This is to certify that the

thesis entitled

Development of Initiator Systems for Ultraviolet Photopolymerization of Thick Polymers and Composites

presented by

Lindsay Scott Coons

has been accepted towards fulfillment
of the requirements for

Ph.D. degree in Chemical Engineering

Alec Scranton
Major professor

Date 6/12/96

DEVELOPMENT OF INITIATOR SYSTEMS FOR ULTRAVIOLET PHOTOPOLYMERIZATION OF THICK POLYMERS AND COMPOSITES

By

Lindsay Scott Coons

A DISSERTATION

Submitted to
Michigan State University
in partial fulfillment of the requirements
for the degree of

DOCTOR OF PHILOSOPHY

Department of Chemical Engineering

1996

ABSTRACT

DEVELOPMENT OF INITIATOR SYSTEMS FOR ULTRAVIOLET PHOTOPOLYMERIZATION OF THICK POLYMERS AND COMPOSITES

By

Lindsay Scott Coons

The general objective of this research project is the development of novel curing strategies based upon photopolymerizations for high-speed, low-cost production of polymeric composites. Developing new technology based upon photopolymerizations could have a significant impact in current polymer and composite processing methods. A host of products and processes could be improved by incorporation of this technology into their development. Although photopolymerizations offer several advantages over current processing methods such as cure on demand, its use has been limited largely to the production of thin films, inks and coatings due to problems arising from the fact that severe light intensity gradients exist initially in the bulk of thicker systems. Two strategies for overcoming the limitations imposed on thick systems by the existence of the light intensity gradient are disclosed here. The first strategy combines careful selection of the initiating wavelength with the reactive system including the resin/monomer, initiator formulation and their relative concentrations to produce light intensity gradients that may be described as "self-eliminating". In the second strategy, a hybrid photo/thermal initiating mechanism is employed where the heat evolved from the highly exothermic photochemical reaction elevates the temperature of the system causing a second, thermal reaction which results in the production of additional active sites. A number of important

operating conditions such as initiator formulation including concentration of thermal and photoinitiators as well as photosensitizers, initiating light including wavelength, intensity and illumination time, and fiber selection including fiber type and degree of loading have been investigate to validate these novel strategies. These studies have successfully demonstrated the potential of these polymerization strategies for the production of composites and thick polymers. Prototypical composites and thick polymers in excess of two centimeters have been cured in cycle times ranging from less than a minute to ten minutes or less depending on the thickness of the composite.

To Julie and The Kernel.

ACKNOWLEDGMENTS

I would like to thank the members of my doctoral committee, Dr. Jack Giacin, Dr. Martin Hawley, and Dr. Andre Lee for their role in this research both in forming the path of the research and in insuring that I never strayed too far from that path. I would especially like to thank Dr. Alec Scranton for serving as my graduate advisor throughout this project. His contributions to the advancement of my professional career have gone above and beyond the scope of this research and I will always look to him as a mentor in the area of photopolymerizations.

I would like to thank the staff in the Chemical Engineering Department including: Candy, for always having a fresh supply of coffee and donuts for seminars; Julie, for turning in our paperwork so that we always got paid; and Faith, for being a young "mother" to all the graduate students.

I would also like to thank the graduate members of ABSLAB including Julie Jessop, Arvind Mathur and Shail Moorjani for their ongoing contributions and mutual support both in and out of the lab. I would also like to thank the numerous undergraduate members whose path I have crossed throughout the years for making the laboratory a fun place to work. David Godshall deserves special mention for the outstanding contributions he has made to this project.

Bharath Rangarajan was my closest cohort in this research and together we conducted some of the most important research in this laboratory. We also teamed up to carry out some of the least successful experiments in the laboratory, but his support was constant regardless of the successes or failures of the particular day. I will undoubtedly miss the morning and late night trips we took in search of hash browns and endless cups coffee and/or alternative beverages. Some of these trips provided intellectual stimulation, but mostly they provided caffeine.

I would also like to thank my family for their understanding and support throughout my graduate career. Never once did anyone suggest I think about "getting a real job" even when everyone around me seemed to be doing just that.

Finally, I would like to acknowledge the person who I am most fortunate to share my life with, my wife Julie. Four years ago she uprooted herself and moved to Michigan without a job or any friends and offered me support and encouragement even at times when I might not have appreciated it. She is truly special, and I am forever grateful for her kindness, compassion and unconditional love.

TABLE OF CONTENTS

LIST OF TABLES

LIST OF FIGURES

Chapter 2

Chapter 4

Chapter 5

Chapter 6

Chapter 7

Chapter 8

CHAPTER 1.

INTRODUCTION

Polymer science is constantly changing and developing. Research in this area has advanced from its primitive stages over a century ago when scientists were simply studying natural polymers such as rubber, starch and some proteins, to the current development of literally hundreds of advanced synthetic polymers. The trend to replace traditional materials with synthetic polymers has provided a constant motivation to develop new products without increasing costs and/or decreasing quality. Rather than developing entirely new polymers to meet this demand, it is often more cost-effective to modify or blend existing polymers using novel processes. As research progresses, it is becoming more and more difficult to develop "new" materials, thus a major research objective is to now either modify current methods used to develop these polymers to make them more cost-effective or to develop entirely new methods for producing these polymers. Methods that focus on photoinitiated polymerization reactions have seen and continue to see rapid expansion as scientists seek to reach the changing research objectives of new and improved polymer processing methods.

1.1. Characteristics and Advantages of Photopolymerizations

Photopolymerizations are simply polymerizations of reactive mixtures initiated by light. The unreacted mixtures are stable at room temperature but will polymerize readily once exposed to light of the appropriate wavelength. This wavelength typically lies in the ultraviolet or visible region of the light spectrum.[1] The active site produced may be either a radical or a cation depending on the photoinitiator formulation present in the system.

Photopolymerizations provide excellent control over the reaction both spatially because the light can be directed and/or focused to a particular area of the reactive formulation and temporally because the light can be shuttered on and off during the reaction. In addition, the rate of photoinitiation can be controlled by a combination of variables including initiator formulation, incident source and intensity, and initial temperature of the system. Photocuring is a simple procedure that uses highly targeted, efficient light sources to cure systems that are often environmentally "friendly" because the polymerizations are typically carried out in bulk,[2] hence no volatile solvents are released during the course of the reaction.

While the exact value of the financial savings varies as a function of the polymer produced, photopolymerizations do present a number of economic advantages. First, production of initiating species is efficient because the light sources are highly targeted and specific light sources may be selected for particular processes. Thus light sources are typically selected for a particular process because they emit light at a wavelength where the photoinitiator (or photosensitizer) absorbs appreciably. Second, the more expensive components of the formulation, namely the photoinitiators or photosensitizers, are used in

much smaller quantities (typically 1 wt% or less as the thickness of the sample increases). Third, because all components of the reaction may be premixed and stored for extended periods of time and the reaction takes place under ambient conditions, there is no need for expensive mixing or heating equipment. Lastly, most photopolymerization processes are carried out in bulk, thus there is no cost associated with purchasing solvents and the need for expensive ventilating systems is also greatly reduced or eliminated altogether depending on the volatility of the monomer.

1.2. Applications of Photopolymerizations

Historically, commercial applications for photopolymerizations date back as far as the 1940s. A number of industrial processes based upon photopolymerizations have been developed for the production of a variety of thin polymer applications including films, inks and coatings. More recently, photopolymerizations have been used for a number of applications in the electronics industry including coating of optical fibers, replication of optical disks and printed copper circuitry. These applications make up what can be described as "traditional" photopolymerization applications, namely thin polymeric products which are cured using some type of photoinitiated polymerization method. The number of products fabricated by photopolymerization methods is increasing at rate of approximately 20-30 % per year, suggesting that the general public is beginning to realize the potential of photopolymerizations for a wider variety of applications. However, the majority of newer applications would still be considered "traditional" in the sense that

photopolymerizations are being used for the production of thin systems. Few examples can be offered that use photopolymerizations to produce three-dimensional polymers.

For the most part, commercial use of photopolymerizations to produce thicker polymers or composites has been limited to the production of composite dental materials and additive or layering processes such as photolithography. Photolithography provides an excellent working example for how the advantages of photopolymerizations can be employed in the production of thicker systems. This particular process combines the excellent spatial and temporal control afforded by photopolymerizations with the computer-aided design capabilities of traditional stereolithgraphy to rapidly produce three-dimensional prototypes and other complex structures. Focused light sources such as helium-cadmium (HeCd) lasers may be employed to produce detailed structures such as intricate electronics patterns or complex products. Briefly, three-dimensional polymers are produced by lowering a platform (which may support a substrate in some applications) into a vat containing an excess of the reactive formulation. A pattern predetermined by computer design is then photocured in a matter of seconds using a point-focused light source capable of producing an intricate polymer. Once the pattern is has been cured, the platform is lowered into the vat, thereby allowing a deliberate layer of reactive monomer to flow over the sample. The photocuring process is then repeated a number of times until the desired specifications of the polymer are reached to produce a detailed, three-dimensional polymer. Photolithography has become a standard and accepted method for producing polymers and prototypes for a number of free-radical systems. For example, Neckers[3] reported polymerizing acrylates in three dimensions by using an additive modeling process based on stereolithography while a patent was issued

in 1986 to Charles Hull[4] for the invention of a three-dimensional photolithography process similar to the one described herein. In the past five years, the scope of photolithographic processes has expanded to include the production of three-dimensional polymeric composites.[5-7]

As mentioned previously, photopolymerizable compositions have been utilized in the production of dental composites. In particular, three patents pertaining to photopolymerizable dental compositions were issued to Sasaki *et al.*[8-10] An obvious advantage of a photocurable dental composite is the ability to cure the material directly in the mouth of the patient quickly and at atmospheric conditions (no external heating requirements). Also, these reactions are carried out in bulk so the patient is not subjected to the release of volatile organic compounds at any time during the procedure. Clearly photopolymerizable dental composites and photolithography demonstrate the potential of photopolymerizations for "non-traditional" or three-dimensional applications. It can still be said that with the exception of these two specific applications, photopolymerizations have been limited to thin systems.

Until very recently, one could safely state that no method has been developed which is capable of photocuring thick polymers and/or composite structures either quickly or uniformly. That statement is now only partially true, thanks to a joint effort of Sunrez Corporation (El Cajon, CA) and Film Technology Incorporated (Houston, TX). The new venture, titled Synergistic Composites Systems, combines vacuum-assisted resin transfer molding and UV-irradiation to produce polymeric composites.[11] While the process is an exciting advance for photopolymerizations, it still comes with a few bugs. For example, the cure time of the process is relatively slow, ranging from 3 to 15 minutes

depending on the thickness of the laminate, and the process is limited to light-permeable laminates, meaning that only glass fibers may be used as reinforcing material.[11] In addition, the technology is currently limited to single cycle production of laminates whose thickness is 0.5 inch or thinner and requires 7-10 minutes to cure. Curing thicker samples requires at least two cycles which increases the overall time required to produe the structures. Still, the development of this process is a significant advance in the current state-of-the-art used to produce thick parts and composites and could make sizable inroads into mainstream composites processing technology with a few modifications and improvements such as increasing the thickness of cured composites, improving the number and type of usable reinforcing materials, and reducing the overall cycle time.

1.3. Composite Materials

A composite may be defined as any two-phase material which consists of a reinforcing phase supported by a binder phase. Composite materials offer significant advantages over other materials such as metals, alloys and wood. For example, composite products are significantly lighter than their steel counterparts and exhibit outstanding strength to weight ratios. A number of methods have been used to produce composites with the most common of these being hand lay-up and resin transfer molding (RTM). A strength of RTM is its ability to produce composites in large quantities while hand lay-up offers the ability to produce highly detailed composites for a number of smaller, specialty applications.

Composites have been employed industrially for over half a century, with the first reported use occurring during World War II when fiber-reinforced plastics were used in a variety of structural applications.[12] Composites were initially developed to solve the problems associated with the lack of a single, lightweight material having desired attributes such as resistance to fatigue and corrosion as well as excellent mechanical properties. Currently, composites are used in a much broader array of applications ranging for example from the transportation industry (automobile, marine and aerospace) to kitchen appliances. When coupling their unique combination of high strength and light weight with relatively inexpensive production costs, it is easy to understand why composites are tested for and ultimately used in a wide variety of applications.

A variety of resin systems have been used in conjunction with an equally varied assortment of reinforcing materials to produce composites. Common resin systems include: epoxies, polyimides and polyesters, as well as a number of thermoplastic resins.[13-16] Reinforcing materials range from short, discontinuous glass, carbon or aramid fibers to continuous fiber strands to fiber mats and other fabrics and preforms.[17-20] While they are not present for their reinforcing capabilities, inorganic filler materials have also been added to polyester resins. While addition of these fillers often enhances the stiffness of the polyester resin,[15] their main role is to reduce the overall cost of the cured material and/or reduce its density. Inert fillers are also added to various resins to alter the physical, mechanical, thermal or electrical properties of the composite.

Through careful selection of the binder material and the type of reinforcement, a composite can be designed for just about any application. The selection of each phase is extremely important in composite design because the properties of the composite are

dictated by the type and orientation of the fiber *and* the resin used as the polymeric binder. Thus it is difficult to classify composites in any way other than by the type of reinforcement used in the composite. Dividing composites in this manner typically means that the composite will fall into one of three classes: particulate, fiber or laminar.[12] Particle composites are identified by the fact that all dimensions of the reinforcing material are roughly equal or uniform while laminar composites consist of reinforcing materials that are layered with two dimensions being far more significant than the third dimension. Fiber composites describe systems where the length of the reinforcing material is much greater than its cross-sectional area. A fiber-reinforced composite may be further classified as continuous or discontinuous depending on whether or not its properties are dependent on fiber length.

1.4. Necessity for Development of Thick Photopolymerization Methods

The previous sections detail the advantages of photopolymerizations and its potential for a variety of applications. In addition, it has been established that the scope of photopolymerizations has been restricted to thin systems and a few specialty applications involving moderately thicker systems. However science is setting its sights too low by limiting photopolymerizations to the domain of the aforementioned systems. The benefits associated with photopolymerizations are rapidly gaining industrial acceptance as evidenced by the rapid growth rate of processes and products based on this technology. Thus by expanding the realm of photopolymerizations to include three-dimensional polymer systems, both academia and industry could realize significant

technological advancements for a much broader array of applications as well as improving current or developing altogether new polymer processing techniques.

There are a few potential explanations for the limited advancement of photopolymerizations into the domain of three-dimensional systems. The most obvious reason for this is the initial existence of severe light intensity gradients throughout the bulk of the reactive system. It is widely accepted that this light intensity gradient virtually eliminates the possibility of uniform degrees of cure throughout the bulk of the polymer. While the existence of this light intensity gradient does affect thick polymerizations, it does not preclude the possibility of polymerizing in three dimensions if careful attention is paid to the selection of a wide variety of system variables.

1.4.1 Impact in Technology

This research could result in the development of novel photopolymerization processes for high-speed, low-cost production of polymeric composites. Although photopolymerizations offer tremendous advantages, problems associated with light intensity gradients and scattering, have limited their use to the production of thin films. This research demonstrates that photopolymerizations may be used to produce thick and fiber-filled specimens with proper system design, and development of applications based on photocurable composite systems could have an important impact on commercial composites processing. For example, in the realm of liquid molding, photopolymerizations may allow decoupling of mold-filling and reaction, thereby eliminating many problems and limitations of current liquid molding processes. Armed with this fact, it is not inconceivable that photopolymerizations could be incorporated into

a continuous process for the production of fiber reinforced composites. This scheme, if successful, represents an important breakthrough since it will allow composites to be produced continuously at low pressure with a relatively small and inexpensive tool. A second area where this research could have a significant impact in current technology is we will develop in this research is polymer prepregs. Since light rather than heat provides the initiating energy, photocurable prepregs would have the unique characteristics of having practically unlimited working time (without UV illumination), but short cure times (upon illumination) at room temperature. Although these photocurable prepregs may find many applications, they are ideally suited for the production of perforated composite acoustic panel face-sheets for the aerospace industry.

1.4.2. Impact in Science

This research may have a significant impact in the area of radiation curing. To date, nearly all of the new radiation curable products being developed are for thin systems. While there is still remarkable growth in this area, it has been needlessly limited. By providing experimental evidence supporting the possibility of photocuring thick polymers and/or composites, possible radiation curing has been exposed to an entirely new, undeveloped area. On a more basic level, it is hoped that this research will serve as a springboard for future scientists to determine for themselves what are the limits of photopolymerizations and not restrict their research to what has been established as "acceptable" applications for radiation curing.

1.5. References

1. G. Odian, *Principles of Polymerization*, Wiley-Interscience, New York, 222 (1991).

2. R. Sastre, M.Conde and J.L. Mateo, "Photoinitiated Bulk Polymerization of Lauryl Acrylate by N-Acetyl-4-nitro-1-naphthylamine in the Presence of N,N-Dimethylaniline," *J. Photochem. and Photobiol., A: Chem.*, **44**, 111 (1988).

3. D.C. Neckers, "Architecture with Photopolymerization," *Polym. Eng. Sci.*, **32(20)**, 1481 (1992).

4. C. Hull, "Apparatus for Production of Three-Dimensional Objects by Stereolithography," *U.S. Patent No.* 4,575,330, issued March 11, 1986.

5. T. Renault, A.A. Ogale, R.L. Dooley, A. Bagchi, C.C. Jara-Almonte, "Photolithography for Composites Manufacturing: Continuous Glass Fiber/-Polyacrylate Composites," *SAMPE Quarterly*, **22(2)**, 19 (1991).

6. A.A. Ogale, T. Renault, R.L. Dooley, A. Bagchi, C.C. Jara-Almonte, "3-D Photo-lithography for Composite Development: Discontinuous Reinforcements," *SAMPE Quarterly*, **23(1)**, 28 (1991).

7. T. Renault, A.A. Ogale, M.J. Drews, "Influence of Reinforcements on Photocuring: Photo Dynamic Mechanical Analysis," *Proceedings of Annual Technical Conference*, Society of Plastics Engineers, 2352 (1993).

8. I. Sasaki, N. Mukai, H. Ige, "Photopolymerizable Dental Composition Containing a Hexafunctional Urethane Methacrylate Based on Isocyanuric Acid," *U.S. Patent No.* 4,762,863, issued August 9, 1988.

9. I. Sasaki, N. Mukai, H. Ige,"Photopolymerizable Dental Composition," *U.S. Patent No.* 4,933,376, issued June 12, 1990.

10. I. Sasaki, N. Mukai, H. Ige,"Photopolymerizable Dental Composition," *U.S. Patent No.* 4,977,197, issued December 11, 1990.

11. "Vacuum-Assisted RTM Increasingly Popular," A. Hudson, ed., *Composites Technology*, p.24, March/April 1996.

12. T.J. Reinhart, L.L. Clements, "Introduction to Composites," in *Composites*, vol 1, ASM International, Metals Park, OH, 27 (1987).

13. C.A. May, "Epoxy Resins," in *Composites*, vol 1, ASM International, Metals Park, OH, 66 (1987).

14. D.A. Scola, "Polyimide Resins," in *Composites*, vol 1, ASM International, Metals Park, OH, 78 (1987).

15. C.D. Dudgeon, "Polyester Resins," in *Composites*, vol 1, ASM International, Metals Park, OH, 90 (1987).

16. R.B. Gosnall, "Thermoplastic Resins," in *Composites*, vol 1, ASM International, Metals Park, OH, 97 (1987).

17. J.C. Watson, N. Raghupathi, "Glass Fibers," in *Composites*, vol 1, ASM International, Metals Park, OH, 107 (1987).

18. N.W. Hansen, "Carbon Fibers," in *Composites*, vol 1, ASM International, Metals Park, OH, 112 (1987).

19. J.J. Pigliacampi, "Aramid Fibers," in *Composites*, vol 1, ASM International, Metals Park, OH, 114 (1987).

20. F.P. Magin, "Multidirectionally Reinforced Fabrics and Preforms," in *Composites*, vol 1, ASM International, Metals Park, OH, 129 (1987).

CHAPTER 2.

BACKGROUND

The purpose of this chapter is to provide a relatively detailed historical background of polymerizations and composites. The first half of this chapter will be devoted entirely to polymers, polymerization mechanisms, and the compounds used to produce these structures. General mechanisms for radical and cationic chain polymerizations will be discussed before presenting a section dedicated to radical and cationic photopolymerization processes. The second half of this chapter focuses on composites including current applications and methods for producing composites, various types of composites, and typical materials used in both the reinforcement phase and the binder (polymer) phase. This section will provide a historical perspective on the composites industry as well as establishing the current state of composites processing as well as a possible direction for its future.

2.1. Polymers and Polymerization Reactions

The term polymer applies to a broad spectrum of chemical structures which can be characterized into more specific groups based on a number of traits including the method used to form the polymer, its physical properties such as thermal stability and physical

appearance, and its mechanical properties such as flexural strength and modulus. The task of classifying polymers can be a difficult one since many polymers are actually networks of several different polymer chains, thereby having one or several qualities which make it difficult to easily categorize the polymer accurately. While polymers have been characterized using a number of methods including structural differences between monomer and polymer, the most effective classification method seems to be based on the chemical reaction that occurs when monomer is converted to polymer.

2.1.1. Classifying Polymers

The original polymer classification system was developed in the early 1900's by W.H. Carothers,[1] who defined *condensation polymers* and *addition polymers* based on compositional differences between the polymer and its monomers. Polymers formed by elimination of a small molecule (i.e. water) were called condensation polymers, while polymers formed without losing a molecule were known as addition polymers. A second classification system was developed by Flory in the 1950's.[2] In his scheme, Flory focused on the mechanism of the polymerization and defined two classes: *step polymers* and *chain polymers.* Although many people tend to use the terms condensation and step as well as addition and chain interchangeably, this is not always accurate because of the fundamental differences in the basis of these classifications. For example, polyurethanes would be defined as addition polymers in the Carothers scheme but step polymers using Flory's classification. All of the polymer systems studied experimentally in the course of this research were formed as a result of a *chain* reaction, therefore the focus of this

section will be on chain polymerizations with a brief overview of step polymerizations provided simply as a method of comparison.

2.1.1a. Step Polymerizations. Step polymerizations propagate through a series of reactions between functional groups of two reactants. In this mechanism, monomers will react with monomers to form dimers, dimers will react with monomers to form trimers or with other dimers to form tetramers and so on until a long-chain polymer is been formed. Step polymerizations can generally be characterized by the following six statements made by Rudin[3] in the early 1980's: 1) a single reaction type is involved in the reaction; 2) monomer units can react with each other, or a polymer of any size; 3) the reactivity of a functional group is not dependent on polymer (or monomer) size; 4) in order to produce high molecular weight polymers, high conversion of the monomer species must occur; 5) an equilibrium may exist between reactants and macromolecules; and 6) condensation polymers are usually produced in step polymerizations.

2.1.1b. Chain Polymerizations. In addition to the monomer(s), chain polymerizations require the addition of a separate compound known as the "initiator", which will undergo some type of chemical reaction when subjected to a change in initial conditions (heating, irradiation, microwave or ultrasound) to form a product which becomes an active site capable of reacting with the monomer to initiate the reaction. Depending on the initiator, a radical, cation, anion or a combination of the three may be produced during the initiation reaction. Polymerization proceeds with propagation of the active species by successive addition of large numbers of monomer molecules in a

relatively short period of time, often on the order of one second or less. A significant fact in chain reactions is that monomer will not react with monomer unless an active site is present on (at least) one of the monomer units. Termination of the growing polymer chains may occur by a number of possible reactions including: chain transfer, disproportionation or combination to name a few.

Chain polymerizations are classified as radical or ionic, with ionic mechanisms further designated as cationic or anionic, depending on the active site responsible for propagation of the polymer chain. Each of these chain polymerizations has a distinctive reaction mechanism because of the differences in the active species. It should be stressed that reactive species are not indiscriminate since all three reactive centers do not initiate polymerization in all monomers. In fact, monomers show varying degrees of selectivity to the type of reactive center that will initiate polymerization, therefore some monomers may undergo ionic initiation exclusively while other monomers (such as styrene) will polymerize in the presence of any type of reactive center. Radical chain polymers are most prevalent in industry to date because most monomers will undergo radical polymerization under modest reaction conditions without being overly sensitive to impurities, while industrial use for ionic reactions has been limited mainly to the rubber industry in part because of the selectivity of many monomers to reactive ionic centers. The following subsections will detail the radical mechanism as well as the cationic mechanism, elaborating on the similarities and differences of each.

2.1.2. The Radical Mechanism

There are two main classes of bonds that will undergo chain polymerization: vinyl bonds and carbonyl bonds.[4] Radical species will not polymerize through a carbonyl group due to the polarity of the double bond. Although a vinyl bond in the monomer does not guarantee that the monomer will polymerize radically because of the resonance structures of the substituents present in the monomer, most vinyl bonds are likely to undergo radical polymerization in part because the radical species is a neutral one which does not have strict "requirements" for attacking the π-bond. Also, nearly all substituents are able to stabilize the radical by delocalizing the radical over two or more atoms.[4]

In the radical mechanism, as is common to each chain polymerization, there is initiation, propagation, and termination. The initiation step is really a two-step process in which the initiator is first dissociated into two radicals (Equation 2.1) before it attacks a single monomer unit to produce an active site on the monomer itself (Equation 2.2).

$$I \Rightarrow 2R\bullet \qquad (2.1)$$

$$R\bullet + M \Rightarrow M_1\bullet \qquad (2.2)$$

A number of initiators are used in radical reactions including many peroxides and azo compounds such as 2,2'-azobisisobutyronitrile. In addition to these initiator, which are susceptible to thermal initiation, there are a number of photoinitiators, or initiators that will undergo dissociation after absorbing light. The photoinitiation mechanism will be detailed more extensively in the following sections of this chapter. Once the monomer becomes "active" (as shown in Equation 2.2), it has the ability to add to any other monomer that comes in close contact. This occurs in the same manner as the reactive

initiator added to the original monomer, making the second monomer an active site (Equation 2.3). Successive additions of monomer units will

$$M_1\bullet + M \Rightarrow M_2\bullet \qquad (2.3)$$

continue to increase the size of the polymer in such a way that each radical will be identical to the previous one except for the fact that the polymer chain will have grown by a single monomer unit. This process is repeated and the polymer chain continues to grow until termination of the radical, which may occur when the active polymer reacts with an active radical species of another polymer, resulting in termination by coupling.

Termination is the final step in the radical mechanism, and can occur by a number of reactions, although the most common is coupling of two active polymer chains (Equation 2.4). A less common method of termination is disproportionation, shown in Equation 2.5.

$$M_n\bullet + M_m\bullet \Rightarrow M_{n+m} \qquad (2.4)$$

$$M_n\bullet + M_m\bullet \Rightarrow M_n + M_m \qquad (2.5)$$

The method of termination is not always specified, hence it is often represented as a general termination reaction, shown in Equation 2.6.

$$M_n\bullet + M_m\bullet \Rightarrow \text{Dead Polymer} \qquad (2.6)$$

As one would expect, rate constants differ for each step of the reaction and are generally represented as k_d for dissociation of the initiator (Equation 2.1), k_i for the addition of the radical to the monomer (Equation 2.2), k_p for propagation of the polymer (Equation 2.3), k_{tc} for termination by coupling (Equation 2.4), k_{td} for termination by

disproportionation (Equation 2.5), and k_t to represent general termination of the polymer (Equation 2.6).

The propagation constant, k_p, and the termination constant, k_t, are used to determine the rate of polymerization, R_p. In order to determine R_p, one begins by deriving an expression for the rate of monomer disappearance, which Odian[4] states is synonymous with the rate of polymerization. Monomer is used up in both the initiation step and the propagation step, therefore the rate at which monomer disappears is given by

$$-d[M]/dt = R_i + R_p \tag{2.7}$$

where R_i is the rate of initiation and [M] is the monomer concentration. An assumption is then made that the amount of monomer reacting in the propagation step is much greater than the monomer used up in the initiation step, therefore (2.7) may be simplified to

$$-d[M]/dt = R_p \tag{2.8}$$

which is a very close approximation of (2.7). The rate of propagation consists of several repetitions of Equation (2.3), which has as its constant k_p. The single rate constant allows the rate of propagation to be expressed as

$$R_p = k_p[M][M\bullet] \tag{2.9}$$

where [M•] represents the concentration of all chain radical species.

Since it is extremely hard to experimentally measure the concentration of radicals in a polymerizing system, Equation (2.9) is not in an acceptable form. Therefore the *quasi steady-state* assumption (QSSA) is commonly made for the concentration of radicals. Stating that the concentration of radicals remains constant throughout

propagation is equal to stating that R_i and R_t (the rate of termination) are equal. This means

$$R_i = 2k_t[M\bullet]^2 \tag{2.10}$$

This equation can then be rearranged to yield an expression for [M•]

$$[M\bullet] = (R_i/2k_t)^{1/2} \tag{2.11}$$

which can be substituted into Equation (2.9) to yield the following expression

$$R_p = k_p[M](R_i/2k_t)^{1/2} \tag{2.12}$$

which gives a general equation for determining the rate of polymerization.

It is clear from Equation (2.12) that the rate of polymerization is proportional to the square root of the rate of initiation and directly proportional to the monomer concentration. This leads to the expectation that polymerization rates would decrease with conversion due to depletion of monomer and initiator; yet this is not always the case in radical polymerizations due to an effect known as *autoacceleration*. Autoacceleration is a process that occurs in radical polymerizations when there is a reduction in the rate of diffusion-controlled termination as a result of reduced mobility in the growing radical chains. This effect causes dramatic increases in the rate of polymerization as well as an increase in the molecular weight with conversion.

2.1.3. The Cationic Mechanism

Cationic polymerizations occur in much the same fashion as their radical counterparts with the exceptions that the propagating center is a cation and termination by coupling will not occur. Termination may occur by chain transfer of the reactive center,

or occasionally by counterion combination. Termination by chain transfer will typically decrease the average primary polymer chain length, although it will not affect the rate of polymerization due to the continued propagation by the resulting cation.[4] For this reason, these reactions are well-suited for the formation of crosslinked structures or ladder polymers which rely on network structure, not long linear chains, for their properties. Classes of monomers that will not polymerize by a free radical mechanism but can be cationically polymerized include α-olefins, 1,3-dienes, vinyl ethers and epoxides to name a few.

Each of these monomer systems has potential advantages that make them industrially useful. Epoxides for example exhibit tremendous adhesion to a variety of substrates. Nevertheless, these monomers are rarely used in applications where they are polymerized via a cationic mechanism to date. A potential explanation for this is the lack of understanding of the cationic mechanism in general.[5] Despite this problem, scientists are still able to formulate a reaction scheme for cationic polymerizations involving the same three steps as radical polymerizations.

Like other chain polymerizations, the first step is the initiation step. Commonly used thermal initiators include Lewis acids such as $AlCl_3$, BF_3, $SnCl_4$ and $TiCl_4$ to name a few; and to a lesser extent Brønsted acids and iodine. Another type of initiator that has been investigated over the last fifteen or so years has been the photoinitiator, ordinarily an iodonium or sulfonium salt. In this initiation sequence, the onium salt undergoes photolytic cleavage to yield a radical-cation which then reacts with HY to yield an active cationic species.[6] Aside from the photoinitiators, Lewis acids are widely considered to be

the most important initiator of cationic polymerizations because they yield high molecular-weight polymers at low to intermediate temperatures.

In the initiation sequence, the Lewis acid either undergoes self-ionization (Equation 2.13) or ionization via a coinitiator, XY (Equation 2.14)

$$2AlCl_3 \Leftrightarrow AlCl_2^+(AlCl_4)^- \quad (2.13)$$

$$I + XY \Leftrightarrow Y^+(IX)^- \quad (2.14)$$

Whether or not an initiator-coinitiator scheme or single initiator is used, the second step of the initiation sequence involves the addition of the active species to the monomer, M

$$AlCl_2^+(AlCl_4)^- + M \Rightarrow AlCl_2M^+(AlCl_4)^- \quad (2.15)$$

At this point, the active species is a carbonium ion in the monomer, which is then capable of propagating with unreacted monomers.

$$AlCl_2M^+(AlCl_4)^- + M \Rightarrow AlCl_2M_2^+(AlCl_4)^- \quad (2.16)$$

Successive addition of monomers will yield high molecular-weight molecules which will terminate through chain transfer, or more rarely spontaneous termination or counterion combination. Chain transfer occurs when a proton is transferred from the reactive center to a monomer, thus terminating the growing polymer while at the same time creating a reactive monomer capable of undergoing polymerization the same way as the terminated polymer

$$AlCl_2M_n^+(AlCl_4)^- + M \Rightarrow M_n + AlCl_2M^+(AlCl_4)^- \quad (2.17)$$

Like radical polymerizations, a general expression describing the kinetics of a cationic polymerization (as seen in Equations 2.13 - 2.17) can be derived. there are rate constants associated with these. The terms used to describe rate constants for initiation

and propagation are the same as those for the radical mechanism, specifically k_i and k_p. However, chain transfer to monomer is almost always responsible for termination of cationic chains, therefore a specific rate constant for termination by chain transfer to monomer is given by $k_{tr,M}$.

Deriving a general expression for the rate of a cationic polymerization is nowhere near as simple as the derivation for radically-initiated systems. There are a number of variables associated with the cationic mechanism which make it virtually impossible to derive a general equation capable of accounting for each of these variables. For example, the rate of polymerization is dependent on the method of initiation. To illustrate this, one need only examine initiation by ionizing radiation. This method of initiation yields an equation in which the rate of polymerization is dependent on the square root of the rate of initiation, while other methods used to initiate cationic polymerizations tend to produce first-order dependence of the polymerization rate on the rate of initiation. Another variation in the rate of polymerization is the method of termination.

Polymers that undergo termination by counterion combination will exhibit a rate expression that can be derived in the same manner as the rate expression for radical polymers.[4] However, the most common method of termination in cationic polymerizations involves chain transfer. Thus the following derivation focuses specifically on termination by chain transfer, either to monomer ($k_{tr,M}$) or to a chain transfer agent ($k_{tr,S}$).

The rate of initiation is given by Equation (2.18) where K is the rate constant for the ionization step, while the rate of propagation is given by Equation (2.19)

$$R_i = Kk_i[I][XY][M] \quad (2.18)$$

$$R_p = k_p[YM^+(IX)^-][M] \quad (2.19)$$

where $[YM^+(IX)^-]$ is the concentration of *all* reactive centers. The rate expression for termination must be divided into two transfer reactions, one for transfer to monomer (Equation 2.20) and one for transfer to chain-transfer agent (Equation 2.21)

$$R_{tr,M} = k_{tr,M}[YM^+(IX)^-][M] \quad (2.20)$$

$$R_{tr,S} = k_{tr,S}[YM^+(IX)^-][S] \quad (2.21)$$

The formation of $[YM^+(IX)^-]$ is dependent upon the initiation step, therefore one must know what the rate-limiting step in the initiation process is to derive an expression for $[YM^+(IX)^-]$. Therefore, if one assumes that Equation (2.14) is rate-limiting *and* that R_i is equal to R_t (QSSA), then $[YM^+(IX)^-]$ can be expressed by

$$[YM^+(IX)^-] = Kk_i[I][XY][M]/(k_{tr,M}[M] + k_{tr,S}[S]) \quad (2.22)$$

Substituting Equation (2.22) into Equation (2.19) yields the following expression for the rate of polymerization for a cationic reaction mechanism

$$R_p = Kk_ik_p[I][XY][M]^2/(k_{tr,M}[M] + k_{tr,S}[S]) \quad (2.23)$$

This is a simple, straightforward method for deriving the rate of cationic polymerization, however there are a number of inconsistencies and assumptions associated with its derivation, and these inconsistencies have the potential to create large discrepancies in the actual rate of polymerization versus the theoretical R_p determined using Equation (2.23). As reported in Odian,[4] various rate constants are calculated using unsubstantiated reaction kinetics and mechanisms. Additionally, it is not known how to

interpret any rate constants because of the known multiplicity of propagating cationic species.[4] The net result of these discrepancies is R_p values calculated using Equation (2.19) will be incorrect when the actual kinetics of the cationic reaction deviate from this equation.

Cationic polymerizations exhibit unusually high reaction rates because they exhibit higher propagation rate constants and lower termination rate constants than typical free radical reactions. Furthermore, the concentration of propagating species is usually two orders of magnitude higher for cationic polymerizations. In fact, these reactions proceed so rapidly that they do not achieve steady-state under most conditions.[7] This makes the assumption that the concentration of active cationic species is maintained at steady-state (QSSA) invalid, which furthermore renders the entire derivation invalid because of its dependence on the cationic species achieving steady-state conditions. In addition, when the rate of initiation is greater than the rate of termination more cations are produced than are used up, consequently steady-state is not achieved during the course of reaction. These disparities exemplify the problems associated with attempting to mathematically describe the rate of polymerization in cationic reactions.

2.2. Photopolymerizations

Photopolymerizations are simply polymerization reactions initiated by light, typically in the ultraviolet (UV) or visible region of the light spectrum. Photopolymerizations are initiated by certain types of compounds which are capable of absorbing light of a particular wavelength. The wavelength or range of wavelengths of

the initiating source is determined by the reactive system including the monomer(s), the initiator(s), and any photosensitizers, pigments or dyes which may be present. An active center is produced when the initiator absorbs light and undergoes some type of decomposition, hydrogen abstraction, or electron transfer reaction. If necessary, the effective initiating wavelength may be shifted by adding small amounts of a second compound, termed a photosensitizer, to the reaction mixture. The photosensitizer absorbs light and populates an excited state which may then react with the photoinitiator to produce an active cation or radical capable of initiating the polymerization. Upon generation of active centers, photopolymerizations propagate and terminate in the same manner as traditional (i.e. thermal) polymerizations.

There are two main types of radiation curing currently being used in industrial applications: UV and electron beam (EB) processing. UV processes are based on the generation of photons upon absorption of light, typically in the ultraviolet or visible region of the light spectrum, while EB processes are based on electrons generated using an e-beam accelerator. While both processes are extremely efficient due to direct interaction between the photon/electron and the chemical bonds, implementation of EB technology is limited to an extremely small portion of the radiation curable market since it is extremely expensive. Thus chain polymerizations initiated by radicals or cations generated by a light-induced reaction are responsible for the majority of new products and developing processes.

2.2.1. General Attributes of Photopolymerizations

There are a tremendous number of advantages inherent in photopolymerizations which make them the technology of choice for a rapidly increasing number of industrial applications. The initiating light can be directed to a specific area of the reaction, providing excellent spatial control over the polymerization; and the start of the reaction can be controlled as can the overall temperature of the reaction at any given point during reaction by shuttering the light. The production of active sites begins immediately upon exposure to light, hence once the initiation reaction begins, active sites may be produced rapidly even at room temperature. The reactive formulation can be premixed and stored for extended periods of time as long as it remains free of light, and the requirements for initiating the process are easily automated. Hence the process is very simple. Additionally, photopolymerizations quite often involve solvent-free reactions, thus they are environmentally "friendly". One fact often overlooked in photopolymerization processes is the fact that they can be operated at room temperature, which is extremely important when curing on substrates which are susceptible to damage at elevated temperatures.

The financial benefits and energy efficiency attributed to UV-cured systems are impressive. The fact that UV curing eliminates the need for expensive post-cure systems combined with the fact that UV systems use approximately 20% of the energy consumed by comparable thermal systems leads to a method which is both energy efficient and less expensive. One final advantage of UV systems is their "portability". Because UV systems require only a fraction of space occupied by thermal curing systems, they free valuable space for a variety of alternative uses.

2.2.2. *Traditional Applications for Photopolymerizations*

These attributes as well as additional advantages have established photopolymerizations as standard technology in a number of "traditional" applications. Traditional applications for photopolymerizations include films, inks; and coatings, for a variety of substrates including wood, metal, plastic, paper and glass. Photopolymerizations have also been incorporated into traditional stereolithography processes. Photolithography capitalizes on the excellent spatial control afforded by photopolymerizations to produce detailed images either by "tracing" predetermined patterns or by masking. An excellent example of the flexibility afforded by photopolymerizations is seen in their use for dental applications.[8,9] Photopolymerizations allow for *in vivo* curing of dental fillers by using optical fibers to direct light to the uncured filler material after it has been placed inside the mouth. The light carried through the optical fiber to the filler initiates a reaction *in the mouth of the patient*, producing a solid filling in a matter of minutes or less without subjecting the patient to potentially hazardous emissions from evaporating solvents or burns as a result of heating sources. Recently, photopolymerizations have been used in a variety of high-tech applications including coating of optical fibers, replication of optical disks and production of printed copper circuitry.[10-14]

UV curing methods are currently being employed in many industries with saturation of the radiation curable market nowhere in sight. In fact, the number of new polymer applications that utilize photopolymerization techniques are expanding at a rate of approximately 20-30% per year. The growth of new photopolymer applications is an excellent measuring stick for the potential of photopolymerizations and the flexibility to

adapt UV curing into the fabrication of existing products and processes as well as new products.

2.2.3. Radical Photoinitiation Processes

2.2.3a. Photoinitiator Compounds. Photopolymerizations involving radical species have been around for many years and the initiation process has been well-documented.[15,16] A number of photoinitiators are available with absorption ranging from the deep UV region well into the visible region of the light spectrum. The most common UV-curable radical photoinitiators include ketones, benzoin ethers, and benzil ketals, along with well-established compounds such as Michler's ketones.[4,17-19] Initiator formulations in the visible region of the light spectrum include many commonly used dyes such as eosin[20] and organic pigments and coinitiators such as camphorquinone/amine[21] formulations. In general there are some important advantages of initiating in the visible region of the light spectrum. However the focus of this research has been in the area of UV-initiated photopolymerizations, therefore attention will be paid to initiators that absorb in this region of the light spectrum. Detailed studies of various radical photoinitiators exist, with Ledwith[22,23] and Pappas[16] providing some of the more exhaustive studies regarding these compounds. In general, radical photoinitiators yield radicals by one of two processes: fragmentation or hydrogen abstraction. Understanding and being able to characterize (and potentially control) the process used to produce the propagating radical is a focal point of this research.

The process by which a reactive radical is produced has a potentially dramatic effect on the absorbance of the polymerizing system, and hence the rate of propagation

and thickness of the cured polymer. While production of radicals via abstraction alters the structure only slightly and results in an initiator fragment having substantially the same chemical structure as the unreacted initiator (see *Figure 2.1a*), fragmentation produces two radicals whose chemical structures are significantly different than the original initiator (see *Figure 2.1b*). Thus initiator fragments resulting from the abstraction reaction may continue to absorb initiating wavelengths while the absorbance characteristics of the fragmentation reaction products are substantially different than those of the unreacted initiator in many initiator formulations. In fact, for the systems

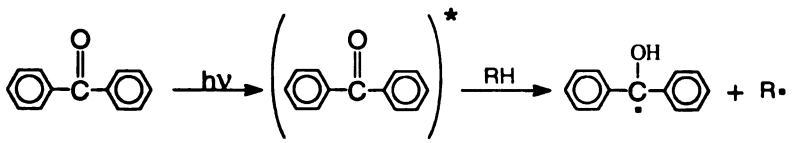

(a)

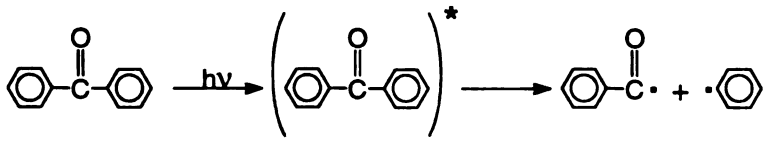

(b)

Figure 2.1. Dissociation of initiator to produce radical by hydrogen abstraction (a) and fragmentation (b).

investigated in this research, the absorbance of initiator fragments resulting from fragmentation proved to be essentially nonexistent in comparison with their unreacted initiator counterparts.

While hydrogen abstraction is more efficient than fragmentation, it will only occur in the presence of hydrogen donors. The most common hydrogen donors are tertiary amines, which have easily abstractable α-hydrogens. While not as efficient as the amines, alcohols and ethers may also be used as hydrogen donors with varying degrees of effectiveness. Historically, tertiary amines have been used successfully in conjunction with a number of photoinitiators such as benzil, benzoin ethers and benzil ketals, to photocure thin polymeric systems.[4,16,24-26] In general, photoinitiator formulations for radical systems have incorporated some type of hydrogen donor in their initiator formulation, thus serving two purposes. First, the presence of a hydrogen donor will tend to promote hydrogen abstraction over fragmentation, therefore improving the overall efficiency of the initiation reaction. Second, hydrogen donors, especially amines, tend to act as oxygen scavengers, thereby removing oxygen molecules that will otherwise serve as inhibitors for free radical polymerizations. The net result of the oxygen-scavenging process is an increase in the rate of polymerization that is dependent on the ability of compounds to serve as oxygen scavengers.

One well-known drawback of simple aromatic or aliphatic amines is the fact that they act as chain transfer agents through a well-established hydrogen abstraction mechanism. While this reaction does not result in direct or immediate termination of an active site, it does terminate the growing polymer chain, resulting in a reduction in the average molecular weight of the polymer chains. In practice, this is very significant since

a number of mechanical and physical properties are directly related to the molecular weight of the polymer. A simple representation of this mechanism is shown in *Figure 2.2*.

To eliminate or minimize any problems caused by chain transfer reactions involving aromatic or aliphatic amines, scientists have attempted to incorporate the amine functionality into a monomer which is capable of participating in the reaction.[27-29] Perhaps the study most relevant to this research is the work performed by Hoyle *et al.*[28] reporting the effects of benzoin ether/amine photoinitiator formulations on the molecular weight of photopolymerized acrylates. In this study, a simple aliphatic amine was functionalized with an ethyl methacrylate monomer unit to produce *N,N*-dimethylaminoethyl methacrylate (DMAEMA).[28] The authors reported minimal effects on the (viscosity average) molecular weight for DMAEMA-promoted reactions, even though this amine is still subject to chain transfer via a hydrogen abstraction mechanism similar to the one seen in *Figure 2.2*. The increased molecular weight of functionalized amines in comparison with simple amines can be attributed to the "crosslinking" nature of the functionalized amines, which have the potential to crosslink because they become "locked" into the polymer backbone upon reaction with an unsaturated monomer. This occurs because polymerization can propagate through two spots on the compound (shown in *Figure 2.3*): the radical formed in the chain transfer reaction; and through the monomer unit incorporated into the backbone of the amine. In addition to these results, the authors[28] reported that the rate of polymerization passed through a maximum before decreasing significantly as the concentration of DMAEMA was increased from 0 - 2

mol/g. The importance of accelerator concentration was also addressed in studies by Seretoudi and Sideridou.[29]

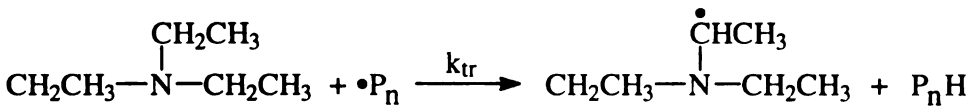

Figure 2.2. Termination by chain transfer of growing polymer chains by amines via a hydrogen abstraction mechanism.

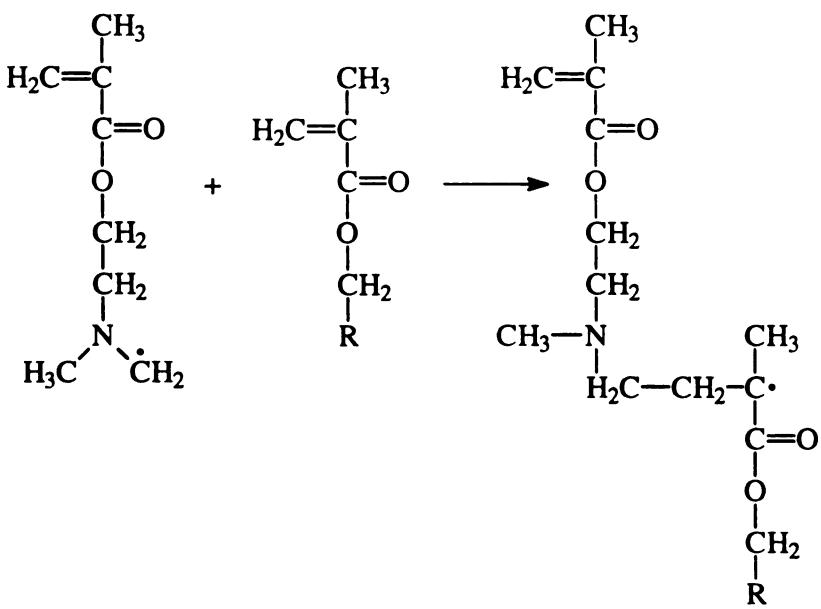

Figure 2.3. Incorporation of N,N-dimethylaminoethyl methacrylate amines into acrylate polymer backbone.

In contrast to the results published by Hoyle,[28] Seretoudi and Sideridou[29] reported that DMAEMA emphatically increases the rate of reaction at the expense of achieving high molecular weights. The authors of this study concluded that 10:1 benzil/DMAEMA photoinitiator formulations increased the rate of polymerization by a factor of ~ 6 while reducing the number-average molecular weight by a factor of ~ 5.[29] The authors agreed with previous studies in the sense that the relative concentrations of photoinitiator and hydrogen donor had a significant effect on the overall reaction kinetics and the molecular weight of the photocured samples.

These examples illustrate the widely accepted method of using amines and/or other hydrogen donors to accelerate polymerizations for traditional (i.e. relatively thin) systems. However, research in this laboratory has indicated that the presence of such compounds may actually inhibit photopolymerizations involving thick (0.1 - 4 cm) polymeric systems. The reasons for this were alluded to earlier in this section and involve continuing absorption by certain compounds even after generation of reactive radicals. Detailed explanations for this effect are offered in a later chapter.

While the aforementioned compounds are far and away the most prevalent UV-curable radical photoinitiator systems, alternative formulations have been investigated. Moderate attention has been focused on the development of photoinitiators based on phosphine oxide derivatives.[30-32] According to Angiolini et al.,[30] these compounds absorb at higher wavelengths than most of the better-known compounds, with peaks centering around 380 nm and extending over 400 nm. This information is useful for extending the operating window of thick photopolymerizations into the near-visible region of the light spectrum.

2.2.3b. Kinetics of The Radical Photoinitiation Step. The derivation used to characterize the rate of polymerization for a radical photoinitiation process is simple and straightforward. The first step in the derivation is to determine the rate of photoinitiation. The general expression used to describe the rate of photoinitiation is shown in Equation 2.24 where ϕ can be described as either the quantum yield for the initiator or the

$$R_i = 2\phi I_a \qquad (2.24)$$

number of propagating chains initiated per photon of light absorbed. The factor 2 is included in the expression because two radicals are generated for every photoinitiator molecule that undergoes reaction. The absorbed light intensity, I_a, can be expressed as a function of the incident intensity, I_o, concentration of photoinitiator, I, the extinction coefficient (or molar absorptivity) of the photoinitiator at the initiating wavelength, ε, and the sample thickness, b. Incorporating these terms into Equation 2.24 yields an alternative expression for R_i.

$$R_i = 2\phi\varepsilon I_o[I]b \qquad (2.25)$$

Equations 2.24 and 2.25 can be substituted into Equation 2.12 to yield two alternative expressions (Equations 2.26 and 2.27, respectively) for determining the rate of polymerization for a photoinitiated system.

$$R_p = k_p[M]\{\phi I_a/k_t\}^{1/2} \qquad (2.26)$$

$$R_p = k_p[M]\{\phi\varepsilon I_o[I]b/k_t\}^{1/2} \qquad (2.27)$$

A limitation of Equation 2.27 in regards to this research effort is the fact that it assumes a relatively uniform distribution of incident light (i.e. little or no absorbance) throughout the bulk of the sample. While this effect may not inhibit uniform

photochemical initiation in thin systems, it would have a severe effect on thick systems because even slight absorbance will result in measurable light intensity gradients throughout the bulk of thicker systems. Hence Equation 2.26 is a more useful equation for calculating the rate of polymerization in thick systems because the amount of absorbed light can be measured directly in polymerizing systems using chemical or electrical actinometry. Experimental studies[33] have shown that typical values for the initiation rate constant can be expected to be on the order of approximately 10^9 M^{-1} sec^{-1} for many photoinitiator formulations including several combinations of benzil/amine derivatives.

2.2.4. Cationic Photoinitiation Process

Cationic photopolymerizations have not received as much attention as their radical counterparts. A possible explanation for this is the fact that cationic photopolymerizations are relatively new and have not been detailed to the same extent as radical systems. Recent Discoveries of thermally stable cationic photoinitiators in the late 1970s and early 1980s have led to more concentrated efforts in understanding and characterizing the cationic mechanism. Crivello has been instrumental in developing an ever-increasing list of cationic photoinitiators including numerous diaryliodonium and triarylsulfonium salts.[6, 34-41] Much of Crivello's early work seemed to focus on developing initiator only so that he could polymerize important classes of monomers such as epoxides and vinyl ethers, however he has been instrumental in developing many of the onium salts that are now widely accepted as excellent initiators for many cationic systems. There now exist a wide variety of onium salt initiators which are extremely

useful because they can be "tailored" to specific systems by manipulating the initiator counterion.

The development of suitable initiators coupled with the rapid reaction rates of vinyl ethers and other cationically polymerizable monomers has led to significant advances in the area of cationic polymerizations. For example, numerous compounds are now being investigated as potential photosensitizers for cationic systems. Photosensitizers such as perylene, pyrene, and numerous anthracene derivatives are added in small amounts to cationic formulations to expand the effective initiating wavelength of the photoinitiator from the deep UV to the visible region of the light spectrum. It is widely accepted that photosensitization proceeds by an electron transfer mechanism.[38,42,43] However, there still exists some disagreement in the scientific community regarding the source, or excited state (singlet or triplet), responsible for electron transfer when anthracene photosensitizes diaryliodonium salts. Recent studies by Nelson *et al.*[44] have reported on the photosensitization mechanism for anthracene and similar derivatives.

The system described by Nelson *et al.*[44] includes a diaryliodonium salt initiator and an anthracene photosensitizer. In systems studied during the course of this research, the monomer (vinyl ethers, epoxies, acrylates) and the photoinitiator were transparent to the initiating light. Therefore anthracene (the photosensitizer) is the only component of the reactive system that absorbs light appreciably in the 350-400 nm range. This is significant because the absorbance of anthracene (and anthracene derivatives such as 9-vinylanthracene and 9,10-dimethylanthracene) changes dramatically as it reacts due to a significant change in its chemical structure. Anthracene absorbance between 350-400 nm

is related to the highly conjugated nature of the compound. However, when anthracene absorbs light and undergoes electron transfer to produce a cationic species, its structure changes and is no longer highly conjugated,[44] resulting in a structure that is transparent to the initiating wavelength (in the 350-400 nm range).

2.2.5. Radical and Cationic Propagation and Termination Processes

Radical and cationic polymerizations proceed in a similar manner once an active species has been produced. The radical (or cation) attacks a bond or group of bonds which are susceptible to radicals (or cations). In either case the first "link" of the polymer chain is established when the active species adds to a monomer unit, resulting in the creation of a new active site at the functionality on the monomer unit. Successive additions via this method result in the formation of a long polymer chain.

Termination of growing radical chains occurs by coupling or disproportionation. Coupling (Equation 2.4) occurs when one radical chain (length A) reacts with a second radical chain (length B) to form a single, dead polymer (length A+B). Disproportionation (Equation 2.5) occurs when radicals from two chains (length A and B, respectively) react to produce two dead polymers (one of length A and the other of length B). These methods of termination are different from termination in cationic polymerizations, which are most commonly terminated by chain transfer to monomer (Equation 2.17) or more rarely by spontaneous termination. Chain transfer occurs when a hydride is transferred from the reactive center to a monomer, thus terminating the growing polymer while at the same time creating a reactive monomer capable of undergoing polymerization in the same manner as the terminated polymer. Thus while one polymer chain is terminated, there is

no reduction in active centers, hence cationic polymerizations may be considered "living" because there is little or no reduction of active sites and more polymer could theoretically be produced if additional monomer were added to the system.

2.3. Composites

Composites may be loosely defined as any material consisting of two phases: a discontinuous phase that composed of a reinforcement or filler material; and a continuous phase that may be described as the polymeric matrix, or binder phase. Composites have been employed in industrial applications for over half a century, with the first reported uses occurring during World War II, when fiber-reinforced plastics were used in a variety of structural applications.[45] Composites were initially developed to solve the problems associated with the lack of a single material having desired attributes such as resistance to fatigue and corrosion , excellent mechanical properties, and light weight. Currently, composites are used in a much broader array of applications ranging for example from the transportation industry (automobile, marine and aerospace) to kitchen appliances. When coupling their unique combination of high strength and light weight with relatively inexpensive production costs, it is easy to understand why composites are tested for and ultimately used in a wide variety of applications.

Composites are suitable for a large number of applications because the properties of the composite are affected by such things as the type and orientation of the fiber and the polymeric material used in the binder phase. Thus it is difficult to classify composites in any way other than by the type of reinforcement used in the composite. Composites

may be characterized as reinforced or "filler" composites depending on the role of the discontinuous, or fiber phase. In the case of filler composites, the filler materials are added either to lighten the material, improve heat resistance, minimize creep, or to reduce the overall cost of the material and not to reinforce the matrix, though that may occur to a degree. Reinforced composites, as the name implies, utilize the strength of the reinforcing material to enhance the polymeric binding phase. These composites may be further divided into one of three subcategories: particulate, fiber or laminar.[45]

"Particulate composites" may be defined as composites where all of the dimensions of the reinforcing material are approximately equal. The reinforcing particles are typically very small (around 1μ), thus they strengthen the composite by resisting movement of the surrounding matrix phase.[46] The particles should be small and well-distributed throughout the matrix because they can interact with other particles only over a limited area; and they should be approximately the same size because this results in optimal use of the particles as reinforcement material. The most common method for formulating particulate composites involves some type of powder metallurgy process using either metallic or nonmetallic reinforcing materials.[45,46]

"Laminar composites" are layered structures where two of the dimensions of the reinforcing material are significantly larger than the third.[45] The layering effect makes it difficult to classify the continuous and discontinuous phases of the composite, since neither the reinforced layers nor the matrix are truly "continuous". Examples of applications that may use laminar composites include low-performance products such as household utensils and automotive trim components.[47]

The majority of composite processes and products are considered "high-performance", thus the focus of composite research is in the area of "fiber composites", although the knowledge gained in the generation of these materials may easily be translated to the production of low-performance composites. Fiber composites offer tremendous advantages over materials such as wood and metal because they combine extremely high strength and stiffness and excellent resistance to corrosion and fatigue, all the while maintaining a very low strength to weight ratio. High-performance, fiber composites are used in a variety of applications ranging from the transportation industry (automotive, aerospace and marine) to the production of various sporting equipment such as fishing rods, tennis rackets and golf clubs.

2.3.1. Methods for Producing Composites

Selecting a composite fabrication method plays an important role in the overall development of the composite. How the fibers are placed in the mold affects the physical properties of the part and ultimately impacts the decision of selecting a molding process.[48] A number of processes are currently being used in the fabrication of composites. Composites are currently being produced on both large and small scales, in continuous and batch processes, for both high and low-performance applications. Depending on the particular application, a process might be entirely automated or highly labor-intensive and it may use either closed or open molds to form the composite. While the current state of the art for composite fabrication processes are labor-intensive to a degree, the general consensus and goal in the composites industry is to move to the point where even highly complex products such as aircraft components are almost entirely

automated.[45] It is believed that the next-generation composites will compare favorably with metallic structures, hence it is necessary to automate the processes used to fabricate these systems in order to rapidly produce composites capable of meeting the increasing demands such as material specifications and cost. By achieving complete or near-complete automation, low-quality operations such as laying out the prepreg and transferring the material between stations will be eliminated.[45]

2.3.1a. Filament Winding. Continuous filament winding is one of the most commonly used methods for continuous composite processing. There are a number of advantages associated with filament winding including: repetitive placement of fibers, ability to use continuous fibers over an entire part without forming any joints, high degrees of fiber loading, elimination of expensive autoclaves.[49] Unfortunately, the complexity of parts produced using filament winding is limited and the surface of the cured composite is typically not finish quality.[49] There are three methods used to unite the binder and reinforcing phases of filament winding processes: preimpregnation (prepreg), wet rerolled prepreg, and wet winding.

Prepregs are systems where the binder phase has been added to the reinforcement phase and gelled to an intermediate stage before cure. This is the most expensive filament winding method and must be cured at elevated temperatures, however it is also the cleanest method and provides the best control of resin content and product quality. In direct contrast to prepregs, wet winding involves addition of the resin to the reinforcement *at the time of winding*.[49] While this results in poor control of resin content and product quality, it is the least expensive winding process and can be used with the

widest variety of fibers available to filament winding.[49] Wet rerolled prepregs lie somewhere between prepregs and wet winding. This process involves a combination of preimpregnation and wet winding. Thus it is less expensive than prepregs and provides better control over resin content and product quality than wet winding.[49] In general, filament winding is a favorable alternative to many composite processing methods because it effectively couples expensive fibers with inexpensive resins to produce relatively inexpensive composites.

2.3.1b. Resin Transfer Molding. Resin transfer molding (RTM) is a composites fabrication technique in which a reactive resin is injected into a closed mold containing a preplaced fiber mat, or preform. The fact that the dry reinforcement and resin are combined within the mold distinguishes RTM from other liquid molding processes. The curing of the resin (typically a thermoset) results in the formation of a fiber reinforced composite which assumes the shape of the mold. Unlike well-developed processing techniques such as hand lay-up, compression molding, and non-structural injection molding, RTM is relatively new and undeveloped.[47] However, RTM offers important advantages since it is considerably less labor-intensive than hand lay-up methods, and may be used to produce more complex reinforced composites than compression molding or injection molding. For these reasons, RTM has already established itself as a viable cost-effective alternative for the production of complex parts in quantities too large to justify hand lay-up, and the production of less complex parts in quantities too small to justify the capital costs associated with compression molding.[50] As RTM is developed it will undoubtedly expand further into both processing domains.

Examples of the tremendous promise of RTM for composite fabrication in the automobile industry were recently provided by Johnson[50] and Chavka and Johnson.[51] These authors describe the production of complex composite support structures for the Ford Escort and the Ford Aerostar, respectively, by HSRTM of a vinyl ester resin with glass fiber preforms. In the former case, two composite parts can replace a 90 piece steel structure with substantial weight savings and improved stiffness and strength. Production cycle times for mass production were projected to be in the 6 to 9 minute range. However it was concluded that mold filling, heat transfer, and gelation of resin in the transfer lines are all issues that must be resolved before the process may be successfully used in medium or large scale production.

Although it is a versatile method capable of producing composites of increasing complexity, RTM is not without limitations or problems. For example, RTM processing methods are complicated by the fact that the resin begins to cure *before* entering the mold. In order to produce acceptable products, the resin must meet some rather stringent requirements. The curing resin should exhibit a moderate viscosity plateau of 0.1 to 0.5 Pa · s (1 - 5 poise) for 20 seconds while flowing into the mold, but should cure rapidly once the mold has been completely filled. RTM has already found extensive application for low volume production of a variety of specialty products,[47] however further developments are required in order to reach high volume RTM production for many composite applications. A considerable challenge exists in meeting the two fundamental requirements of mass production: low cost and high speed. The fact that a curing resin enters the mold makes meeting *both* of these requirements extremely difficult. In general, RTM processes are operated at relatively high mold pressures to reduce the overall cycle

time of the process. While this is an effective method for obtaining more rapid cure rates, it inevitably results in increased costs because the process requires more expensive pumping systems to increase the flow rate and more expensive, stronger molds to withstand the increased pressure.

Many technical problems associated with resin transfer molding arise during mold filling. The problem of mold filling is very complicated since a reacting liquid is being forced through a porous medium (the preform). As the liquid reacts it becomes more viscous (actually viscoelastic). Thermoset systems typically exhibit a tremendous increase in viscosity as they cure due to branching and crosslinking in the system. Due to the moderately high initial (uncured) resin viscosities which only increase during reaction, most current RTM processes exhibit significant mold filling problems associated with high operating pressures required to fill the mold and poor resin impregnation into the fibers. Moreover, preform displacement and/or compression often occurs as the curing resin flows into the mold. Preform displacement is an extremely significant problem in the sense that it undermines a major advantage of RTM: precise control over fiber placement. A final occurrence which can cause considerable delay and downtime is gelation of the resin in the transfer lines before they enter the mold.

In addition to the mold filling problems discussed above, further complications arise from the facts that the mold geometry may be highly irregular and the process is typically not isothermal. Furthermore, it has been found that it is important to differentiate flow on the microscale (within a fiber bundle) from flow on a macroscale (between fiber bundles). It is suggested[52] that micro-flow improves the wetting and the bonding at the fiber-matrix interface, and therefore improves the strength of the final

composite. The importance of the micro-flow was underscored by Patel *et al.*,[52] who found that the best composite properties were under low-pressure conditions in which the mold filled slowly, allowing ample time for micro-flow within the fiber bundles. The time required for micro-flow depends upon the viscosity of the penetrating fluid, but may be on the order of hours for large parts using commercial resins. There are a large number of studies dealing with the problem of mold filling on the macro- and microscales,[53,54] under isothermal and non-isothermal conditions,[55,56] accounting for compression of preforms,[57] and for the viscoelastic behavior of the resin.[58]

In general, many RTM limitations in high volume production arise from the fact that the resin system begins to react before it enters the mold, thereby creating high viscosities, high operating pressures, poor "wet out," and preform displacement. Additionally, attempts to decrease the cycle time by increasing the operating pressure to accommodate faster reactions may actually decrease the quality of the composite by allowing insufficient time for micro-flow. Finally, the high capital costs associated with higher operating pressures create an inevitable trade-off between high speed and low cost under the current technology.

2.3.1c. Reaction Injection Molding. Reaction injection molding (RIM) and compression molding processes are used for molding polyurethanes, epoxies and other liquid systems. In general, injection molding processes involve two to four component systems that are mixed using some type of high-pressure, impingement-mixing technique. In a typical RIM process the fluid is forced into a *closed* mold. This is the fundamental difference between RIM and compression molding, where the resin fills an *open* mold

which is then forcibly closed.[59] Both RIM and compression molding can be readily automated, although RIM is a superior alternative to compression molding for the production of detailed parts. Injection molding processes are categorized as thermosets or thermoplastics based on the resin being cured. Thermosets are typically injected into a warm mold where the resin undergoes further polymerization or crosslinking to produce a solid polymer while thermoplastic resins are first melted, then placed in a relatively cool mold which allows the material to solidify and take the shape of the mold before removal.[59] It has been stated that compression molding is the most developed method in terms of its ability to incorporate continuous or chopped fibers into structural composites, however some compression molding processes involving regions of high fluid flow rates may result in orientation of fiber in the direction of fluid flow.[60] This can be an advantage if oriented fibers are desired because flow patterns could be studied and developed in such a manner to achieve this effect.[60]

Unlike compression molding, RIM is not used to produce structural composites. However, processing methods based on variations of reaction injection molding are currently used to produce composites. These methods have been classified[50] as i) vacuum-assisted resin injection (VRIM), ii) structural reaction injection molding (SRIM), and iii) high speed resin transfer molding (HSRTM). These methods are essentially classified according to the pressure used to inject the resin, and the time required to fill the mold. VRIM uses very low mold pressures and very long fill times with cycle times approaching hours or days. Therefore relatively inexpensive molds may be used and slow curing resins are required. SRIM uses more reactive resins and higher mold pressures approaching 50 to 100 psi. Typically two highly reactive resins are held in separate

holding tanks before injection, and are impingement mixed immediately before entering the mold. The resin flows into the mold and "wets out" the preform while the reaction is occurring. HSRTM is similar to SRIM except that higher mold pressures are used (100 - 500 psi), resulting in faster filling times; and the mold is maintained at elevated temperatures to minimize cure times. HSRTM typically requires stronger and more expensive metallic molds and has relatively short cycle times on the order of 1 to 10 minutes.

2.3.1d. Hand Lay-up. Hand lay-up is used in the production of highly detailed composites, where the complexity of the part eliminates the possibility of molding; and specialty composites in which the cost of setting up a molding process becomes prohibitive. In either case, hand lay-up methods play an important role in the production of composites. Hand lay-up has the advantages of great part complexity, precise placement of the fiber reinforcement, the ability to allow time for superior micro-flow, and production of finish-quality products in a single step. Unfortunately, each of these advantages come at the expensive of time and are highly labor-intensive. Composites produced by hand lay-up methods are very expensive because their production is highly labor-intensive and time-consuming. An additional disadvantage of hand lay-up is the fact that it can not be used for large-scale production. However hand lay-up methods are still the state of the art for producing highly complex, specialty composites.

2.3.2. Materials used in the Fabrication of Composites

Choosing a combination of reinforcing materials and binder matrices is indeed a daunting task. The availability of materials which may be incorporated into the design of a composite are so vast that a task as simplistic in theory as selecting materials for the eventual composite design is in fact highly involved in practice. Recent developments in the areas of fiber technology and resin formulation have only served to exacerbate this situation. This section should not be thought of as a comprehensive review of all materials available for composite design, rather it should serve as an illustrative guide as to the wide range of materials which are currently being used in the design and fabrication of composites.

Materials that are used as the binder phase for composites are selected for a variety of reasons such as chemical resistance, heat resistance, cost, and general purpose (or overall properties of the material). The ability to be used as an all-purpose binder phase make polyester and vinyl ester resins the most commonly used resins in the production of composites.[61] There are, however, a great number of alternatives to these resins which afford tremendous flexibility in designing a composite for a specific application. For example, epoxy resins provide a broad range of physical properties which make them possibly the most flexible alternative for a variety of high-performance applications while polyimide resins are particularly well-suited for composites designed for high temperature applications.[62,63] *Figure 2.4* is a schematic (adapted from ref. 64) which provides a qualitative comparison of some physical properties for a number of polymeric resins.

In general, the polymeric resin serves the role of matrix material while the reinforcing material defines the overall performance of the composite. Scientists are constantly investigating new reinforcing materials or modifying existing fibers to meet the ever-increasing demand for better, cheaper, lighter composites. While current state of the art reinforcing fibers may be made out of E-glass, S-glass, aramid, silicon carbide, boron, alumina, fused silica, alumina-boria silica, or carbon graphite, the technology is still evolving. A list of a few well-developed resin/filler systems is shown in Table 2.1 (adapted from ref. 64). Rosato[64] provides a far more comprehensive description of both resins and filler materials as well as the strengths and weaknesses of numerous materials/composite formulations in his review.

Table 2.1. Compatibility of polymeric resins with reinforcement materials.

	Alumina	**Calcium Carbonate**	**Carbon Black**	**Clay**	**Glass Fibers**	**Quartz**	**Talc**
Alkyds	NO	YES	NO	YES	YES	NO	YES
DAP	NO	YES	NO	YES	YES	NO	YES
Epoxy	YES	YES	YES	YES	YES	YES	NO
Phenolic	YES	YES	YES	YES	YES	N	YES
Polyester	NO	YES	NO	YES	YES	NO	NO
Silicone	YES	YES	YES	NO	YES	YES	NO
Urethane	YES	YES	YES	YES	YES	YES	NO

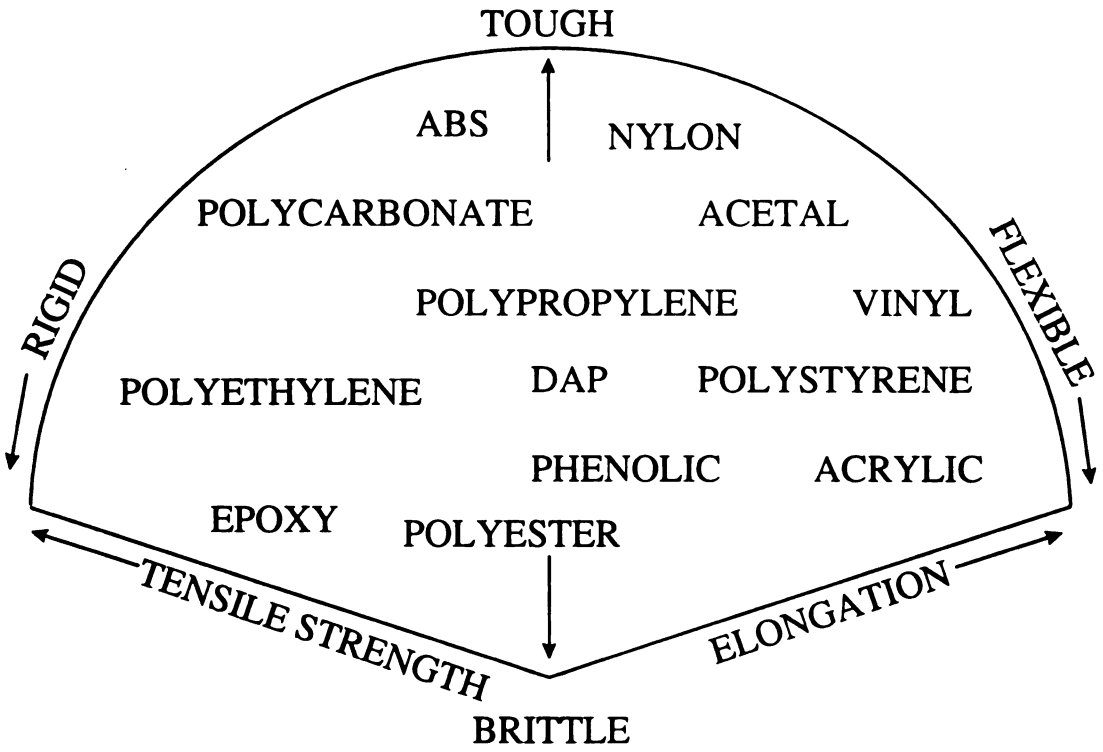

Figure 2.4. Diagram of physical properties for a number of commonly-used polymeric resins.

2.4. References

1. W.H. Carothers, *J. Am. Chem. Soc.*, **51**, 2548 (1929).

2. P.J. Flory, *Principles of Polymer Chemistry*, Cornell University Press, Ithaca, NY, 1953.

3. A. Rudin, *Elements of Polymer Science and Engineering*, Academic Press, New York, NY, 1982.

4. G. Odian, *Principles of Polymerization*, 3rd edition, Wiley & Sons, New York, NY, 1992.

5. J.P. Kennedy, E. Marechal, *Carbocationic Polymerization*, Wiley & Sons, New York, NY, 1982.

6. J. Crivello, "Triarylsulfonium salts as photoinitiators of free radical and cationic polymerization," *J. Polym. Sci., Polym. Letters*, **17**, 759 (1979).

7. S.P. Lapin, "Radiation-induced cationic curing of vinyl-ether-functionalized urethane oligomers," *Radiation Curing of Polymeric Materials*, C.E. Hoyle, J.F. Kinstle, Eds., ACS Symposium Series 417, ACS, Washington, DC, 363 (1989).

8. A.D. Wilson, S. Crisp, H.J. Prosser, B.G. Lewis, S.A. Merson, "Aluminosilicate glasses for polyelectrolyte cements," *Ind. Eng. Chem. Prod. Res. Dev.*, **19**, 263 (1980).

9. E.A. Wasson, J.W. Nicholson, "New aspects of the setting of glass-ionomer cements," *J. Dent. Res.*, **72**, 481 (1983).

10. W. Michaeli, E. Krampe, M. Langen, *Kunst. Plast. Eur.*, **84**, 9 (1994).

11. J.P. Fouassier, S.K. Wu, *J. Appl. Polym. Sci.*, **44**, 1779 (1992).

12. W. Radak, "Radiation Curing: New Market Rx," *Chemical Business*, October 1990.

13. T. Yamaoka, Y.-C. Zhang, K. Koseki, *J. Appl. Polym. Sci.*, **38**, 1271 (1989).

14. D.C. Neckers, O. Valdes-Aguilera, K.S. Raghuveer, D.G. Watson, "Production of Three-Dimensional Bodies by Photopolymerization," *U.S. Patent No. 5,137,800*, Issued August 11, 1992.

15. G. Oster, N.-L. Yang, *Chem. Rev.*, **68**, 125 (1968).

16. S.P. Pappas in "Encyclopedia of Polymer Science and Engineering," **11**, H.F. Mark, N.M. Bikales, C.G. Overberger, G. Menges, Eds., Wiley-Interscience, New York, 186 (1988).

17. L. Angiolini, D. Caretti, C. Carlini, E. Corelli, P.A. Rolla, "Polymeric photoinitiators having benzoin methyl ether moieties connected to the main chain by the benzoyl group and their activity for ultra-violet curable coatings," *Polymer*, **35**, 5413 (1994).

18. M. Zheng, M. Yang, S. Liu, L. Zhang, "Photopolymerization of propargyl acetate with Michler's ketone as photoinitiator," *Chin. J. Polym. Sci.*, **13**, 74 (1995).

19. B. Glad, K. Irgum, P. Horstedt, "Photopolymerization and characterization of methacrylate-based reactive composite membranes," *J. Membrane Sci.*, **100**, 171 (1995).

20. R. Mallavia, F. Amat-Guerri, A. Fimia, R. Sastre, "Synthesis and evaluation as a visible-light polymerization photoinitiator of a new eosin ester with an *O*-benzoyl-α-oxooxime group," *Macromolecules*, **27**, 2643 (1994).

21. J.L. Mateo, P. Bosch, A.E. Lozano, "Reactivity of radicals derived from dimethylanilines in acrylic photopolymerization," *Macromolecules*, **27**, 7794 (1994).

22. A. Ledwith, *J. Oil Col. Chem. Assoc.*, **59**, 157 (1976).

23. A. Ledwith, *Pure Appl. Chem.*, **49**, 431 (1977).

24. N.T. Lipscomb, Y. Tarshiani, "Kinetics and mechanism of the benzoin isobutyl ether photoinitiated polymerization of styrene," *J. Polym. Sci. Polym. Chem. Ed.*, **26**, 529 (1988).

25. M.V. Encinas, J. Garrido, E.A. Lissi, "Polymerization photoinitiated by carbonyl compounds. VIII. Solvent and photoinitiator concentration effects," *J. Polym. Sci. Polym. Chem. Ed.*, **27**, 139 (1989).

26. M.V. Encinas, C. Majmud, J. Garrido, E.A. Lissi, "Methyl methacrylate polymerization photoinitiated by pyrene in the presence of triethylamine," *Macromolecules*, **22**, 563 (1989).

27. G. Jiang, Y. Shirota, H. Mikawa, *Polym. Photochem.*, **7**, 311 (1986).

28. C.E. Hoyle, M. Keel, K.-J. Kim, "Photopolymerization of 1,6-hexanediol diacrylate: the effect of functionalized amines," *Polymer*, **29**, 18 (1988).

29. G. Seretoudi, I. Sideridou, " Benzil/N,N-dimethylaminoethyl methacrylate system as photoinitiator for methyl methacrylate polymerization," *J.M.S. - Pure Appl. Chem.*, **A32(6)**, 1183 (1995).

30. L. Angiolini, D. Caretti, C. Carlini, N. Lelli, P.A. Rolla, "Polymeric photoinitiators bearing side-chain acyldiphenylphosphinoxide moieties for UV surface coatings," *J. Appl. Polym. Sci.*, **48**, 1163 (1993).

31. T. Kimura, M. Kajiwara, "The synthesis of phosphinylphosphorimidic hydroxyethyl acrylate and the electrical properties of its polymer produced by ultraviolet-irradiation-induced polymerization," *Polymer*, **36**, 713 (1995).

32. T. Sumiyoshi, W. Schnabel, "On the reactivity of phosphonyl radicals towards olefinic compounds," *Makromol. Chem.*, **186**, 1811 (1985).

33. J.C. Scaiano, "Photochemical and free-radical processes in benzil-amine systems. Electron-donor properties of α-aminoalkyl radicals," *J. Phys. Chem.*, **85**, 2851 (1981).

34. J.V. Crivello, J.L. Lee, D.A. Conlon, "New monomers for cationic UV-curing," *Society of Manufacturing Engineers*, **4**, 28 (1982).

35. J.V. Crivello, "Photoinitiated cationic polymerization of coatings," *Organic Coatings, Science and Technology*, **Vol. 5**, G.D. Parfitt, A.V. Patsis, Eds., Marcel Dekker Inc., New York, NY, 35 (1983).

36. J.V. Crivello, D.A. Conlon, "Aromatic bisvinyl ethers: a new class of highly reactive thermosetting monomers," *J. Polym. Sci., Polym. Chem.*, **21**, 1785 (1983).

37. J.V. Crivello, J.L. Lee, D.A. Conlon, "Photoinitiated cationic polymerization with multifunctional vinyl ether monomers," *J. Rad. Cur.*, **10**, 6 (1983).

38. J.V. Crivello, "Cationic polymerization - iodonium and sulfonium salt photoinitiators," *Adv. Polym. Sci.*, **62**, 1 (1984).

39. J.V. Crivello, "Recent progress in the design of new photoinitiators for cationic photopolymerization," *Cationic Polymerization and Related Processes*, E.J. Goethals, Ed., IUPAC, Oxford, UK, 289 (1984).

40. J.V. Crivello, D.A. Conlon, D.R. Olson, K.K. Webb, "Accelerators in UV cationic polymerization," *Polym. Paint Colour J.*, **178**, 696 (1988).

41. J.V. Crivello, J.L Lee, "Alkoxy-substituted diaryliodonium salt cationic photoinitiators," *J. Polym. Sci., Polym. Chem.*, **27**, 3951 (1989).

42. G. Manivannan, J.P. Fouassier, "Primary processes in the photosensitized polymerization of cationic monomers," *J. Polym. Sci., Polym. Chem.*, **29**, 1113 (1991).

43. J. Pelgrims, "Cationic UV polymerization of cyracure cycloaliphatic epoxies," *Pigment and Resin Technology*, 5, September, 1987.

44. E. W. Nelson, T. P. Carter, A. B. Scranton, "The role of the triplet state in the photosensitization of cationic polymerizations by anthracene," *J. Polym. Sci., Polym. Chem.*, **33**, 247 (1995).

45. T.J. Reinhart, L.L. Clements, "Introduction to composites," in *Composites*, **Vol. 1**, ASM International, Metals Park, OH, 27 (1987).

46. Z.D. Jastrzebski, *The Nature and Properties of Engineering Materials*, 2nd edition, Wiley & Sons, New York, NY, 1976.

47. P. Beardmore, "Manufacturing processes: consumer products," in *Composites*, **Vol. 1**, ASM International, Metals Park, OH, 554 (1987).

48. A.B. Strong, "Molding," in *International Encyclopedia of Composites*, **Vol. 3**, S.M. Lee, ed., VCH, New York, NY, 420 (1990).

49. S.T. Peters, W.D. Humphrey, "Filament winding," in *Composites*, **Vol. 1**, ASM International, Metals Park, OH, 503 (1987).

50. C.F. Johnson, "Resin Transfer Molding," in *Composites*, **Vol. 1**, ASM International, Metals Park, OH, 564 (1987).

51. N.G. Chavka, C.F. Johnson, "The Taming of Liquid Composite Molding for Automotive Applications," *Advanced Composite Materials*, New Developments and Applications, Conference Proceedings, Detroit, MI, 115 (1991).

52. N. Patel, M.J. Perry and L.J. Lee, "Influence of RTM and SRIM Processing Parameters on Molding Mechanical Properties," *Advanced Composite Materials*, New Developments and Applications, Conference Proceedings, Detroit, Michigan, 105 (1991).

53. A.W. Chan and R.J. Morgan, "Modeling Preform Impregnation and Void Formation in Resin Transfer Molding of Unidirectional Composites," *SAMPE Quarterly*, **23(3)**, 48 (1992).

54. F.R. Phelan, "Modeling of Microscale Flow in Fibrous Porous Media," *Advanced Composite Materials*, New Developments and Applications, Conference Proceedings, Detroit, MI, 175 (1991).

55. M.J. Owen, C.D. Rudd and K.N. Kendal, "Modeling the Resin Transfer Molding Process," *Advanced Composite Materials*, New Developments and Applications, Conference Proceedings, Detroit, MI, 187 (1991).

56. A. Bruno, G. Mollna, G. Bertacchi, A. Moroni, "Flow Behavior in Resin Transfer Molding: Numerical Simulations," *Advanced Composite Materials*, New Developments and Applications, Conference Proceedings, Detroit, MI, 149 (1991).

57. A.C. Loos and M.H. Weldeman, "RTM Process Modeling for Advanced Fiber Architecture," *Advanced Composite Materials*, New Developments and Applications, Conference Proceedings, Detroit, MI, 209 (1991).

58. K. Jayaraman and C.N. Satyadev, "The Role of Fluid Rheology in Resin Transfer Molding," *Advanced Composite Materials*, New Developments and Applications, Conference Proceedings, Detroit, MI, 225 (1991).

59. A.D. Murray, "Injection Molding," in *Composites*, **Vol. 1**, ASM International, Metals Park, OH, 555 (1987).

60. C.F. Johnson, "Compression molding," in *Composites*, **Vol. 1**, ASM International, Metals Park, OH, 559 (1987).

61. I.H. Updegraff, "Unsaturated polyester resins," in *Handbook of Composites*, G. Lubin, Ed., Van Nostrand Reinhold, New York, NY, 17 (1982).

62. C.A. May, "Epoxy resins," in *Composites*, **Vol. 1**, ASM International, Metals Park, OH, 66 (1987).

63. D.A. Scola, "Polyimide resins," in *Composites*, **Vol. 1**, ASM International, Metals Park, OH, 78 (1987).

64. D.V. Rosato, "Materials selection, polymeric matrix composites," in *International Encyclopedia of Composites*, **Vol. 3**, S.M. Lee, ed., VCH, New York, NY, 148 (1990).

CHAPTER 3.

RESEARCH OBJECTIVES

The preceding chapters illustrate many of the advantages afforded by photopolymerizations. Although they have been well-characterized and used extensively for the production of thin films and coatings, few attempts have been made to incorporate photopolymerizations into the production of thick polymers and/or composites. It is difficult to hypothesize why the domain of photopolymerizations has not been expanded to include these products, however there are at least two potential explanations for the lack of research in the area: the importance of the initiation step in the overall reaction mechanism has been overlooked and is therefore not completely understood; and there are a number of logistical problems associated with light intensity gradients and light scattering throughout the sample which make it difficult to photopolymerize in three dimensions. While chain polymerizations propagate and terminate in the same manner once an active site has been produced, the initiation reaction is specific to the initiating source be it heat, light, microwave, or ultrasonic frequency. Thus it is extremely important in a photopolymerization to be able to predict with some degree of certainty what exactly is occurring in the initiation step(s) and what is its significance. However, this is easier said than done, since it can be difficult to characterize the products of a polymerization *in situ*, which makes it difficult to understand their relative importance in

the overall reaction. In addition, the fact that the existence of severe light intensity gradients in thicker systems has been well-established may serve as a major deterrent when trying to convince one of the possibility of using photopolymerizations for the production of thick or composite structures.

The general objective of this research project has been to verify the applicability of photopolymerizations for the high-speed, low-cost production of thick polymers and composites by developing novel polymerization strategies based on ultraviolet photoinitiation methods for uniform cure in three dimensions. Specific objectives of this research were: i) to develop a set of guidelines which would predict whether or not a particular photoinitiator (or class of initiators) could be used in the production of three-dimensional polymers; ii) to thoroughly characterize the initiation step of free-radical and cationic photopolymerizations which could provide an explanation for why some systems are susceptible to three-dimensional polymerization while other formulations fail to polymerize in thick or 3-D geometries; iii) to determine an optimal initiator concentration and formulation for a representative system including photoinitiator, photosensitizer and thermal initiator which can be used to demonstrate how photopolymerizations afford control over the general kinetics of the polymerization reaction as well as how minute alterations in the initiation mechanism affect the entire polymerization; iv) characterization of the mechanical properties of the composites cured using the novel methods which would provide experimental evidence as to the potential of photopolymerizations as a method for the production of high-performance composites; v) determine the effects of a number of processing conditions on the kinetic and mechanical properties of the cured polymers and composites.

CHAPTER 4.

DEVELOPMENT OF THE THICK PHOTOINITIATION STRATEGIES: FUNDAMENTAL EXPERIMENTS

4.1. Introduction

A great number of compounds have been studied as initiators for free radical photopolymerizations.[1-12] Benzoin ethers are the most commonly used class of these compounds, and their use as free-radical photoinitiators has been well-documented.[7-9] There are a number of advantages associated with photopolymerizations that make them a practical alternative to current methods for industrial applications. Included among these advantages are excellent spatial and temporal control over the reaction and superior energy efficiency. These and other advantages are largely responsible for the rapid growth rate of photopolymerizations, roughly 20-30% per year, for industrial applications. This growth rate is even more significant when one takes into consideration the fact that the majority of applications for photopolymerizations have focused on thin systems, thus targeting only a small portion of the polymer industry.

Although photopolymerizations are used in a number of applications involving thin films, inks, coatings and electronics, their development for thick polymers and polymeric composites has basically been restricted to a few specialty applications that utilize techniques such as photolithography and screen printing.[13-15] While

photolithography is an excellent method for creating detailed polymeric structures, its industrial usage is largely restricted to the production of prototypes and electronics applications such as printed copper circuitry and replication of optical disks due to the fact that the products typically have relatively low mechanical and physical properties.

One industry where it is common practice to use photopolymerizations to produce composites is the dental industry. Photocurable dental composites based on acrylate resins have been used for years as long-term fillings for teeth that have been damaged by cavities or other dental problems. This process demonstrates both the flexibility and the spatial and temporal control afforded by photopolymerizations. This application, while it is an excellent example of the potential of photopolymerizations for the production of composites, differs from the research conducted in this project in at least two areas. First, it uses point focused light sources (lasers) to cure the sample whereas the light sources used in this research were less expensive arc lamps and other sources which produce light over a much larger wavelength range at a sacrifice of intensity at any given wavelength. Second, the method of cure is based on "overexposing" the reactive resin (using enough light so that even with losses due to absorption, a sufficient amount of light is able to penetrate through the bulk of the sample) with initiating light, which can be done in this case because the thickness of samples is relatively limited (less than 1 cm).

Alternatives to current photoinitiator systems have coupled some of the traditional photoinitiators with well-known hydrogen donors such as tertiary amines in an attempt to accelerate the polymerization process.[16,17] While these efforts have proven to be effective in thin-system photopolymerizations,[17] the presence of tertiary amines may in fact inhibit efforts to photopolymerize thicker systems. The possible interference of certain

accelerators in thick systems coupled with the fact that severe light intensity gradients initially exist in thick samples are likely responsible for the general consensus in the scientific community that photopolymerizations cannot be employed to cure thick polymers.[18] However, detailed investigations of common photoinitiator systems have revealed that it is in fact possible to use photopolymerizations to produce thick polymers and composites if every component of the reactive system is chosen judiciously.

In this chapter, two strategies for photocuring thick polymers and composite structures in relatively short cycle times using moderate light sources are presented. In the first strategy, samples in excess of two centimeters have been polymerized using relatively low intensity light sources (less than 1 mW/cm^2) by carefully selecting the initiator (both formulation and concentration) and the incident wavelength. The second strategy capitalizes on the fact that the polymerization reactions are highly exothermic by using the heat generated by polymerization to "kick off" a second reaction where a thermal initiator undergoes some type of dissociation reaction which results in the generation of additional active sites. In essence, the heat caused by the photopolymerization causes the thermal initiator to dissociate, and radicals are produced concurrently by thermal and photoinitiation, allowing for more complete cure, especially in partially opaque systems or complex geometries where it is difficult or impossible for the incident light to reach the sample in every corner or crevice of the mold.

4.1.1. Self-Eliminating Light Intensity Gradients

By carefully selecting the initiator formulation and concentration along with the initiating wavelength and intensity, vinyl ester polymers as thick as 3-4 cm can be cured

in relatively short cycle times (ranging from 2 - 7 minutes) depending on the light source. These polymerizations have been possible due to the existence of a light intensity gradient that is "self-eliminating". In these systems, a compound absorbs light at a particular wavelength and is excited to a higher energy state before reacting to produce an active site (either a cation, radical or anion). A result of this reaction is the production of a compound which no longer absorbs light at the initiating wavelength, thereby allowing incident light to penetrate into the bulk of the sample. In short, the light which is initially absorbed at or near the surface of the system and thus responsible for any light intensity gradients in this system is also responsible for initiating the reaction to produce active sites, which results in a substantial decrease in the light intensity gradient in the system, thus the system can be described as "self-eliminating". The idea of a decreasing light intensity gradient has been discussed in previous literature,[19] however the decay is attributed to "photobleaching". It can be argued that a self-eliminating gradient is simply a photobleaching effect. However, the term photobleaching is a generic statement for all events, chemical or otherwise, which result in a decrease such as the one that occurs in self-eliminating systems. What distinguishes this type of system from other photobleaching effects is that it can be specifically attributed to a chemical reaction; and in direct contrast to other photobleaching effects,[19] it is a very efficient method of photobleaching. While this effect may not occur in all photoinitiating systems, a set of loose guidelines to determine which systems will likely exhibit this self-eliminating characteristic has been developed.

The characteristic of a self-eliminating gradient is likely to be found in systems which contain initiators (photoinitiator, photosensitizer, or co-initiator) with the

following characteristics. The initiator system should consist of at least two aromatic rings which are either conjugated or otherwise coupled in such a manner that the resulting molecule has a considerable or continuous pi-electronic structure. This excess of pi electrons, in this highly coupled aromatic structure, enables the molecule to absorb light in the ultraviolet or near ultraviolet region of the spectrum. Upon irradiation, the excited state of this molecule should initiate either a free radical or an ionic polymerization reaction by some type of electron transfer or dissociation process. The resulting initiator molecule should lose its characteristic absorbance in the near-UV region of the spectrum, due to the loss of the coupled aromatic pi structure. If a compound maintains its general structure even after it has reacted to produce a radical, its characteristic absorbance could remain largely unchanged. In such situations, the light intensity gradient would not be sufficiently reduced even after long periods of irradiation. Hence the reacted initiator would continue to absorb initiating light, thus limiting the absorption and subsequent reaction of initiators in the bulk of the sample.

As stated earlier, the success of any photocurable system is highly dependent on the initiator formulation. An example of this is an initiator system consisting of BEE and a tertiary amine (tributylamine, TBA). While TBA and other compounds have been successfully employed as accelerators for thin photocurable systems,[17,18,20-23] experiments performed during the course of this research have shown that in fact some hydrogen donors have a negative, inhibiting effect on the polymerization reaction when thicker systems are photocured.

The addition of a tertiary amine will likely promote hydrogen abstraction as the dominant method for producing radicals as opposed to fragmentation. H^+ abstraction is

typically more efficient than fragmentation and thus serves to enhance cure in thin systems, however radicals produced via H^+ abstraction maintain a structure very similar to that of the unreacted initiator (see *Figure 4.1, a-b*), thus they may continue to absorb incident light appreciably. In this instance the light intensity gradient is not significantly eliminated and the incident light is not able to effectively penetrate the bulk of the sample, thereby limiting the depth of polymerization. However, when BEE fragments to produce active radicals, its structure is altered drastically (*Figure 4.1c*) and its absorbance of the initiating light decreases almost completely. In this instance, light is able to penetrate deeper into the system allowing for more uniform and deeper polymerization in the bulk of the sample.

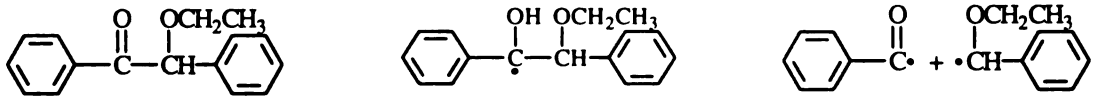

a) Benzoin ethyl ether

b) BEE radical produced via H^+ abstraction

c) BEE radicals produced via fragmentation

Figure 4.1. Benzoin ethyl ether photoinitiator (a) and corresponding radicals produced via H^+ abstraction (b) and fragmentation (c).

This research has focused not on developing novel photoinitiators but on thoroughly characterizing commonly used photoinitiators and initiator formulations to determine if they have any utility for photocuring thick polymeric systems. To this end, a number of well-reported radical photoinitiator formulations have been investigated, including: camphorquinone / triethylamine;[5] several benzoin ethers such as benzoin methyl ether (BME), benzophenone and benzoin ethyl ether (BEE);[7-9] and 2-benzyl-2-

(dimethylamino)-1-[4-(4-morpholinyl)phenyl]-1-butanone and α,α-dimethoxy-α-phenyl-acetophenone, marketed by Ciba-Geigy (Hawthorne, NY) under the names Irgacure 639 and Irgacure 651, respectively. However, the bulk of this research has focused on photoinitation based on benzoin ether initiator formulations, and this will be reflected in the results presented in this chapter.

4.1.2. Photo/Thermal Initiation Mechanism

Addition of a thermal initiator to the reactive formulation can greatly enhance the degree of cure in systems where the sample is largely opaque such as a composite with a high degree of fiber loading. This initiating mechanism capitalizes on the highly exothermic nature of these systems by using a photoinitiator to initiate reaction at or near the surface of the sample and "using" the heat generated by this reaction to cause some type of dissociation reaction involving a second, thermal initiator which is then capable of creating active sites in areas where light may not be able to sufficiently penetrate the system.

This initiating method is favorable to traditional, thermally-cured systems because it is more energy-efficient, highly targeted, and can be initiated at or near room temperature. The thermal initiator should not absorb the initiating light as it is far less likely to exhibit self-eliminating characteristics than the photoinitiator. Additionally, the thermal initiator should be susceptible to rapid dissociation at relatively moderate temperatures (80 - 100°C). As our results will show, the observed effect of a thermal initiator such as benzoyl peroxide (BP) on the mechanical properties of cured polymers can be dramatic.

4.2. Experimental

Benzoin methyl ether (BME), benzoin ethyl ether (BEE), benzil, benzophenone, camphorquinone, tributylamine (TBA), Eosin B, anthracene, 9,10-diphenylanthracene, 9,10-dihyroanthracene and 9-phenylanthracene were obtained from Aldrich (Milwaukee, WI). Benzoyl peroxide (BP) was obtained from Polysciences (Warrington, PA). Irgacure 639 and 651 were obtained from Ciba-Geigy (Hawthorne, NY). Derakane resins 470-45, 411c-50 and 441-400 were obtained from Dow Chemical (Midland, MI). The cationic photoinitiator UV9310C (GE Silicones, Schenectady, NY) had a composition of 5-10 wt% linear alkylate dodecylbenzene, ~50 wt% 2-ethyl-1,3-hexanediol, and ~50 wt% bis(4-dodecyclphenyl)iodoniumhexafluoroantimonate. Cationic initiator concentrations specified in the remainder of this chapter correspond to the overall UV9310C concentration. 3,6,9,12-tetraoxatetradeca-1,13-diene (DVE-3) (GAF Chemicals Corp.) was also used as a cationic monomer. All materials were used without further purification.

Absorption Experiments. UV-Vis absorption experiments were conducted in a Hewlett-Packard Diode Array Spectrophotometer (Model 8452A). Hexanol was used as the solvent unless otherwise specified. Absorbance decay experiments were conducted by irradiating samples in a quartz cuvette for a predetermined amount of time before mixing the sample and placing it in the spectrometer to measure the absorbance. By mixing the sample, an average absorbance for the entire sample is collected.

Irradiating Light Sources. The primary light source for this research was a 1000 watt Hg(Xe) arc lamp (model 6293) produced by Oriel Corporation (Stratford, CT). The light source was fitted with a water filter obtained from Oriel Corporation to eliminate

infrared (IR) light and reduce thermal effects. The filter was attached to a circulating water bath to maintain constant temperature in the filter so as to avoid possible effects caused by evaporation of water inside the filter during reaction. Additional light sources included a 200 watt Hg(Xe) arc lamp (model 6291), also produced by Oriel Corporation, and a 100 watt Black-Ray long wave UV lamp (model B100AP) produced by UVP (San Gabriel, CA). A hand-held UV meter designed by UVP was used to monitor the incident intensity to insure that it remained constant for given sets of experiments.

Monitoring Thickness of Photocured Samples. A method was devised for measuring polymer thickness that consisted of placing 5 gram samples in a glass cylinder (1 cm inner diameter). The sample was then placed in an enclosure in such a manner that it could only be irradiated from light entering the enclosure through a circle having a cross-sectional area approximately equal to that of the glass cylinder. This setup guaranteed that light could only penetrate the sample from a single direction, thus insuring that only one surface of the sample would be directly exposed to initiating light throughout the course of the polymerization.

4.3. Optimizing the Initiator Formulation

4.3.1. Developing an Operating Window

There must exist at least one region in the light spectrum where only the unreacted initiator (or sensitizer) absorbs light appreciably in order for a reactive formulation to be successfully photocured. In addition, the initiator absorbance in this region must decrease to the extent that it does not absorb appreciably after excitation and subsequent

production of radicals. Consequently, light is able to penetrate into the bulk of the sample because it becomes transparent to the initiating light once it reacts. If these criteria are met, then there is a region in the light spectrum where the polymerization can be photoinitiated without interference from species that do not participate in the initiation reaction. It should be noted that the operating window is specific to each reactive formulation, hence the existence of an operating window must be determined before a reactive formulation can be photocured in three dimensions.

4.3.1a. Radical Systems. *Figures 4.2-4.3* show an operating window for a typical vinyl ester system studied in this research including thermal and photoinitiators, monomer/resin, and initiator fragments produced by photofragmentation and hydrogen abstraction mechanisms. This system consists of an oligomer (470-45) and an initiator formulation (BEE and BP) present in a 99.6 / 0.4 ratio by weight (initiator formulation is 0.2 wt% each for BEE and BP). It should be noted that the absorbance of benzil, whose structure is essentially that of a BEE radical produced by a fragmentation reaction, does not absorb appreciably above 310 nm. *Figure 4.2* clearly shows that the only species in this system that absorbs light appreciably in the 320-360 nm region is the benzoin ether photoinitiator. *Figure 4.3* shows the absorbance spectra for BEE radicals generated via hydrogen abstraction (illustrated in *Figure 4.1b*) and photofragmentation (illustrated in *Figure 4.1c*). *Figures 4.2-4.3*, when observed together, make it abundantly clear that it should be possible to initiate the polymerization by irradiating the sample using light in this region of the spectrum. In fact, a more broad description of the operating window for a vinyl ester based system would simply be that the photoinitiator must absorb light above

310 nm. This simple strategy will prevent any light intensity gradient as a result of monomer absorption. However, absorption of light by the initiator (at the initiating wavelength) will still result in the formation of light intensity gradients, even though the initiator is present in relatively small quantities (~0.1 wt. %). A strategy for reducing or eliminating even these gradients is required for the successful photoinitiated polymerization of thick parts.

A strategy to reduce or even eliminate the light intensity gradients arising from the initiator has been developed. In most systems, light intensity gradients arise not only from the initiator molecules before they have reacted to produce active centers, but also from the residual initiator fragments after reaction. If these residual initiator fragments absorb light at substantially the same wavelengths as the unreacted initiator, the light intensity gradient will persist even after initiation of the polymerization reaction. However, if the absorbance (at the initiating wavelength(s)) of the residual initiator fragment is significantly lower than that of the parent molecule, then the light intensity gradient will disappear at a rate proportional to the rate of disappearance of parent molecules. Using this criteria, photoinitiators which become non-absorbing at the initiating wavelength upon reaction have been identified. It has been found that these initiators may be used to polymerize systems of considerable thickness since light intensity gradients that exist at the beginning of the reaction are self eliminating. Therefore these initiators allow continuously increasing light penetration in the sample, and consequently allow the relatively rapid and uniform polymerization of thick polymeric structures. In this study, three separate photoinitiator formulations were tested for the self-eliminating characteristic: benzoin ethers (BEE and BME), camphor-

quinone/TBA (abbreviated as C/TBA), and Eosin B. Benzoin ethers absorb UV light, C/TBA absorb in the UV and the visible regions, and Eosin B absorbs in the visible region of the light spectrum. Absorbance spectra for BEE and C/TBA photoinitiator formulations are shown in *Figures 4.2-4.*

To test for a self-eliminating characteristic, absorbance lifetime experiments were performed for each photoinitiator. Two of the initiators (C/TBA and BEE) exhibited marked decreases in their average absorbance the longer they were exposed to the incident light. In the case of C/TBA, the absorbance decrease occurred between 440-490 nm, while the BEE absorbance decrease took place between 320-360 nm. The wavelengths that were monitored and compared (472 nm for C/TBA and 328 nm for BEE) in *Figure 4.5* were selected because they represent the maximum initial absorbance in the decaying region. In order to directly compare the two absorbance profiles in *Figure 4.5*, the data was normalized to an initial value of one. The initial concentration for BEE was 0.2 wt% and the initiator concentration for C/TBA was 0.2/0.2 wt% camphorquinone/TBA, while the solvent for both samples was benzene. The shape of the absorbance profiles observed in *Figure 4.5* show that the average absorbance of both samples decrease exponentially as the exposure to the light source is prolonged. This can be explained by the fact that the initiator fragments do not absorb light in the operating window, hence the average absorbance of each sample decreases as more and more initiator molecules react to produce active sites. The net effect of this situation is a continuing increase in the ability of the incident light to penetrate deeper into the sample as the initiation reaction proceeds towards equilibrium. Unlike the other two formulations, the absorbance profile for Eosin B did not decrease significantly over prolonged periods of

irradiation. This led to the conclusion that Eosin B would not be as effective as either BEE or C/TBA as a photoinitiator for thick polymerizations, hence no further studies involving this compound were conducted in the course of this research.

4.3.1b. Cationic Systems. Like radical systems, cationic operating windows are dependent on the particular system being investigated. One difference between the two systems is the introduction of an additional component into the cationic system. The absorbance of the initiator in the cationic system occurs almost entirely below 300 nm, and this can cause a number of problems including more expensive optics and molds (made out of quartz), potential absorbance by the monomer or resin (which would virtually eliminate any possibility of a thick photopolymerization), and a reduction in the number of commercially available light sources. To alleviate these problems, small quantities of a compound termed a "photosensitizer" are added to the reactive mixture, making it possible to initiate polymerization in the near UV or visible region of the light spectrum. In brief, the photosensitizer absorbs near UV or visible light and is excited to a higher energy state. From this state, the photosensitizer undergoes direct interaction with the initiator to produce an active cation. Absorbance spectra for some common photosensitizers are shown in *Figure 4.6*. In addition, this figure shows the absorbance for anthracene both before and after photosensitization and makes it very clear that there is a region in the light spectrum where the reaction can be photoinitiated (340-380 nm). Because many commercially available lamps utilize mercury bulbs, anthracene is a particularly good choice as a photosensitizer for this system because mercury has strong emission peaks in the 340-380 nm region.

Each of the photosensitizers shown in *Figure 4.6* was tested to determine if it would exhibit the self-eliminating characteristic. Individual samples for each photosensitizer were prepared in hexanol containing 1 wt% UV9310 and 10-2 wt% photosensitizer. Absorbance decay experiments for each sample were conducted using the method described in the previous section. Results for the three systems (shown in Table 4.1) clearly establish that neither perylene nor pyrene absorbance decays sufficiently. In fact, pyrene absorbance actually *increases* slightly (likely a result of sample degradation). In direct contrast to these photosensitizers, anthracene absorbance decayed rapidly to approximately zero even at a low light intensity (0.75 $\mu W/cm^2$). The decay constant, τ_d in Table 4.1, is the rate at which the absorbance decays according to the expression

$$A = Ce^{-t/\tau d} \qquad (4.1)$$

where A is the absorbance at time t, and C is a constant of the equation. *Figure 4.7* shows the rate of decay for the anthracene system at 364 nm. The exponential decay observed in *Figure 4.7* shows that the average absorbance of this sample decreases even more substantially than the radical system, suggesting that an initiator formulation including anthracene could be extremely effective for cationic photopolymerization of thick polymers.

Table 4.1. Absorbance decay characteristics for various cationic photosensitizers.

Photosensitizer	Normalized Absorbance (@ t = 1 hour)	Decay Constant, τ_d (min^{-1})
Anthracene	~ 0.00	1.8
Perylene	0.98	NA
Pyrene	> 1.0	NA

4.3.2. Selection of Suitable Photoinitiators

Since all of the monomers/resins, hydrogen donors (TBA), and thermal initiators (BP) investigated in this research all absorb below ~ 310 nm, it is theoretically possible to initiate a radical photopolymerization consisting of any combination of monomer/ accelerator/thermal initiator using any photoinitiator that absorbs above 310 nm. However, the selected photoinitiator must be self-eliminating. The C/TBA initiator formulation and the benzoin ethers both demonstrated this characteristic, thus they were tested further to determine which initiator system was best suited for this research. Each initiator system was added to the resin such that the weight percent of the formulation consisted of 0.2 initiator / 99.8 470-45 resin.

The effectiveness of these formulations were compared by direct observation and thermal profiles obtained using a computerized thermocouple system (Omega Systems, Stamford, CT). By direct observation it was determined that the C/TBA formulation was not suitable for producing thick polymers from vinyl ester resins because it proved incapable of producing a polymer thicker than roughly 2 mm after a reasonably long period of irradiation (15 minutes) at a moderate incident intensity (approximately 1.2 $\mu W/cm^2$). Thermal profiles of this system indicated that the bulk of the reaction had occurred after 15 minutes by showing that the temperature of the system peaked at 4.9 minutes and subsequently cooled to roughly ambient temperature (40-50°C) after fifteen minutes. This suggested that reaction had occurred only on or near the surface of the sample while the bulk of the sample remained uncured. One possible explanation for this

is the absorbance of camphorquinone in the initiating region (440-490 nm) is extremely modest, thus even slight absorption in this region by initiator fragments or other species is enough to keep additional initiator sites from being excited to a higher energy state and the molecule is not able to dissociate to produce a reactive radical.

The benzoin ethers proved to be far more successful than C/TBA at polymerizing thick polymers, even upon exposure to relatively low intensity (less than 1 $\mu W/cm^2$) light sources. Direct observation and thermal profiles of the BEE system indicated irrefutably that the bulk sample had polymerized after fifteen minutes. The 2 cm thick sample had completely solidified, leaving no discernible traces of uncured monomer at any point in the sample; and the thermal profile indicated that the temperature of the system peaked at 4.1 minutes and had returned to ambient conditions before fifteen minutes. Repeating this set of experiments yielded virtually the same results, making it clear that the benzoin ethers were the most effective class of photoinitiators for this system. Table 4.2 shows the effects of various initiator formulations on polymer thickness for samples irradiated for 5 minutes using the 1000 watt source (measured intensity of 0.40 $\mu W/cm^2$).

Table 4.2. Effect of initiator formulation on polymer thickness.

Initiator Formulation	% Monomer Cured[a]	Polymer Thickness (mm)[b]
Camphorquinone/TBA	11.4 ± 0.2	1.7 ± 0.1
Irgacure 651	41.9 ± 0.6	12.9 ± 0.2
BEE	43.4 ± 0.8	13.5 ± 0.2
BME	42.6 ± 1.2	13.4 ± 0.2
BME/BP	58.6 ± 1.4	22.4 ± 0.3
BME/TBA	38.5 ± 0.5	12.2 ± 0.2

[a]compares the mass of the sample before and after irradiation
[b]measures the polymer thickness at the largest point in the sample

The process of optimizing the photoinitiator formulation began as soon as it was determined that the benzoin ethers were the best class of photoinitiators for this research. Two separate studies were conducted to quantify the optimal initiator formulation. The first study involved monitoring the average absorbance of BEE samples in hexanol with concentrations of photoinitiator ranging from 0.05 - 2 wt%. The second study measured the flexural modulus for polymers photoinitiated using the same range of photoinitiator concentrations. Results from the first set of experiments showed that the average absorbance for initiator concentrations greater than ~ 0.5 wt% were not significantly reduced after irradiation for a period of 15 minutes at moderate (~ 1.0 $\mu w/cm^2$) light intensities. This meant that initial light intensity gradients for samples having initiator concentrations above 0.5 wt% would not decrease significantly during this period of time. Thus few if any active sites would be produced in the bulk of these samples and polymerization would therefore by limited everywhere except at or near the surface.

The second study showed that the maximum value for the flexural modulus for neat (no reinforcing fiber added) 470-45 polymers photocured for 4 minutes occurred around 0.2 wt% of photoinitiator. *Figure 4.8* shows the flexural modulus as a function of initiator weight percent for samples up to 1 wt% photoinitiator. Samples containing greater than 1 wt% of photoinitiator were not completely cured after four minutes of irradiation at this light intensity (~1.3 $\mu w/cm^2$). As seen in *Figure 4.8*, there is an optimum amount of initiator for achieving maximum strength in a given cure time, and further increases in the initiator concentration actually undermine the mechanical properties. In fact, he shape of the curve in *Figure 4.8* can be divided into three regions. In the first region (0.05 - 0.15 wt%), the flexural modulus increases as function of

initiator concentration. This suggests that an insufficient number of active sites are produced at very low initiator concentrations (0.05 wt%). The maximum values for the flexural modulus occur in the second region (0.15-0.25 wt%). The third region (> 0.25 wt%) shows that as the weight fraction of initiator increases the flexural modulus actually *decreases* as a result of an optical effect. At high initiator concentrations, there is a dramatic reduction in the penetration of initiating light, since it is strongly absorbed by the large amount of initiator present. This results in non-uniform initiation and the formation of a polymeric film at or near the surface. It should be state that the optimal initiator concentration depends on a large number of factors such as initiator type, temperature, and light intensity and is specific to each photocurable system.

BEE and other benzoin ethers proved to be the most successful photoinitiators for the vinyl ester resins investigated in this research because they meet all of the criteria necessary for efficient elimination of the light intensity gradient. For example, the absorbance of the unreacted (initiator) and reacted (active radical) states in the operating window is dramatically different. As the initiator reacts to form active sites, its absorbance in the operating window decreases severely, corresponding to a decrease in the overall absorbance in the system due to a reduction in the initiator concentration. Thus the transverse light intensity gradient that exists initially in the bulk of the sample will decrease gradually as the reaction proceeds and more initiators absorb light and react to form active sites. This effect is shown in *Figure 4.9*. This figure shows that the severity of the light intensity gradient decreases as a function of irradiation time.

An important facet of *Figure 4.9* is that it provides *in situ* measurements of the light intensity gradient. Being able to monitor the light intensity gradient during reaction

allows one to extract important information about the system. For example, one can easily study the effects of initiator concentration and type on the gradient as well as qualitatively determine the importance of incident intensity on the intensity gradient. *Figure 4.9* shows that the light intensity gradient decreases even at moderate light intensities (1.0 $\mu w/cm^2$) for the optimal (in terms of flexural properties) photoinitiator formulation. *Figures 4.8-9* help to emphasize the importance of the self-eliminating light intensity gradient. *Figure 4.8* shows that the initiator concentration affects the flexural properties of the resultant polymer while *Figure 4.9* shows that the light intensity gradient does decrease at optimal initiator concentrations. In fact, the intensity increased by ~ 9% after 10 minutes at a depth of 1.1 cm, while the intensity at the bottom of the sample (~ 4.7 cm) increased by ~ 505%. The rate and the degree of elimination are dependent on the intensity of the initiating light and the initial concentration and type of photoinitiator.

4.3.3. Effects of Hydrogen Donors

As stated in Chapter 2, a number of compounds are added to photocurable systems in order to enhance the degree of cure or to increase the kinetics of the polymerization. Hydrogen donors are commonly employed as accelerators to increase the polymerization kinetics. The basic principle behind these compounds is that they enhance the likelihood that a photoinitiator will undergo hydrogen abstraction, which enhances the polymerization kinetics. However, a look back at Table 4.2 shows an unexpected effect. Addition of 0.2 wt% TBA to the 0.2 wt% BEE photoinitiator actually decreases both the degree of cure and the depth of polymerization. At the very least, this result is surprising considering the reputed success of this initiator formulation in the

literature.[17,18,21-23] Additional experiments performed during the course of this research have shown that promoting H^+ abstraction (by addition of traditional hydrogen donors such as TBA) results in a decrease in the rate of absorbance decay in the operating window.

Figure 4.10 demonstrates how the presence of a strong hydrogen donor, in this case TBA, affects the average absorbance of the system at a wavelength (328 nm) used to initiate the polymerization. In this experiment, two initiator formulations were irradiated for a predetermined period of time, removed from the light and placed in a UV-Vis spectrometer to obtain absorbance spectra. This process was repeated several times with the same sample until it had been irradiated for a total of fifteen mintues and corresponding absorbance data had been collected. Each initiator formulation consisted of 0.2 wt% BEE dissolved in hexanol with one sample also containing 0.2 wt% TBA. Upon irradiation, the samples absorbed light and were excited to higher energy state before reacting to produce active radicals. TBA was added to the system to promote one method of radical production (H^+ abstraction) over the other method (fragmentation).

It is clear from *Figure 4.10* that addition of TBA to the system slows the rate at which absorbance in the initiating window decays. Therefore it can be concluded from this data that, while it serves as an accelerator in thin-film photopolymerizations and thermal polymerizations, strong hydrogen donors may and in some cases do inhibit thick photopolymerizations by decreasing the rate at which light intensity gradients in the system decrease.

4.3.4. Effect of Thermal Initiators

As seen in Table 4.2, the degree of curing can be significantly enhanced by adding small amounts (less than 0.2 wt% of the total formulation) of thermal initiators such as benzoyl peroxide (BP). BP does not absorb in the operating window (see *Figure 4.2*) thus it will not interfere with the production of active sites via photopolymerization. In fact, the highly exothermic reaction associated with propagation elevates the temperature of the system to the extent that BP dissociates to produce additional active sites that are capable of reacting with monomers to produce new polymer chains. This method is exceptionally useful in systems that are semi-opaque or systems where light can not travel in a direct path through the bulk of the sample such as composites with high degrees of fiber loading. It is also a useful method for systems where it is difficult or impossible for direct light to reach the entire sample (i.e. complex mold designs).

The addition of thermal initiators can greatly enhance the rate at which thick polymers are cured. *Figure 4.11* shows the effect of BP on the amount of time required to cure samples of predetermined thickness at a modest light intensity (2.15 $\mu W/cm^2$). It is clear from *Figure 4.11* that addition of BP increases the rate of propagation significantly. Furthermore, cure time increased only slightly as sample thickness was increased from 2.5 to 15 mm for samples initiated using the dual-cure method while the amount of time required to cure samples containing only photoinitiator increased by ~ 250% as the thickness of the sample was increased from 2.5 to 6.5 mm. Interestingly, there is virtually no change in the amount of time required to cure the polymer as the concentration of BP is increased from 0.2-1 wt%.

Employing a dual cure initiation mechanism to photocure polymers also reduces the effects of incident intensity on polymer cure time. *Figure 4.12* compares cure times for single-initiation (pure photoinitiator formulation) and dual-cure (photo and thermal initiator) mechanisms at predetermined thicknesses. This figure shows how the effect of light intensity is reduced when a thermal initiator is added to the system. In cases where a single-initiation mechanism is employed, increasing the light intensity from 0.78 to 2.15 $\mu W/cm^2$ significantly decreased the amount of time required to cure samples as the polymer thickness was increased. However, polymers cured using the dual-cure initiation mechanism were essentially independent of light intensity as it was increased from 0.78 to 2.15 $\mu W/cm^2$, indicating that significance of light penetration for completeness of cure is reduced when a thermal initiator is added and active centers are produced from both photo and thermal initiation reactions. Interestingly, there is virtually no change in the amount of time required to cure the polymer as the concentration of BP is increased from 0.2-1 wt%.

4.4. Conclusions/Chapter Summary

Photopolymerizations can be used to cure thick systems if careful attention is paid to: the system formulation including initiator(s), monomer(s) and photosensitizer; the wavelength or wavelengths of light used to irradiate the system; the mechanism responsible for production of active sites; and the use of so-called accelerators or catalysts. These polymerizations can be initiated using low-cost UV light sources such as arc lamps and low-pressure mercury lights. The kinetics and cure times of photocurable

polymer systems are enhanced by addition of small amounts of non-interfering thermal initiators such as benzoyl peroxide to create a so-called dual-cure system. Purely photoinitiated systems and dual-cure photo/thermal systems are more energy-efficient than thermally cured systems. In addition, they react immediately upon absorbance of light of the appropriate wavelength to produce active sites capable of initiating reaction.

The experiments presented in this chapter validate the potential for each of the curing strategies developed in this research as alternatives to current processing methods for the production of composites and thick polymers. Both radical and cationic photoinitiators which exhibit the self-eliminating characteristic have been disclosed and clear operating windows based on these initiators have been established. Additional experiments have shown that careful attention must be paid to every compound in the system because their addition may significantly affect the polymerization.

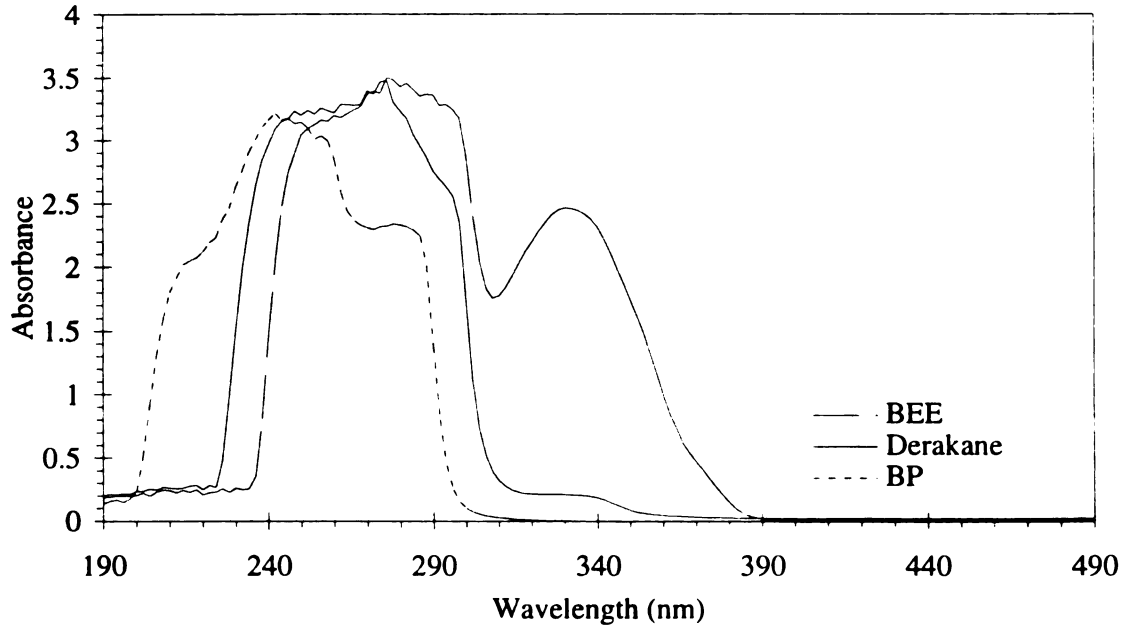

Figure 4.2. UV-Vis absorbance spectra for typical reactive system including monomer (Derakane 470-45), photo (BEE) and thermal (BP) initiators.

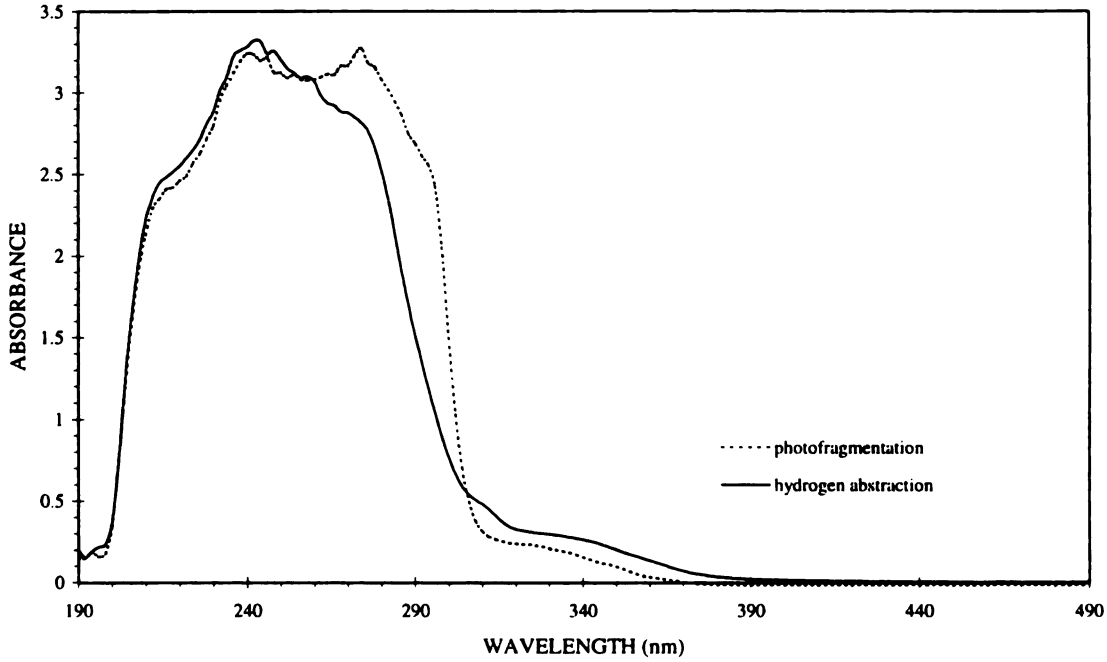

Figure 4.3. UV-Vis absorbance spectra for BEE radicals generated via hydrogen abstraction (—) and photofragmentation (--) reactions.

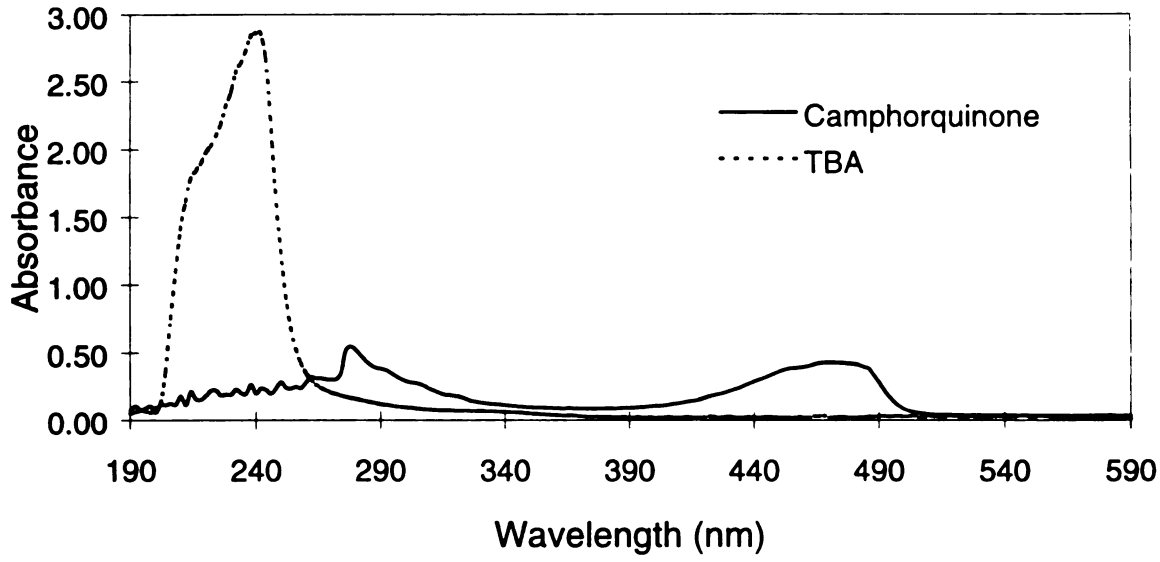

Figure 4.4. Absorbance spectra for the camphorquinone / tributylamine coinitiator system.

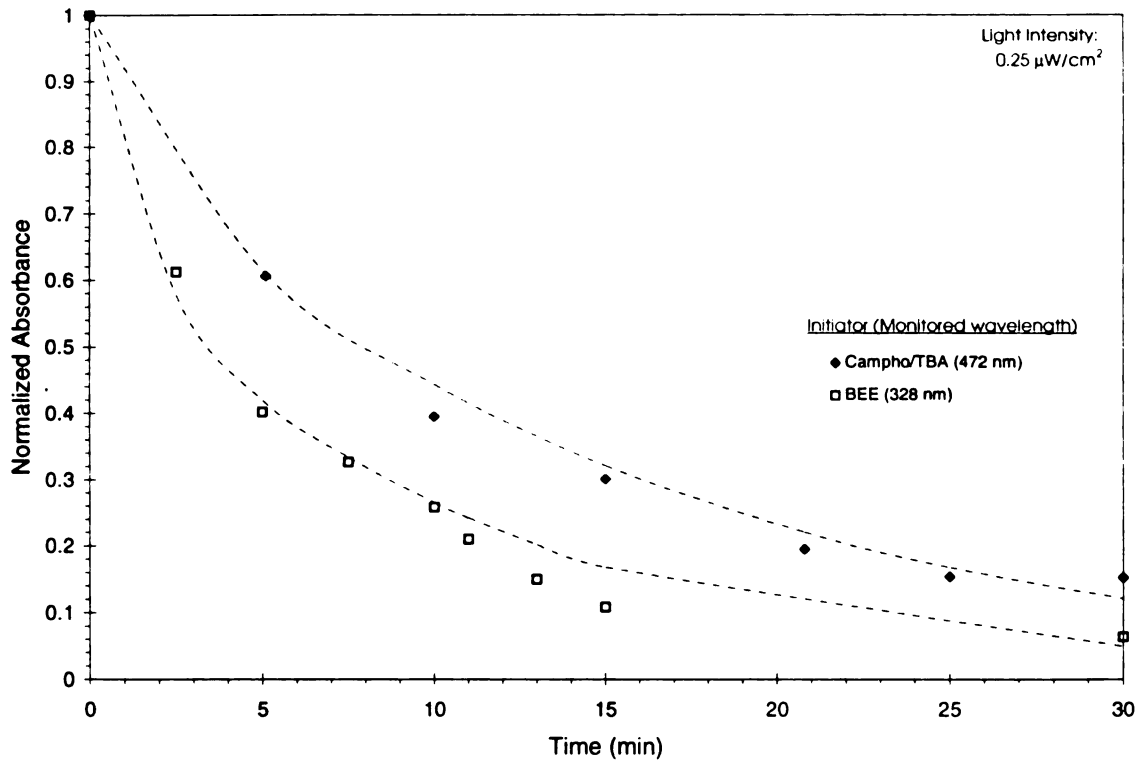

Figure 4.5. Absorbance decay of radical photoinitiators benzoin ethyl ether (at 328 nm) and camphorquinone/TBA (at 472 nm) as a function of time.

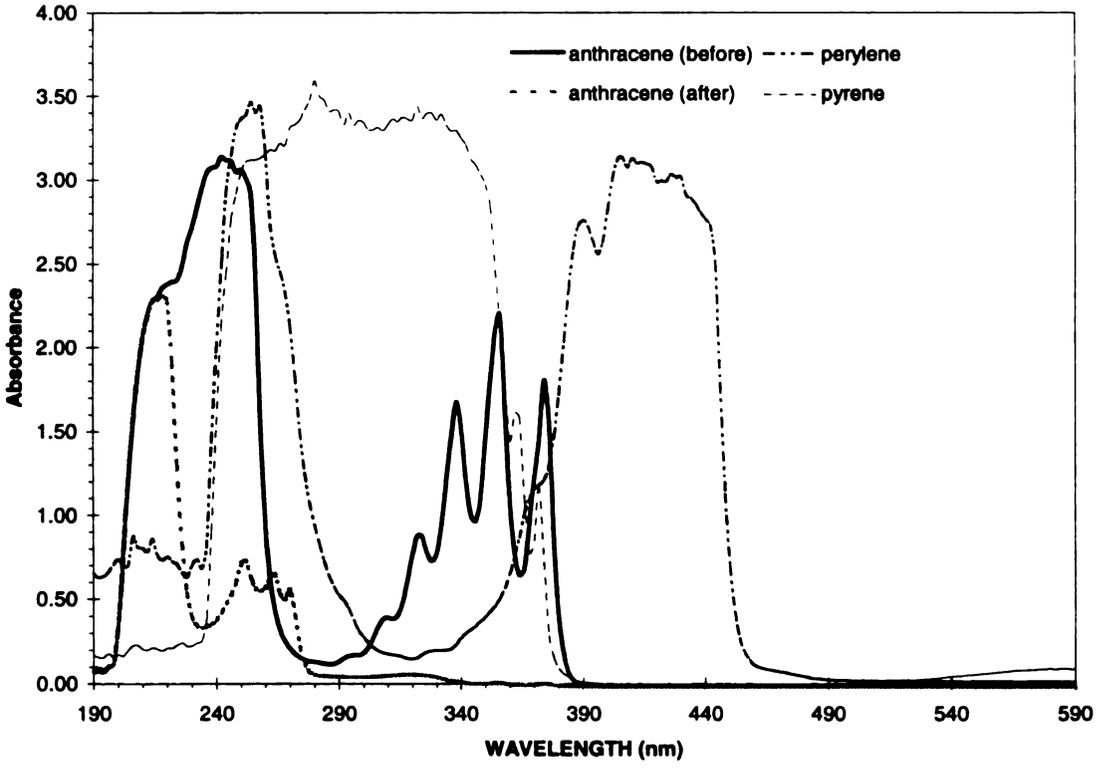

Figure 4.6. Absorbance spectra for cationic photosensitizers including perylene, pyrene, and anthracene (both before and after photosensitization).

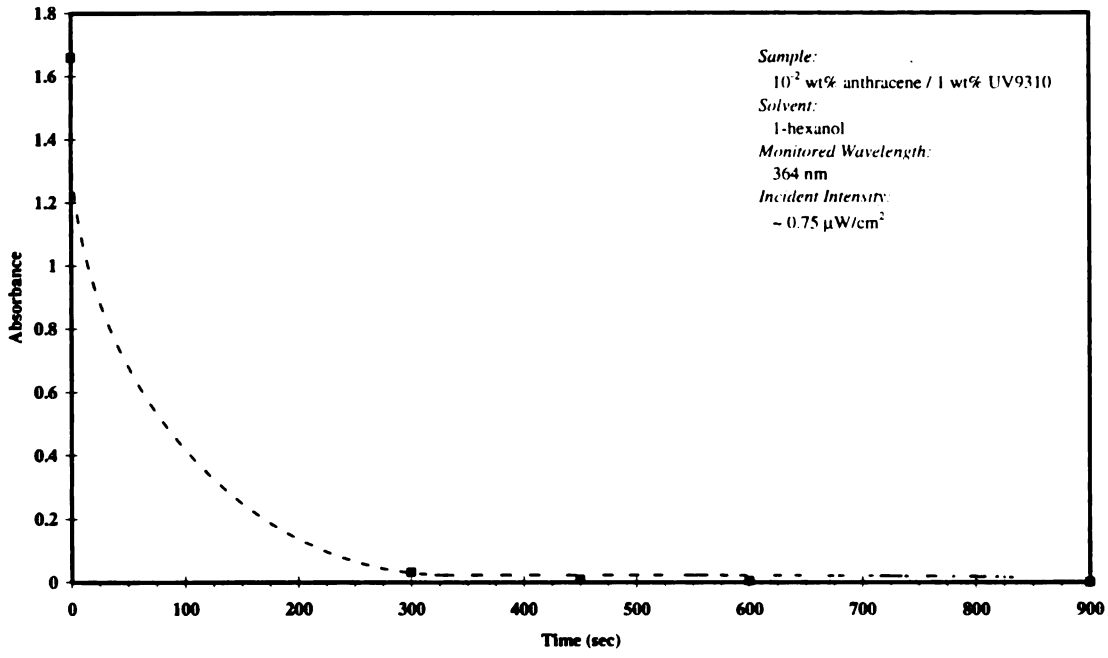

Figure 4.7. Absorbance decay of anthracene at 364 nm as a function of time.

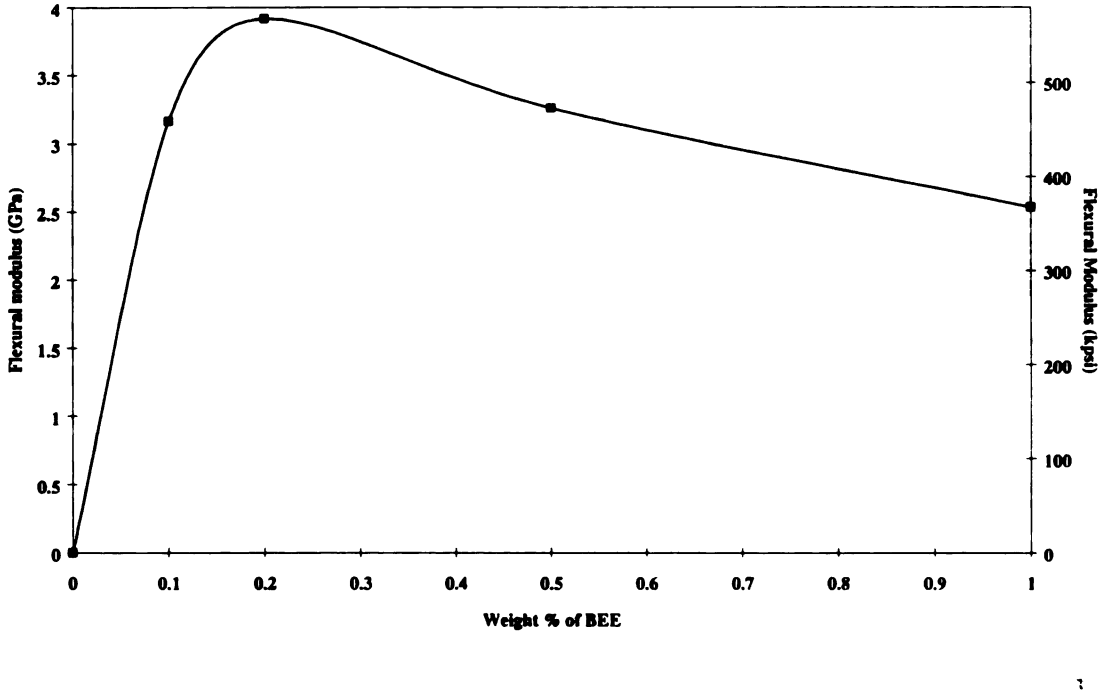

Figure 4.8. The effect of BEE weight fraction on flexural modulus for unfilled vinyl ester polymers photocured for 4 minutes.

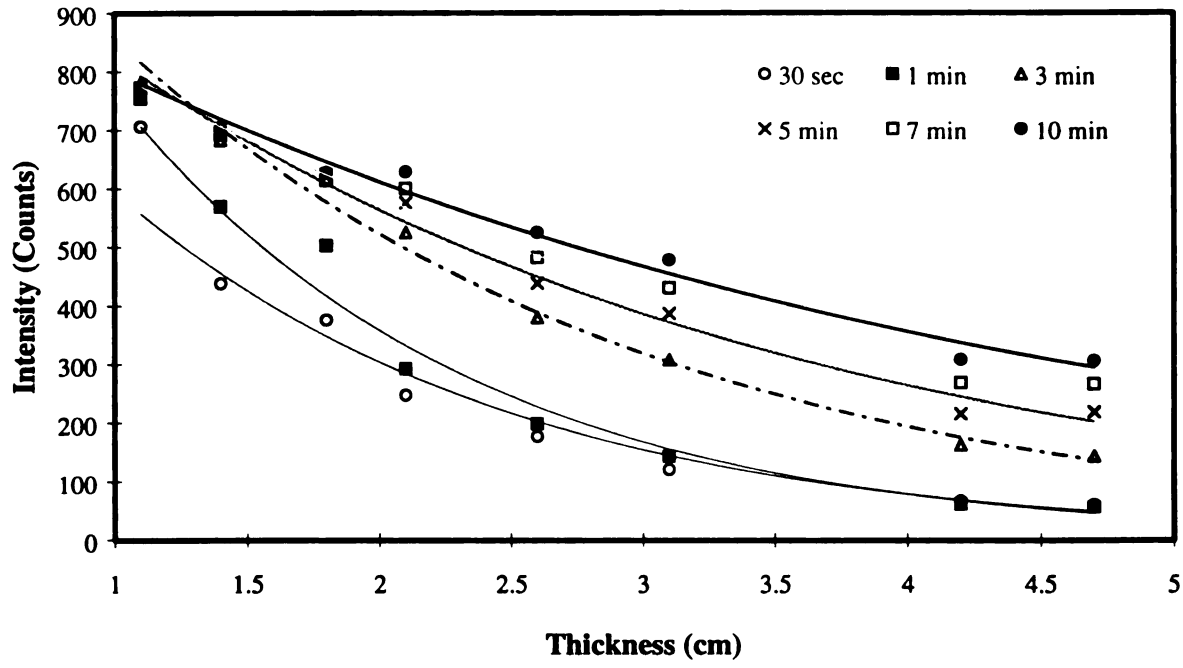

Figure 4.9. Intensity of light as a function of thickness for increasing periods of irradiation.

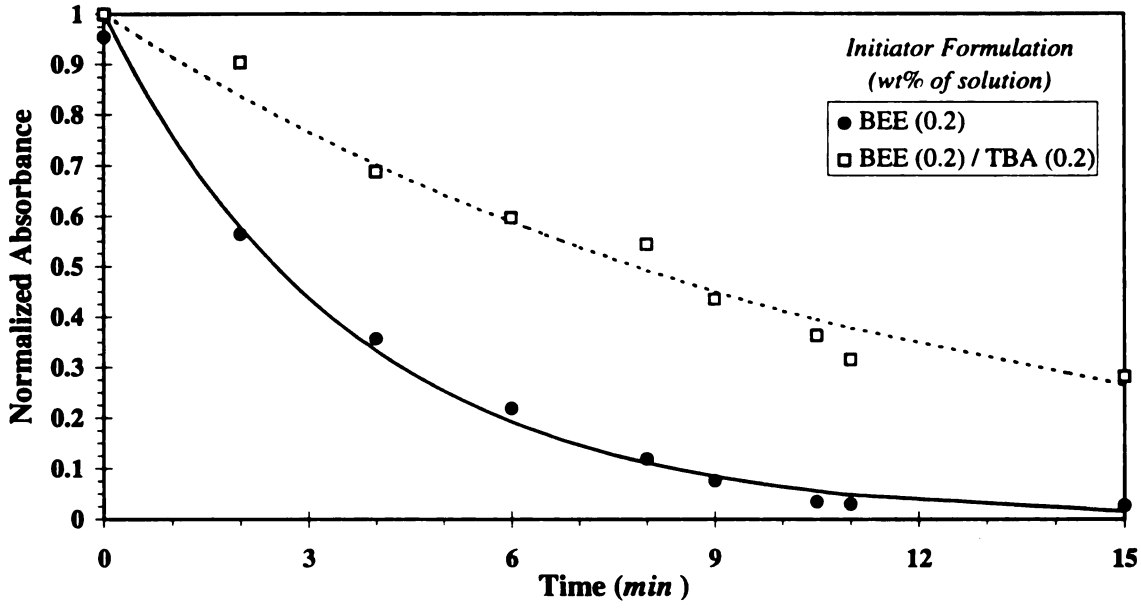

Figure 4.10. Average absorbance at 328 nm for BEE(•) and BEE/TBA() initiator formulations irradiated as a function of time.

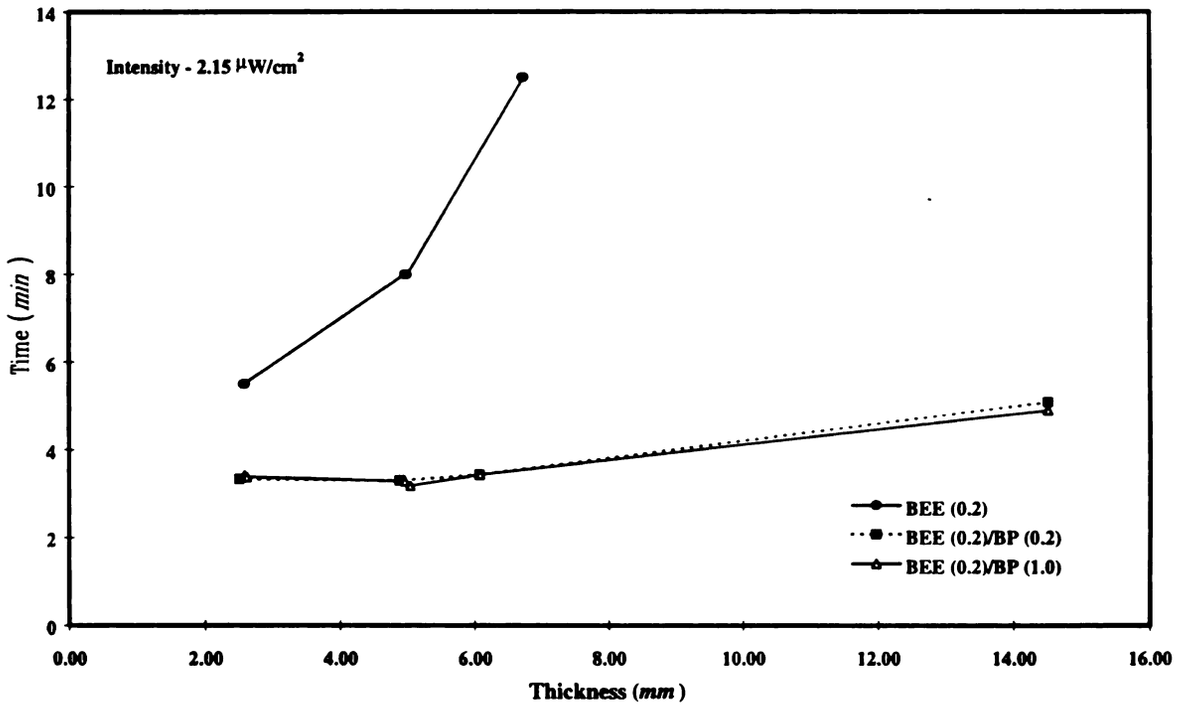

Figure 4.11. Amount of time required to cure samples of varying thickness for a number of initiator formulations including BEE (0.2 wt%) (•), BEE (0.2 wt%)/BP (0.2 wt%) (✪) and BEE (0.2 wt%)/BP (1.0 wt%) (Δ).

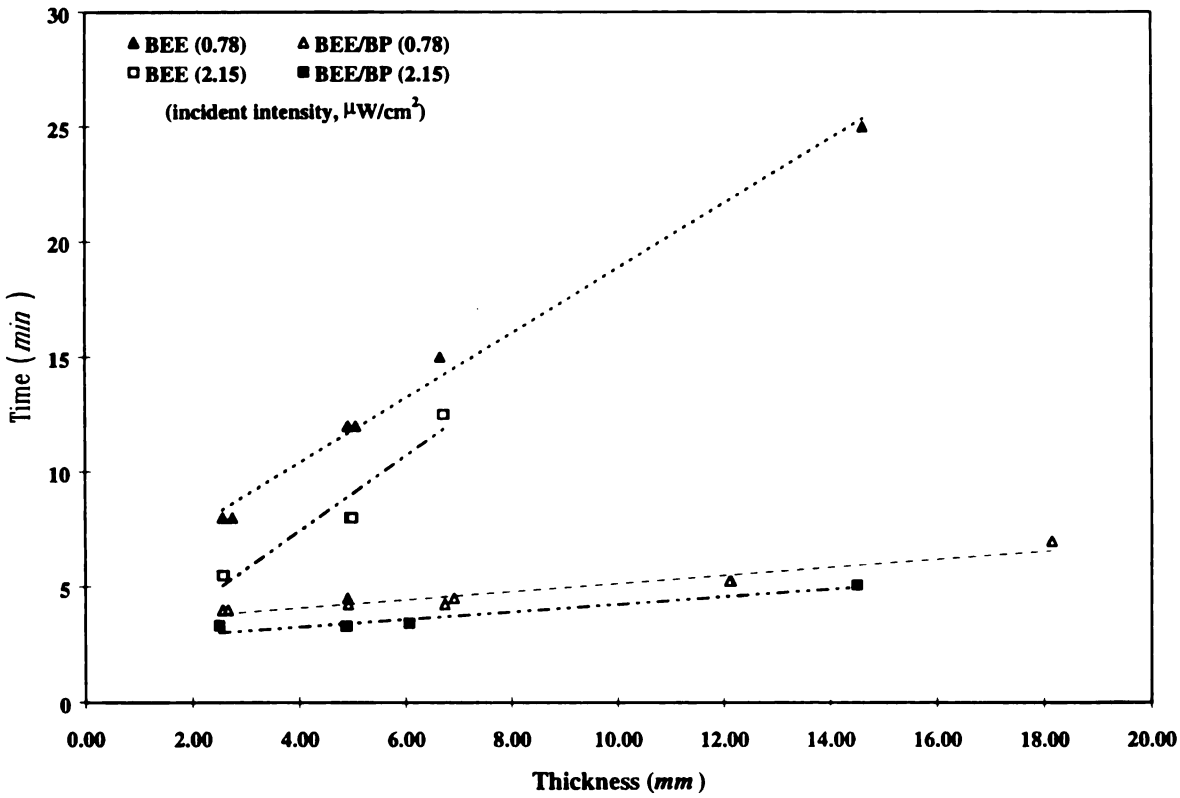

Figure 4.12. Effect of light intensity and thickness on cure time for 411-c50 vinyl ester polymers containing 0.2 wt% BEE and 0.2 wt% BEE / 0.2 wt% BP initiator formulations.

4.5. References

1. M. Zheng, M. Yang, S. Liu, L. Zhang, "Photopolymerization of propargyl acetate with Michler's ketone as photoinitiator," *Chin. J. Polym. Sci.*, **13**, 74 (1995).

2. L. Thijs, S.N. Gupta, D.C. Neckers, "Photochemistry of perester initiators," *J. Org. Chem.*, **44**, 4123 (1979).

3. C.B. McArdle, J. Burke, J.G. Woods, U.S. Patent No. 5,084,490, issued 1/28/1992.

4. O. Nuyken, J. Stebani, A. Lang, "Synthesis and characterization of photopolymers with azo units," *Angew. Makromol. Chem.*, **226**, 143 (1995).

5. J.L. Mateo, P. Bosch, A.E. Lozano, "Reactivity of radicals derived from dimethylanilines in acrylic photopolymerization," *Macromolecules*, **27**, 7794 (1994).

6. R. Mallavia, F. Amat-Guerri, A. Fimia, R. Sastre, "Synthesis and evaluation as a visible-light polymerization photoinitiator of a new eosin ester with an *O*-benzoyl-α-oxooxime group," *Macromolecules*, **27**, 2643 (1994).

7. L. Angiolini, D. Caretti, C. Carlini, E. Corelli, P.A. Rolla, "Polymeric photoinitiators having benzoin methyl ether moieties connected to the main chain by the benzoyl group and their activity for ultra-violet curable coatings," *Polymer*, **35**, 5413 (1994).

8. B. Glad, K. Irgum, P. Horstedt, "Photopolymerization and characterization of methacrylate-based reactive composite membranes," *J. Membrane Sci.*, **100**, 171 (1995).

9. L. Angiolini, D. Caretti. C. Carlini, N. Lelli, P.A. Rolla, "Polymeric photoinitiators bearing side-chain acyldiphenylphosphinoxide moieties for UV surface coatings," *J. Appl. Polym. Sci.*, **48**, 1163 (1993).

10. H. Kaczmarek, L.A. Linden, J.F. Rabek, "Reactions of hydroxyl (HO•) and hydroperoxyl (HO_2•) radicals generated chemically and photochemically with poly(ethylene oxide)," *J. Polym. Sci., Polym. Chem.*, **33**, 879 (1995).

11. S. Knaus, H.F. Gruber, "Photoinitiators with functional groups. III. Water-soluble photoinitiators containing carbohydrate residues," *J. Polym. Sci., Polym. Chem.*, **33**, 929 (1995).

12. T. Kimura, M. Kajiwara, "The synthesis of phosphinylphosphorimidic hydroxyethyl acrylate and the electrical properties of its polymer produced by ultraviolet-irradiation-induced polymerization," *Polymer*, **36**, 713 (1995).

13. D.C. Neckers, "Architecture with photopolymerization," *Polym. Eng. Sci.*, **32**, 1481 (1992).

14. C. Hull, U.S. Patent No. 4,575,330, issued March 11, 1986.

15. I. Rohm, W. Kunnecke, U. Bilitewski, "UV-polymerizable screen-printed enzyme pastes," *Anal. Chem.*, **67**, 2304 (1995).

16. E. Bortel, A. Kochanowski, W. Rys, E. Witek, "Polymerization initiated by the system triethanolamine/hydrogen sulfite with and without the cooperation of hydrogen peroxide. 1. Polymerization of acrylamide," *J.M.S. - Pure Appl. Chem.*, **A32**, 1197 (1995).

17. G. Seretoudi, I. Sideridou, "Benzil/n,n-dimethylaminoethyl methacrylate system as photoinitiator for methyl methacrylate polymerization," *J.M.S. - Pure Appl. Chem.*, **A32**, 1183 (1995).

18. G. Odian, "Principles of Polymerization," 3rd Ed., Wiley, New York, NY, 223 (1991).

19. D.C. Neckers, O. Valdes-Aguilera, K.S. Raghuveer, D.G. Watson, "Production of Three-Dimensional Bodies by Photopolymerization," *U.S. Patent No. 5,137,800*, Issued August 11, 1992.

21. S.P. Pappas in "Encyclopedia of Polymer Science and Engineering," **11**, H.F. Mark, N.M. Bikales, C.G. Overberger, G. Menges, Eds., Wiley-Interscience, New York, 186 (1988).

21. N.T. Lipscomb, Y. Tarshiani, "Kinetics and mechanism of the benzoin isobutyl ether photoinitiated polymerization of styrene," *J. Polym. Sci. Polym. Chem. Ed.*, **26**, 529 (1988).

22. M.V. Encinas, J. Garrido, E.A. Lissi, "Polymerization photoinitiated by carbonyl compounds. VIII. Solvent and photoinitiator concentration effects," *J. Polym. Sci. Polym. Chem. Ed.*, **27**, 139 (1989).

23. M.V. Encinas, C. Majmud, J. Garrido, E.A. Lissi, "Methyl methacrylate polymerization photoinitiated by pyrene in the presence of triethylamine," *Macromolecules*, **22**, 563 (1989).

CHAPTER 5.

CHARACTERIZATION OF THE DYNAMIC LIGHT INTENSITY GRADIENT

To validate the self-eliminating light intensity gradient approach for photopolymerizations of thick polymers and composites, the time-evolution of the light intensity gradient was characterized both experimentally and theoretically. The time evolution of the dynamic light intensity gradients was simulated by first solving the elementary kinetic differential equations for a constant light intensity (to yield the effective kinetic constant for a rate expression which is first order in both the initiator concentration and the light intensity) then solving the governing set of coupled differential equations for the light intensity and the initiator concentration as functions of both position and time. Experimentally, actinometry was used to characterize the light intensity as a function of both time and position. These studies provide insight on the effects of factors such as sample thickness, incident intensity, and initiator formulation (type and concentration) on the time-evolution of the light intensity gradient.

5.1. Simulation of the Dynamic Light Intensity Gradient

5.1.1. Elementary Reactions for a Constant Light Intensity

The discussion in the previous chapter illustrates that benzoin ethyl ether (BEE) is an appropriate initiator for polymerizations of thick systems if care is taken to ensure that

the active centers are produced by a photofragmentation mechanism rather than by hydrogen abstraction. The reaction mechanism for generation of active centers by photofragmentation is described by three elementary reaction step, as illustrated by Equations 5.1-3:

$$h\nu + A \overset{k_{abs}}{\Leftrightarrow} {}^1A \tag{5.1}$$

$${}^1A \overset{k_{nr}}{\Rightarrow} A \tag{5.2}$$

$${}^1A \overset{k_d}{\Rightarrow} 2R\bullet \tag{5.3}$$

where A is the ground state initiator, ^1A represents the excited singlet state, k_{abs} is the rate constant for absorption (the calculation of k_{abs} based upon the incident light intensity is described below), k_{nr} is the rate constant for nonradiative deactivation (from the excited state to the ground state) and k_d is the rate constant for dissociation of the excited state initiator to produce active radicals (R•). Therefore, BEE in the ground state absorbs a photon and is promoted to the excited singlet state, then undergoes an excited-state dissociation reaction to yield radical centers.

Based upon this set of elementary reactions, differential balances on the ground and excited-state initiator yield the following kinetic differential equations:

$$\frac{d[A]}{dt} = k_{abs}([{}^1A] - [A]) + k_{nr} [{}^1A] \tag{5.4}$$

$$\frac{d[{}^1A]}{dt} = k_{abs}([A] - [{}^1A]) - k_{nr} [{}^1A] - k_d [{}^1A] \tag{5.5}$$

These equations may be readily solved numerically once the rate constants have been evaluated. The rate constant for absorption, k_{abs} is equal to the product of the absorption

cross-section of the initiator, σ, and the photon flux of the incident light, ϕ. For BEE, our absorption experiments revealed that σ is equal to 1.8×10^{-18} cm^2, while the value of ϕ is easily calculated as the incident light power divided by the energy of a photon ($h\nu$). For our simulations, these calculations yielded a value of 1.509×10^{-5} for k_{abs}. A value of 1.01×10^6 sec^{-1} was used for the dissociation constant, k_d based upon flash photolysis studies on benzil reported in the literature.[1] The rate constant for the return to the ground state through non-radiative processes, k_{nr}, is readily calculated from the initiator quantum yield, f, as shown below:

$$k_{nr} = k_d(\frac{1}{f} - 1) \qquad (5.6)$$

This equation is derived from the consideration that the excited-state initiator either returns to the ground state nonradiatively, or fragments to produce radical centers. For BEE, a typical value of f is 0.90, yielding a value for k_{nr} equal to 1.12×10^5 sec^{-1}. These values for the elementary rate constants were then substituted into Equations 5.4-5, which were then solved simultaneously using the software package Mathcad. Simulation results for the ground-state initiator concentration as a function of time are shown in *Figure 5.1.* This figure reveals that, for a constant light intensity, the initiator follows a first-order decay with an effective rate constant, k_{eff}, equal to 0.112 sec^{-1} for photopolymerizations initiated by benzoin ethyl ether.

5.1.2. Light Intensity Profiles as a Function of Position and Time

In these reaction systems the initiator concentration and the light intensity in a given location are coupled to one another because the light drives a reaction which consumes the initiator, and the initiator (and its reaction products) in turn absorb light to

reduce its intensity. This interrelationship is described by the set of coupled differential equations and boundary conditions shown below:

$$\frac{d[A]}{dt} = - k_{eff} [A(z,t)] I(z,t) \qquad (5.7)$$

$$\frac{dI}{dz} = -\varepsilon_A[A(z,t)]I(z,t) - \varepsilon_R [R(z,t)]I(z,t) \qquad (5.8)$$

initial condition: @ $t = 0$, $A = A_o$ for all z (5.9a)

boundary condition: @ $z = 0$, $I = I_o$ for all t (5.9b)

where $R(z,t) = [A_o(z,t)] - [A(z,t)]$

where ε_A and ε_R are the molar absorptivities of the original initiator and the initiator fragments, respectively. I represents the transmitted intensity at a particular wavelength and is a function of both position and irradiation time.

In a completely self-eliminating system, the initiator fragments do not absorb in the operating window, therefore light is able to penetrate deeper into the sample as initiator absorbs light and subsequently reacts to produce active sites (initiator fragments). In this case, the second term on the right hand side of Equation 5.8 will equal zero, therefore the intensity will be dependent only on the photoinitiator (or photosensitizer) concentration which decreases monotonically throughout the course of the reaction. If, however, both the photoinitiator and the initiator fragments absorb in the operating window, the light intensity gradient will be either partially eliminated or completely static depending on the absorptivity of the initiator fragment(s). In reality, all of the radical photoinitiator systems investigated in this research lie somewhere between

complete elimination and static light intensity gradients, therefore the second term in Equation 5.8 must be included in any model.

Equations 5.7-8 were solved using finite differences to yield a numerical solution for the light intensity profile. Microsoft Excel software was used to create a spreadsheet based upon the finite difference method to determines the normalized light intensity at a given point in the sample at any given time. The simulations allow the effects of a number of variables on the dynamic light intensity profiles to be determined, including: the effective rate constant, k_{eff},, the initial concentration of photoinitiator, incident intensity, sample thickness, and the total time for illumination.

5.1.3. Simulation Results

For illustrative purposes, simulation results were obtained for three types of reactive systems: i) systems for which the molar absorptivities of the initiator fragments and the original initiator are essentially the same, (representative of many initiators used for thin-film polymerizations); ii) systems for which the molar absorptivity of the initiator fragments is lower than that of the original initiator, but non-zero (representative of benzoin ethers such as BEE); and iii) systems for which the molar absorptivity of the initiator fragment is zero (a desirable characteristic for photopolymerizations of samples exhibited by a few systems such as anthracene/iodonium salt cationic initiators).

The light intensity gradient remains static in cases where the molar absorptivity of the initiator fragments is equal to or greater than the molar absorptivity of the original initiator. An illustrative example of such a system is shown in *Figure 5.2*. In this case, light is not able to penetrate deeper into the sample over time which means that

polymerization will occur at or near the surface while the bulk of the sample remains uncured. If a system has a static light intensity gradient similar to the example shown in *Figure 5.2* then it will not produce thick polymers or composites based on the SEG initiation strategy developed in this research because light will not be able to penetrate into the bulk of the sample efficiently.

In many photoinitiator systems, the molar absorptivity of the initiator fragments, while smaller than the molar absorptivity of the original initiator, is non-zero. In fact, this is the situation when benzoin ethers such as those used most frequently in this research. For BEE, the molar absorptivity of the original initiator is 474 L mol^{-1} cm^{-1} at 328 nm while the molar absorptivity of the initiator fragments ranges from ~ 18 - 48 L mol^{-1} cm^{-1} depending on the initiator fragments generated during the dissociation reaction. Hence the light intensity gradient will never be completely eliminated even if all of the initiator reacts because the initiator fragments will continue to absorb (slightly) in the operating window. However, *Figure 5.3* shows that the severity of the gradient decreases significantly over time and there is a noticeable increase in the amount of light that reaches the bottom of the sample as initiator reacts to produce initiator fragments. Hence the system is more likely to polymerize throughout the bulk of the sample than a system where the light intensity gradient is completely static. *Figures 5.3-4* demonstrate the effect the molar absorptivity of initiator fragments can have on the elimination of the light intensity gradient. When radicals are generated solely by photofragmentation (illustrated in *Figure 5.3*), the molar absorptivity of the initiator fragments is equal to 18 L mol^{-1} cm^{-1}. However, when the initiator undergoes hydrogen abstraction, the molar absorptivity of the initiator fragments is equal to ~ 48 L mol^{-1} cm^{-1} (illustrated in *Figure*

5.4). Thus this system is not as efficient as the system where the initiator fragments are generated by photofragmentation because the light intensity gradient does not eliminate as rapidly or completely.

In the final system, the molar absorptivity of the initiator fragments is zero. This is by far the most idyllic situation for photocuring thick polymers and composites because the light intensity gradient is dictated entirely by the concentration of original photoinitiator in the system. Thus as the initiator absorbs light and reacts, the elimination of the light intensity gradient will eventually be complete if all of the initiator dissociates. *Figure 5.5* is an illustrative example of an initiator system that is completely self-eliminating. This figure clearly shows that the light intensity gradient is completely eliminated, meaning that the amount of light that penetrates through the bulk of the sample is equal to the amount of light that reaches the surface of the sample (i.e. the sample eventually becomes transparent to the incident light). While the molar absorptivity governs the amount of elimination that will ultimately occur, there are consequences associated with initiator concentration.

The importance of initiator concentration is simulated in *Figure 5.6*. This figure simulates the light intensity profile for a system where the molar absorptivity of the initiator fragments is zero, however the original initiator concentration is ~700% larger than the original initiator concentration in *Figure 5.5*. While the light intensity gradient is initially very severe even for "normal" concentrations of photoinitiator (*Figure 5.5*), it decreases quickly until the gradient is completely eliminated. However, when the concentration of photoinitiator becomes excessive (as is the case in *Figure 5.6*), the light intensity gradient remains severe much longer because a greater number of compounds

absorb the initiating light, demonstrating an optical effect which has a devastating effect on the gradient elimination rate. In this case, the initiator at or near the surface absorbs light and reacts, becoming transparent to the initiating light. However, the shear concentration of initiator in this sample dramatically slows the rate at which the gradient eliminates, creating a system where there is no longer efficient penetration of light into the bulk of the sample. Hence it is unlikely that these systems would completely polymerize in reasonable periods of illumination time.

In addition to obtaining three-dimensional profiles of the light intensity as a function of position and time, simulations proved to be useful in predicting how the intensity of the incident light affects the amount of time required for a given amount of light to penetrate to a predetermined depth. This is significant because the amount of light required to initiate a reaction resulting in the production of radical centers depends on a number of variables including: the temperature of the system; initiator type; and presence (or lack thereof) of additional initiator compounds such as thermal initiators, accelerators or photosensitizers. *Figure 5.7* compares the amount of time required for varying amounts of light to penetrate to a depth of 1.5 cm as a function of light intensity for a system where the molar absorptivity of the initiator fragments is zero. This figure compares three different "percentages of light" (60, 75 and 90%), where "percentage of light" represents the amount of light that penetrates to a depth of 1.5 cm divided by the amount of light that reaches the surface of the sample. From the figure it is clear that even at low incident intensities, 60% of light reaches the sample immediately. In cases where more energy (thus more light) is required, the sample will have to be exposed to light for longer periods of time. *Figure 5.7* also shows the effects of incident intensity on

the amount of time required to reach a given percentage of light penetration. For example, while one hour of exposure time is required before 90% of the incident light penetrates through the bulk of the sample for a 1 mW/cm^2 light source, 90% of the incident light will reach the bottom of the sample in less than 5 minutes if a 20 mW/cm^2 light source is employed. Higher light intensities reduce the amount of time necessary to attain the desired levels of energy throughout the bulk of the sample because more intense light sources carry more energy into the sample, thus more molecules absorb photons and react in a given period of time.

5.1.4. Discussion of Simulation Results

Clearly, the molar absorptivity of the initiator fragments has a dramatic impact on the degree of gradient elimination. In an ideal system such as the anthracene/iodonium salt cationic initiator formulation, the molar absorptivity of the initiator fragments would be zero and the light intensity gradient would exist only as long as the original initiator remained in the system, eventually eliminating completely if all of the initiator dissociated. However, when the molar absorptivity of the initiator fragments is non-zero (representative of initiator systems such as BEE), a light intensity gradient will always exist, although it will decrease as the initiator dissociates and it does not prohibit these initiator systems from being used in self-eliminating gradient (SEG) initiation strategies. In these initiator systems, it is often favorable to control the method responsible for generating initiator fragments as some initiator fragments exhibit higher molar absorptivity values than other initiator fragments (illustrated in *Figures 5. 3-4*). In the worst case, the molar absorptivities of the original initiator and the initiator fragments are

equal (representative of most initiators used in thin-film photopolymerizations), creating a light intensity gradient which is static. In this case, the initiator system will likely be ineffective for SEG initiation strategies because there will not be efficient penetration of light into the bulk of the sample.

The simulation results indicate that system variables such as initiator formulation and incident intensity can have dramatic effects on the gradient elimination rate. While the molar absorptivity of the components in the system, particularly the initiator fragments, dictates the degree to which elimination will occur, the incident intensity and initiator formulation govern the rate at which elimination occurs. Increasing the light intensity and/or reducing the concentration of initiator in the system increases the rate at which the light intensity gradient is eliminated. Conversely, high initiator concentrations can effectively decrease the gradient elimination rate, thereby reducing the efficiency of light penetration into the bulk of the sample and negatively impacting the polymerization.

5.2. Experimental Characterization of the Light Intensity Gradient

Actinometry is a general term for techniques which are used to monitor the absorbed light intensity, I_a, of a system during polymerization. It is a valuable technique for photopolymerizable systems because it can be used to directly characterize the rate of polymerization (using Equation 2.26) if the propagation and termination rate constants are known.[2] Three types of actinometers have been used to monitor I_a during polymerization: chemical, thermal and electrical. In general, thermal and electrical actinometers are more convenient than chemical actinometers, possibly because there are

a wider variety of thermal and electrical actinometers. Some of the more common thermal and electrical actinometers include thermocouples which convert photon energy to electrical or thermal energy, photomultipliers and semiconductor photodetectors.[2]

Chemical actinometers present a more complicated system than thermal or electrical actinometers because they are based on using chemical compounds which undergo a reaction where the quantum yield is known. Chemical actinometry could pose a host of problems for thick photopolymerizations including: possibility of the chemical actinometer serving as a photoinitiator, thus distorting the measured I_a value; introduction of additional species into the operating window, thus affecting the elimination of the light intensity gradient; and difficulty getting light to the actinometer. To emphasize some of these problems, one need only examine common actinometers. Although potassium ferrioxalate is used most frequently,[3] benzophenone is also employed as a chemical actinometer.[2] In this function, the benzophenone undergoes a reduction to produce benzhydrol.[2] However, benzophenone is one of the most commonly used radical photoinitiators,[4,5] therefore it would be difficult or impossible to determine if benzophenone were being reduced or was initiating a polymerization reaction. In addition, in order for a chemical actinometer to be effective it must be able to absorb light. However, if its primary absorbance is in the same region as the monomer or another species which is present in excess, its effectiveness will be minimized or eliminated completely. One final disadvantage of chemical actinometers is that they must be placed directly in the reaction vessel where they are subject to the same system variations as the rest of the system. This can be a problem since potassium ferrioxalate is sensitive to changes in temperature and wavelength.[2]

5.2.1. Developing an Experiment Setup for Actinometry Studies

The inherent difficulties associated with chemical actinometers made them a poor option for studying intensity in this research. Consequently, it was determined that an electrical actinometer would be the best option for this research in lieu of thermal or chemical actinometers. The fact that electrical actinometers are non-intrusive and are therefore not sensitive to environmental changes proved to be the deciding factors when selecting between thermal and electrical actinometers. Once the type of actinometer to be used was decided, a setup had to be devised that would be capable of providing *in situ* measurements of the absorbed light intensity. This proved to be an arduous task, more so than it appeared at first glance.

The initial setup employed a highly sensitive photomultiplier (PMT) used in conjunction with fiber optics and a monochromator in such a fashion that a single wavelength could be monitored during reaction. Unfortunately, the sensitivity of the PMT meant that its environment had to be blanketed in total darkness. What made this a problem is that measuring devices attached to the PMT such as a voltmeter and the monochromator also had to be blanketed in darkness. This made it nearly impossible to accurately read the data. While this setup proved to be an inferior one for monitoring the intensity during reaction, it did lead to the setup which was ultimately used to collect intensity data.

A schematic of the experimental setup used in this research is shown in *Figure 5.8*. This setup provided a non-intrusive method for obtaining *in situ* measurements of the light intensity for samples of thicknesses ranging from 0-5 cm. In fact, this setup allows one to construct three-dimensional profiles for the light intensity as a function of

both sample thickness *and* irradiation time by combining light intensity profiles for samples of different thickness. Developing a setup capable of monitoring the light intensity after it has passed through reactive samples provides physical data that supports the importance and the impact of self-eliminating light intensity gradients. The experimental results produced from dynamic light intensity gradient studies can be interpreted to determine if a self-eliminating gradient is both feasible and significant in producing thick polymers and composites using photopolymerization techniques.

A series of optical (bandpass) filters were employed to restrict the wavelength range to the operating window for the system being investigated. A bandpass filter centered around 330 nm (range ± 5 nm) was used to study the benzoin ether photoinitiators while a 360 nm (range ± 5 nm) filter was used to monitor the anthracene photosensitization reaction. Neutral density filters were employed to insure that the spectrometer responsible for "counting" photons was not bombarded with potentially damaging levels of energy. Neutral density filters "cut" the intensity through a series of equations that relate density, D, incident intensity, I_O, transmitted intensity, I_T, and transmittance, T.[6] The relationship between these variables is shown in Equation 5.10.

$$T = I_T/I_O = 10^{-D} \tag{5.10}$$

The effects of neutral density filters are additive, meaning that they can be placed in series to attenuate a beam to a desired factor via Equation 5.11

$$D = - \log_{10}(1/A_T) \tag{5.11}$$

where A_T is the desired attenuation.

5.2.2. Experimental

BEE, BME and anthracene were obtained from Aldrich (Milwaukee, WI). The onium salt cationic photoinitiator, UV9310C, was obtained from GE Silicones (Waterford, NY). All materials were used without further purification. Each of the dynamic intensity experiments were conducted in 1-hexanol instead of monomer. This was done for practical reasons. The absence of monomer prevented either system from polymerizing in the quartz cuvette. If monomer had been added and the samples were allowed to polymerize, the quartz cuvettes would have been destroyed after each individual run. This would have required multiple cuvettes in order to complete the experiments, which would have substantially increased the cost for this study.

In order to construct a three-dimensional intensity profile, samples ranging in thickness from less than 1 cm to 5 cm were irradiated for a total of 10 minutes per sample at a constant light intensity (1 $\mu W/cm^2$). This method produced intensity profiles for a given thickness as a function of time. By varying the thickness from sample to sample, one can obtain intensity profiles over a wide range of sample thickness. A three-dimensional profile of intensity as a function of sample thickness and exposure time can then be constructed by combining the individual profiles.

5.2.3. Experimental Results

Comparing *Figure 5.3* and *Figure 5.9*, we see that there is a general agreement in the trends of the model and the experimental results. For example, at a minimum thickness in each figure, the intensity profile shows a marked increase right from the beginning and the intensity approaches the maximum value in each case. As the

thickness increases, each figure show increases in the intensity profile, although the initial increase is more dramatic experimentally than predicted by the model. And finally, thicker samples in both figures seem to show a slight delay, more pronounced in *Figure 5.9*, before the intensity begins to increase.

A simple explanation is offered to justify the delay, or induction period, observed at the onset of irradiation in thicker samples. This trend stands to reason since the severity of the initial light intensity gradient dramatically limits the amount of light that penetrates through the bulk of the sample and few if any initiator molecules are able to absorb enough energy (light) to undergo reaction. However, as the exposure time increases, initiators in the deepest regions of the sample absorb enough energy to react, resulting in the generation of active sites and in the process becoming transparent (or significantly less absorbent) to the incident light. Another significant result of the experimental study shows that the light intensity gradient is eliminated almost entirely for samples approaching 2 cm in thickness. Were the intensity of the initiating source higher, one would assume that the intensity gradient would be completely eliminated for 2 cm samples in less than 10 minutes.

Figure 5.10 shows intensity profiles for BEE samples at 328 nm before and after irradiation at 1.2 $\mu W/cm^2$ for a total of 10 minutes. It is clear from *Figure 5.10* that the severity of the intensity gradient does in fact decrease as initiator reacts to produce active radicals. In fact τ_h, the decay constant in the exponential expression relating intensity, I, and thickness (denoted by the variable h in Equation 5.12), decreases by a factor of two after the sample has been exposed for a total of 10 minutes.

$$I = \exp(- h / \tau_h) \qquad (5.12)$$

One final glance at *Figure 5.10* shows that the amount of light that reaches the bottom of the sample (~ 5 cm) after irradiation has increased by 433%, meaning that more than four times as many photons reach the bottom of the sample as it reacts to produce active sites.

Results for the anthracene system were far less conclusive than for the BEE system, however similar trends were observed for this system. For example, the amount of 364 nm light intensity measured after passing through a 2 cm sample containing 0.1 wt% anthracene and 1 wt% UV9310C dissolved in hexanol increased by ~ 60% after the sample had been exposed to 1.5 $\mu W/cm^2$ for 20 seconds. However, monitoring the intensity growth in the anthracene system is more difficult than in the BEE system because the reaction is far more rapid and the molar concentration of anthracene is typically much lower than the BEE molar concentration. In order to alleviate this problem, the intensity of the incident light was decreased to < 0.25 $\mu W/cm^2$. The results for this set of experiments are shown in *Figure 5.11*. This figure shows a plot of the light intensity at the bottom of anthracene samples of varying thickness over a period of 900 seconds. The linear increase in light intensity at the bottom of the sample demonstrates the self-eliminating light intensity gradient.

5.3. General Conclusions/Chapter Summary

Obtaining intensity profiles proved to be very important to the success of this research. The modeling experiments verified the importance careful selection of initiators, incident intensity and initiator concentration in the evolution of self-eliminating

light intensity gradients. The experimental results verified both the existence of an initial light intensity gradient and its disappearance upon generation of active centers. Because the experimental data report the amount of intensity that has passed through a sample of a given thickness, the data can be directly related to a decrease in light intensity gradients. In addition, modeling the light intensity gradient provided a framework which served as a qualitative measuring stick for determining if the system would behave experimentally as one would expect it to. Lastly, the model could be a useful tool if one were attempting to determine the amount of energy or light penetration required for a system to polymerize if it were to be photoinitiated.

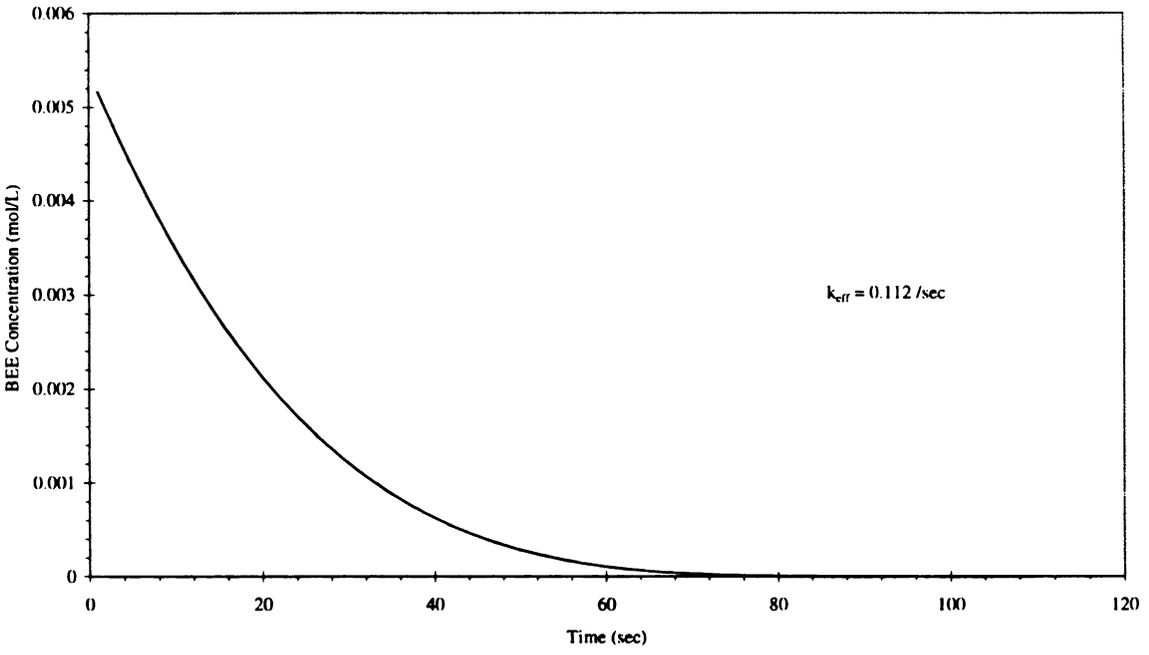

Figure 5.1. Ground-state initiator concentration of benzoin ethyl ether as a function of illumination time.

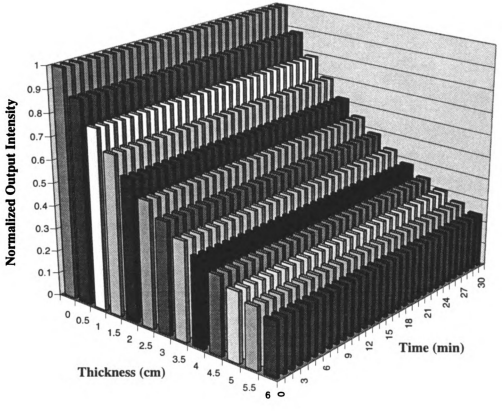

Figure 5.2. Static light intensity gradient (non-eliminating system).

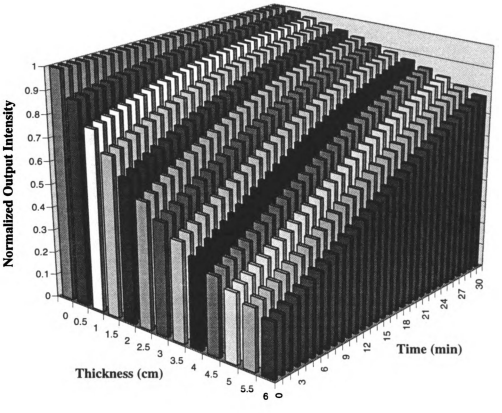

Figure 5.3. Profile of the light intensity for BEE assuming all of the active radicals are produced via photofragmentation.

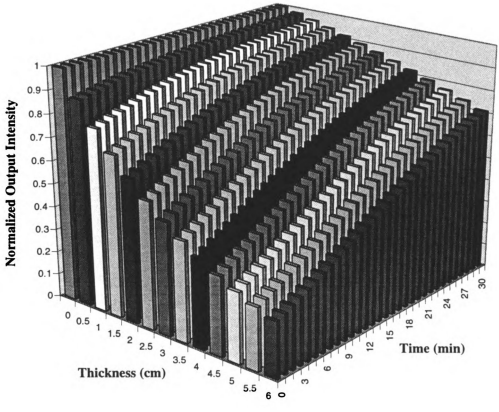

Figure 5.4. Profile of the light intensity for BEE assuming all of the active radicals are produced via hydrogen abstraction.

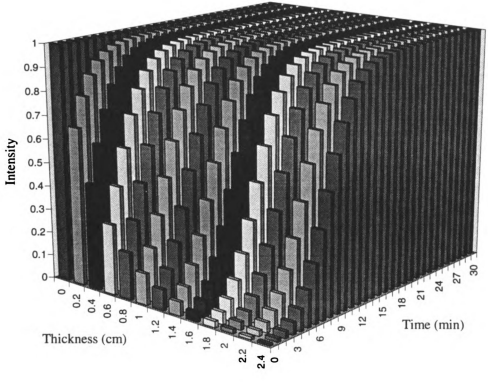

Figure 5.5. Normalized light intensity profile for a completely self-eliminating system with a "normal" photoinitiator concentration.

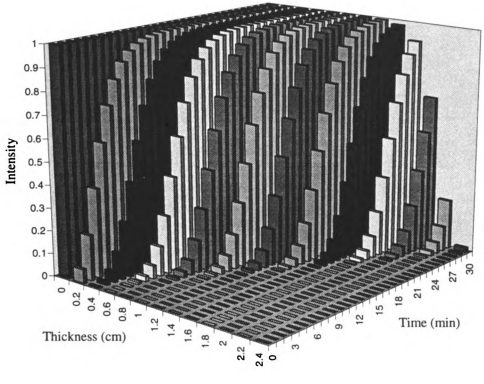

Figure 5.6. Normalized intensity profile for a completely self-eliminating system with a "high" photoinitiator concentration.

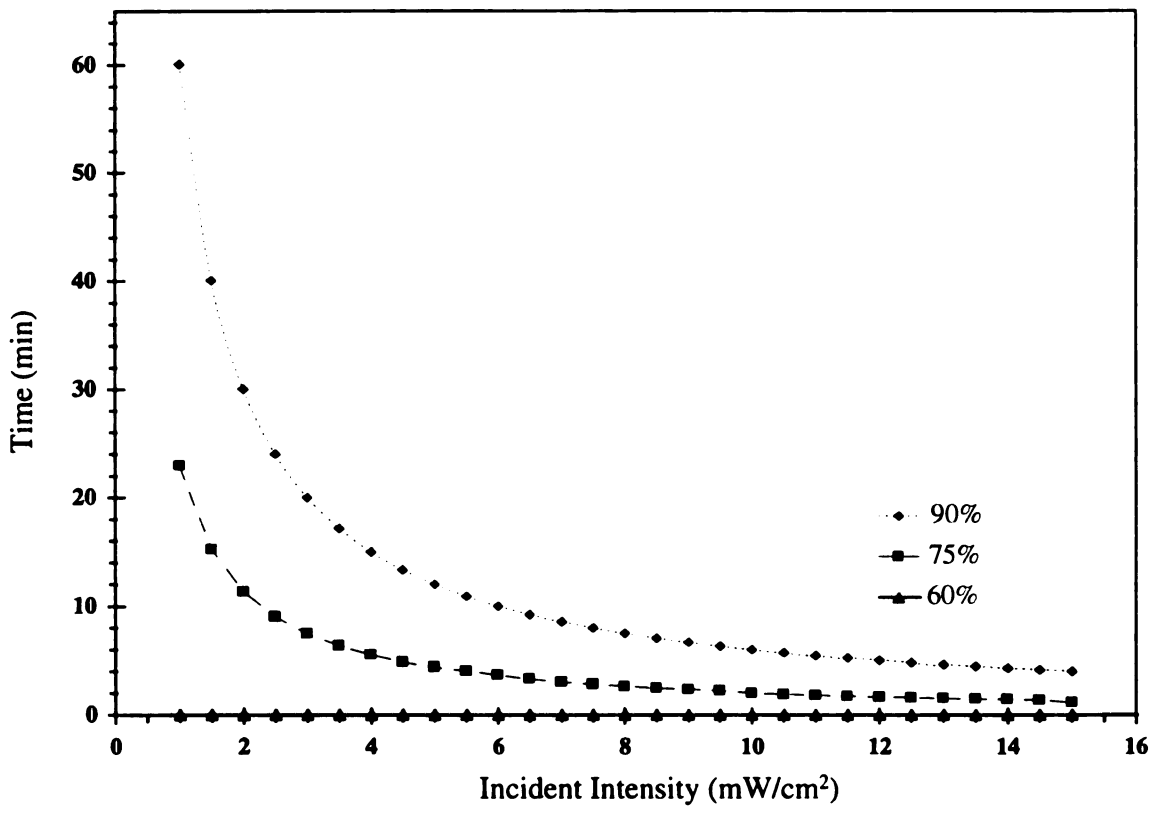

Figure 5.7. Effect of incident intensity on gradient elimination rate.

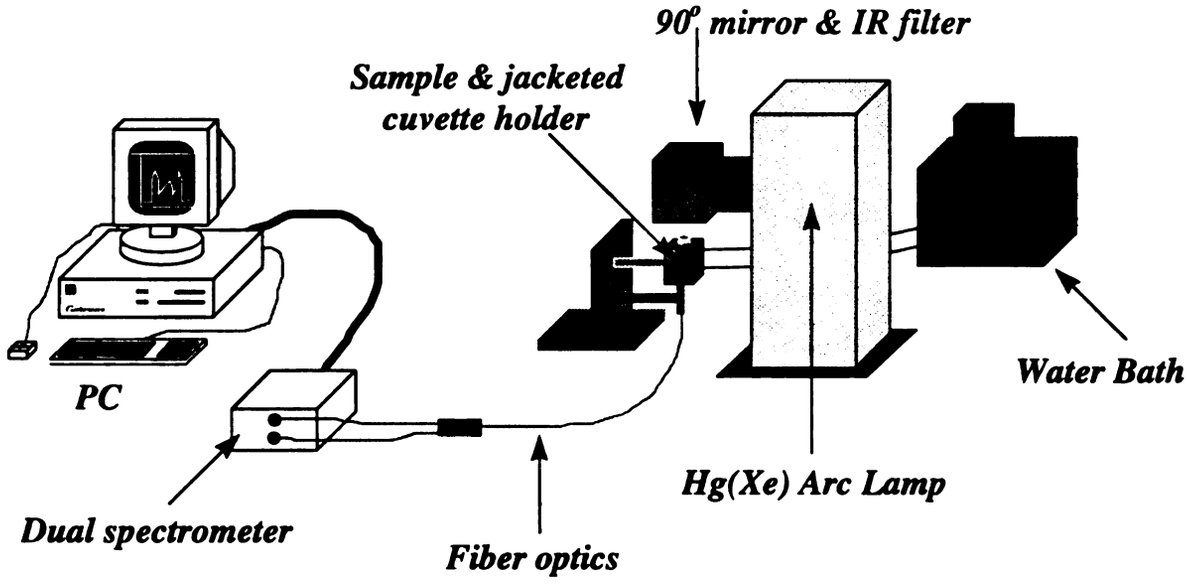

Figure 5.8. Schematic of the experimental setup for actinometry studies.

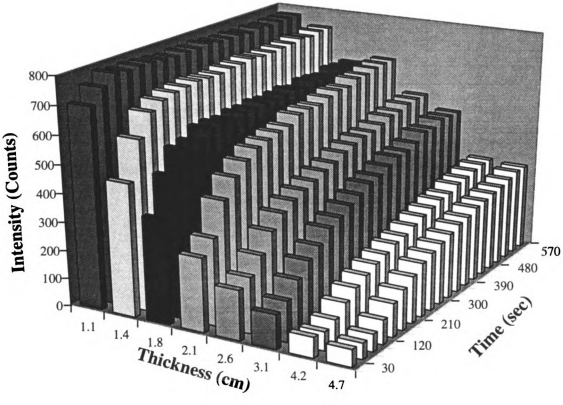

Figure 5.9. Experimental characterization of the light intensity gradient as a function of exposure time and sample thickness for BEE initiation reaction.

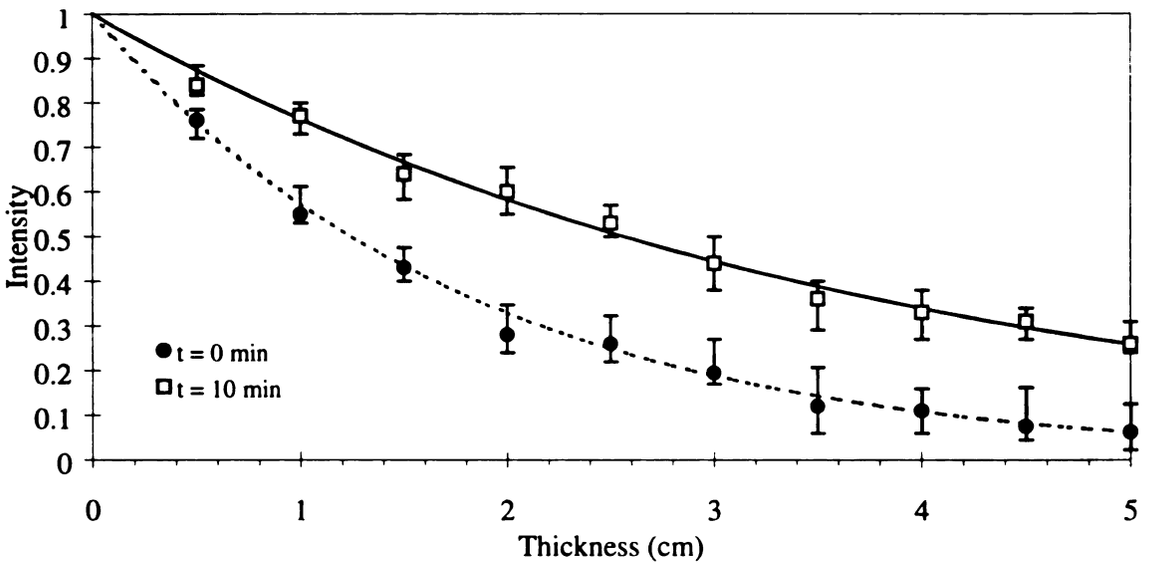

Figure 5.10. Measured light intensity after passing through BEE samples of varying thickness before and after sample exposure for 10 minutes (incident intensity = 1.2 $\mu W/cm^2$).

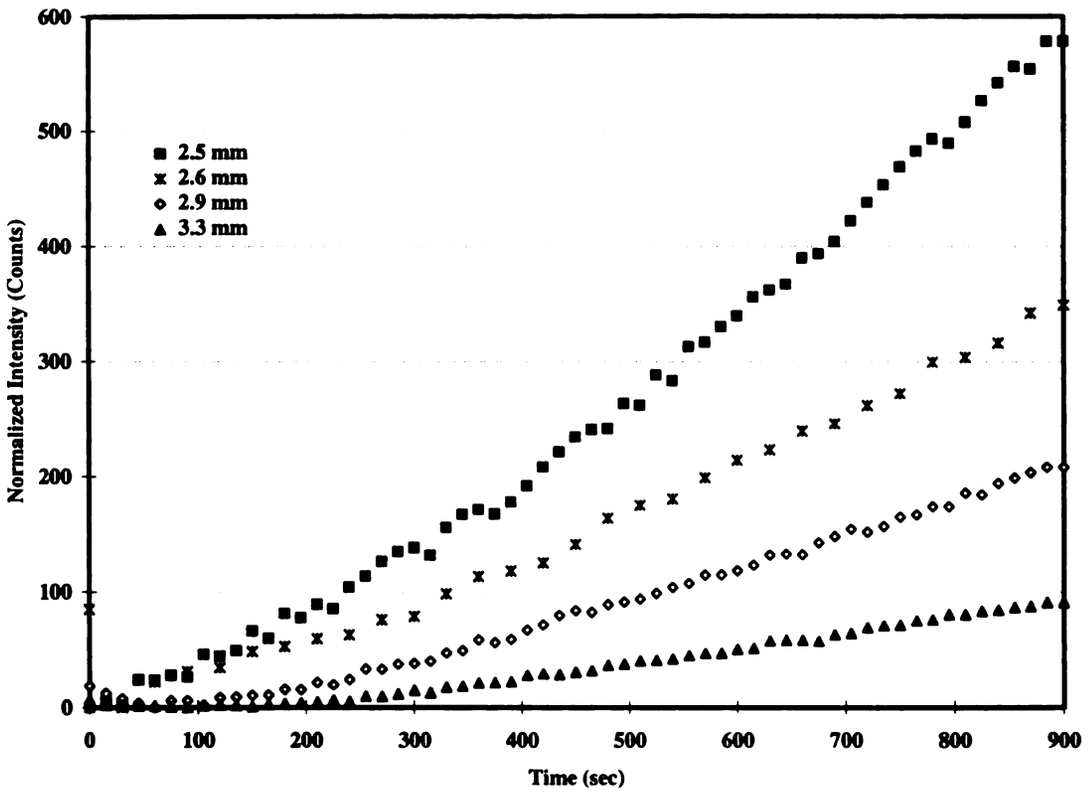

Figure 5.11. Normalized light intensity as a function of time for varying sample thickness of 1 x 10^{-2} wt% anthracene/1 wt% UV9310 in hexanol as a function of time (intensity monitored at 363.96 nm).

5.4. References

1. J.C. Scaiano, "Photochemical and free-radical processes in benzil-amine systems. Electron-donor properties of α-aminoalkyl radicals," *J. Phys. Chem.*, **85**, 2851 (1981).

2. G. Odian, *Principles of Polymerization*, 3rd edition, Wiley & Sons, New York, NY, 1992.

3. N.T. Lipscomb, Y. Tarshiani, "Kinetics and mechanism of the benzoin isobutyl ether photoinitiated polymerization of styrene," *J. Polym. Sci., Polym. Chem.*, **26**, 529 (1988).

4. J.L. Mateo, P. Bosch, A.E. Lozano, "Reactivity of radicals derived from dimethylanilines in acrylic photopolymerization," *Macromolecules*, **27**, 7794 (1994).

5. M.V. Encinas, J. Garrido, E.A. Lissi, "Polymerization photoinitiated by carbonyl compounds. VIII. Solvent and photoinitiator concentration effects," *J. Polym. Sci., Polym. Chem.*, **27**, 139 (1989).

6. "Optics and Filters," Oriel Corporation Product Catalog, **Vol. III**, 2-19 (1990).

CHAPTER 6.

DIFFERENTIAL SCANNING CALORIMETRY STUDIES

6.1. Introduction

In this chapter, a number of variables have been investigated using Differential (DSC) and Photodifferential (PDSC) Scanning Calorimetry. PDSC has been a widely used technique for *in situ* characterization of reaction kinetics and polymerization rate constants involving photopolymerizations.[1-6] The response time of PDSC is relatively fast, on the order of 2-3 seconds,[7] therefore it can be used to monitor the kinetics of most free-radical photopolymerizations including vinyl esters and acrylates. In addition, DSC can be used to determine the degree of conversion in cured polymers as well as to determine the glass transition temperature, T_g, for polymers (results for values of T_g for various polymers are presented in Chapter 7 - *Thermal and Mechanical Characterization of Polymer Systems*).

The fundamental operating principle of DSC is relatively straightforward. It measures the difference between reference and sample cells during a thermal event such as a chemical reaction or a controlled temperature change. The DSC typically uses temperature sensors placed in heat sinks located immediately below the sample and reference cells to monitor changes in temperature.[8] Because the cells are maintained

independently, heat flow can be controlled for each cell. Heat can either be removed or supplied from the sample and reference cells depending on the system being tested which allows DSC to characterize both exothermic and endothermic reactions.[9] The exothermic nature of these polymerization reactions mean that they are well suited to kinetic characterization techniques afforded by DSC.[10,11]

DSC can be used to glean a wealth of information for polymer samples in addition to its ability as a kinetic analysis technique. For example, the degree of conversion for polymeric samples can be measured by measuring the size of the exothermic peak after the sample has been heated above its glass transition temperature.[12] Moreover, DSC has been used to characterize thermodynamic constants; cure rates for monomers and resins; and rates of physical and chemical change.[8] There are a number of advantages afforded by DSC including: the ability to measure all thermal events such as glass transition, melting, and degradation; it responds rapidly to thermal transitions and chemical reactions; and it uses small sample sizes. Unfortunately, DSC may be too slow to characterize extremely rapid reactions such as vinyl ethers; and it can be sensitive to slight deviations in sample size, heating rate, and sample morphology. However, it is without a doubt one of the most versatile and flexible techniques currently available for thermal analysis during and after reaction.

The versatility of DSC was exploited in this research to study the effects of temperature, initiator formulation, and initiator concentration on the reaction rate profile of vinyl ester polymers cured using both the self-eliminating gradient (SEG) and dual-cure initiation strategies. In addition, DSC experiments are shown that provide qualitative proof that the reaction is occurring as a direct result of the light source as

opposed attributing the reaction to a thermal effect. Finally, post-cure DSC analysis was used to characterize the degree of cure for polymers that were cured using both initiation strategies.

6.2. Experimental Procedure

Resins were selected from the Derakane™ family (Dow Chemical Co., Midland, MI). In this research, low viscosity (470-45), medium viscosity (411c-50) and high viscosity (441-400) Derakane resins were investigated, although the majority of research involved the lowest viscosity, 470-45, resin for the sake of convenience. Initiators used in this study included benzoin ethyl ether (BEE, Aldrich Chemical Co., Milwaukee, WI) and benzoyl peroxide (Aldrich Chemical Co.). An additional radical photoinitiator was obtained from Ciba-Geigy (Hawthorne, NY), α,α-dimethoxy-α-phenylacetophenone, which is marketed by Ciba as Irgacure 651. All materials were used without further purification.

Standard samples that were initiated based on the SEG strategy were prepared in a bulk solution by mixing 99.8 wt% 470-75 with 0.2 wt% BEE. Upon mixing, the sample was dark-stored in an amber bottle at room temperature. Standard samples cured using the dual-cure initiation strategy consisted of 99.6 wt% 470-45 with the balance being equal parts benzoyl peroxide thermal initiator and BEE photoinitiator. This bulk solution was also dark-stored at room temperature after mixing. The initiator concentration has been noted for cases where the initiator formulation differs from standard and the concentration refers to the weight percent of the entire sample. Individual samples for

each reaction were weighed out from the bulk solution using a Mettler analytical balance that measures to the nearest 0.1 milligram.

The DSC studies were performed using a Perkin Elmer (Norwalk, CT) Differential Scanning Calorimeter (model DSC 7). For the PDSC studies, the calorimeter was modified so that both the sample and reference cells could be irradiated using UV light generated from a 200 watt Hg(Xe) arc lamp (Oriel Corporation - Norwalk, CT). The samples were maintained isothermally using room temperature water that was stored in a reservoir within the calorimeter. Individual samples were placed in aluminum DSC pans and weighed 15-40 milligrams. Light intensities were measured using a UVP Blak-Ray ultraviolet meter (model J225), and the intensities were varied by either using the condenser lens on the lamp or by altering the distance between the sample and the light source. In separate experiments, a high-speed computerized thermocouple (produced by Omega Systems) was used to obtain in situ temperature measurements of these photo-initiated reactions.

6.3. Results and Discussion

6.3.1. In Situ Characterization of the Reaction

The possibility that the reactions were being thermally initiated instead of photoiniated was raised during this research. This raised an important question: whether the reactions were being thermally or photoinitiated. To answer this question, isothermal DSC experiments were conducted at a series of temperatures ranging from 25-45°C. This was a straightforward series of experiments where two samples were maintained

isothermally for a predetermined period of time. The sole difference between the two samples was that one sample was exposed to light from the 200 watt arc lamp. This provided a controlled environment where the only variable between the two samples was initiating light, therefore any differences in the reaction could be attributed to the presence or absence of UV light. The effect of incident light proved to be the same for samples cured at 25, 35 and 45°C, thus only the results for the system maintained at 25°C are shown here (in *Figure 6.1*).

Figure 6.1 shows conclusively that UV light initiates the polymerization reaction, and the absence of light virtually insures that reaction will not take place at or near room temperature. The measured light intensity for this set of experiments was relatively low ($< 1\ \mu W/cm^2$) therefore it is highly unlikely that the light supplied enough heat to initiate the polymerization. However, to insure that the reaction was in fact photoinitiated, a simple experiment was performed to completely rule out the possibility of the light heating the sample sufficiently to initiate a thermal polymerization.

DSC was used to monitor the reaction profile for a solution containing 99.8 wt% 470-45 resin and 0.2 wt% benzoyl peroxide thermal initiator maintained isothermally at 25°C and irradiated using the same 200 watt arc lamp at the same intensity that resulted in the photopolymerization shown in *Figure 6.1*. As expected, no reaction was observed even after the sample was irradiated for a total of 15 minutes. Even after this time, the sample remained a liquid upon its removal from the DSC.

6.3.2. Post-Cure Studies

DSC was used to determine the presence of uncured resin in the polymer and composite specimens. These measurements show that after 5 minutes of exposure to moderate light intensities (1.2 $\mu W/cm^2$) the samples cured more than 95%. These studies also showed that the addition of thermal initiator (BP) dramatically accelerates the degree of cure of the sample. For example, addition of 0.2 wt% BP reduced the amount of time required to achieve a 95% degree of cure by 60%. A summary of the post-cure studies for the 470-45 and 411c-50 resins are presented in Tables 6.1-2, respectively.

Table 6.1. The effect of initiator and illumination time on the degree of cure for low viscosity vinyl ester resin.

Sample	Initiator	Irradiation time	Degree of Cure %
DER 470-45	0.1 % BEE	3 min	50
DER 470-45	0.1 % BEE	5 min	95
DER 470-45	0.1% BEE	10 min	100
DER 470-45	0.1% BEE, 0.2% BP	2 min	95

Table 6.2. The effect of initiator and illumination time on the degree of cure for a moderate viscosity vinyl ester resin.

Sample	Initiator	Irradiation time	Degree of Cure %
DER 411c-50	0.2 % BEE	3 min	60
DER 411c-50	0.2 % BEE	5 min	~98
DER 411c-50	0.2% BEE	10 min	100
DER 411c-50	0.2% BEE, 0.2% BP	2 min	100

6.3.3. Variable Effects

The effect of temperature on the rate of reaction was monitored by PDSC. In these studies, about 30 milligrams of reactive resin (containing 0.1 wt.% benzoin methyl ether) were polymerized at 70, 90 and 110°C, by exposure to UV light (0.07 $\mu W/cm^2$). As expected, the location of the exotherms show that the rate of reaction increases with increasing temperature. In other words, the amount of time required for complete cure decreases as the temperature of the system increases. For example, at this light intensity, the reaction peaked in 3 minutes at 110°C, 6 minutes at 90°C, and 10 minutes at 70°C. *Figure 6.2* shows reaction rate profiles for photoinitiated samples cured isothermally at 70, 90 and 110°C. The initial shape of the 110°C curve can be attributed to equipment problems associated with heating the sample to the reaction temperature and should be not be considered an indication of reaction (the samples in this experiment were preheated to 50°C, however further heating could have led to production of active radicals through some type of thermal dissociation process).

A result similar to the BEE initiator system was observed for 411c-50 resins photocured using 0.1 wt% Irgacure 651 as the photoinitiator. *Figure 6.3* shows the effects of temperature on the reaction rate profile for samples irradiated using UV light (0.6 $\mu W/cm^2$) from the 200 watt arc lamp. The polymers cured much more rapidly than in the previous system, however the intensity of the initiating light was approximately an order of magnitude larger. Interestingly, as the temperature of the system was increased, the reaction occurred more rapidly, but a comparison of the reaction rate profiles showed that the cooler the sample, the higher the reaction rate. While this result was somewhat

surprising, it is not altogether unexpected, especially when one considers the fact that initiation and termination rates can be assumed to be equal for radical polymerizations[13] (recall kinetic derivation of radical mechanism in Chapter 2 - *Background*). Thus the termination rate constant, k_t, increases as the rate of initiation increases. It follows from Equation 2.12 that an increase in k_t would result in a decrease in the overall rate of polymerization, R_p.

One final variable that was investigated using PDSC was initiator formulation. A hypothesis of this research has been that the addition of polymerization enhancing compounds such as strong hydrogen donors does not accelerate thick photopolymerizations but instead slightly inhibits them. While DSC would seem to be perfectly suited to quantify the effect of hydrogen donors such as TBA on the reaction rate, there are a number of problems which minimize its effectiveness. First and foremost among these concerns is the fact that the sample thickness is also relatively thin because extremely small samples are used in DSC. This is indeed a problem because TBA and other hydrogen donors have previously shown that they do indeed enhance the kinetics of photopolymerizations for thin systems, partially because radicals produced by abstraction are more efficient than radicals produced by fragmentation.[14,15] This minimizes the effectiveness of DSC because there are competing effects (efficiency of radicals and self-eliminating light intensity gradients) which can not be differentiated. However, PDSC can at the very least be used to qualitatively determine if one effect will show dominance over the other effect. The results of this experiment are shown in *Figure 6.4*. This figure seems to suggest that the effect of the self-eliminating gradient is slightly more significant than the efficiency of the initiator fragment for ~ 2mm thick samples because the reaction

occurs a little bit more rapidly for the BEE system than the BEE/TBA initiator formulation.

6.4. Chapter Summary

The experiments discussed in this chapter reinforce the notion that thick photopolymerizations can be cured using ultraviolet light as the sole initiating source. In addition, PDSC studies show that the ambient temperature of the system can be used to increase or decrease the amount of time required for complete polymerization. Achieving complete cure is a concern for any polymerization process. The degree of concern is exaggerated when the process involves production of thick polymers and/or composites based upon photopolymerizations in large part because the general consensus in the scientific community all along has been that photopolymerizations can not be used to produce thick polymers. The results of this research both validate and alleviate this concern. In one sense, the results of this research validate this concern because it is clear from the post cure studies that the degree of cure can be alarmingly low (around 50%) for a photopolymerization if certain conditions are not optimized (initiator formulation, light intensity, exposure time). However, the post cure studies also alleviate the concern because they show that photopolymerization strategies do exist which be used to produce polymers where the percentage of conversion approaches unity.

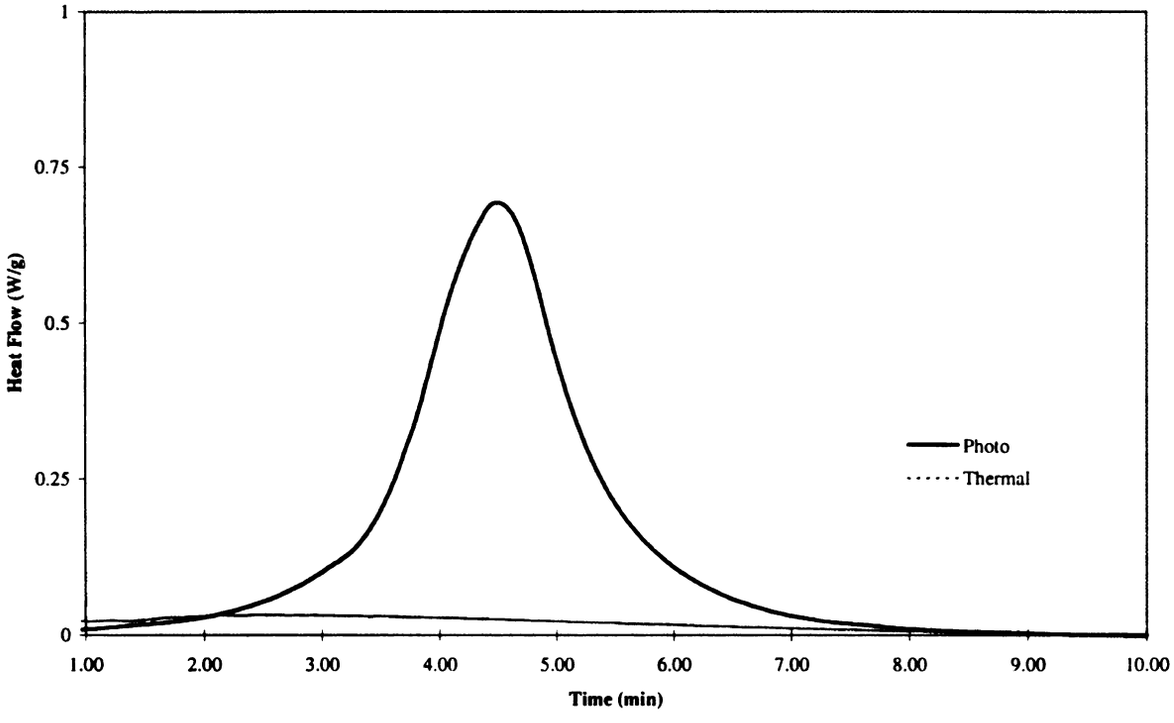

Figure 6.1. Reaction profile for photoinitiated and thermally initiated vinyl ester system at 25°C.

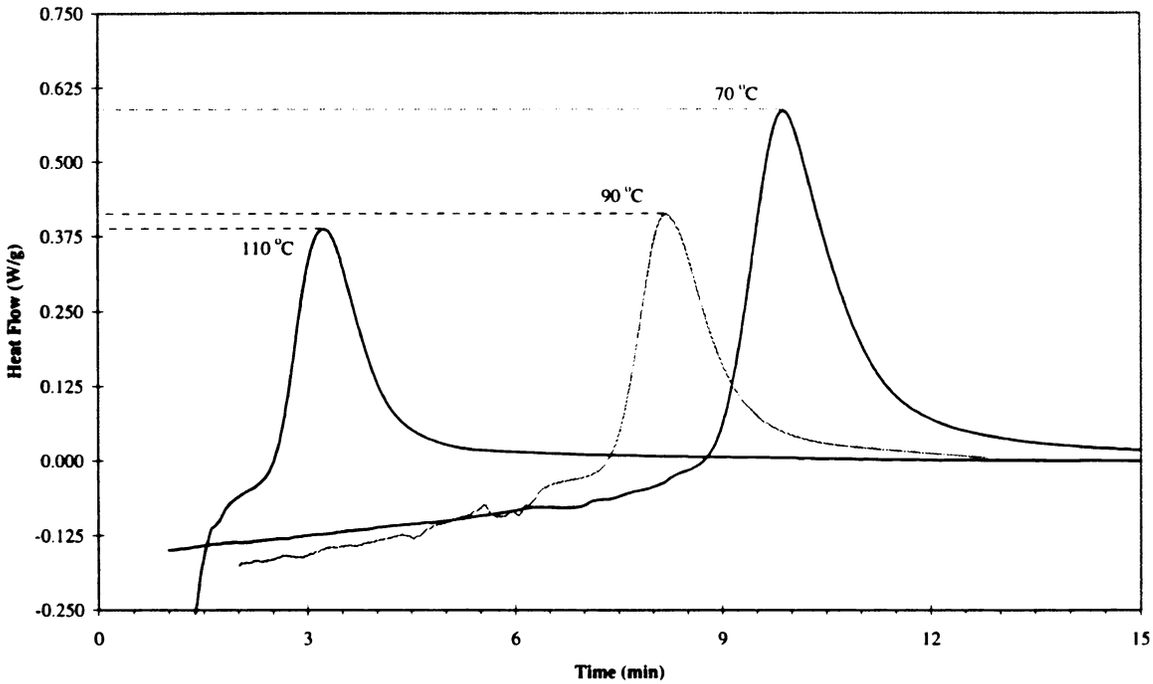

Figure 6.2. Effect of system temperature on the reaction rate profile for samples cured using 0.1 wt% BME to photoinitiate the polymerization.

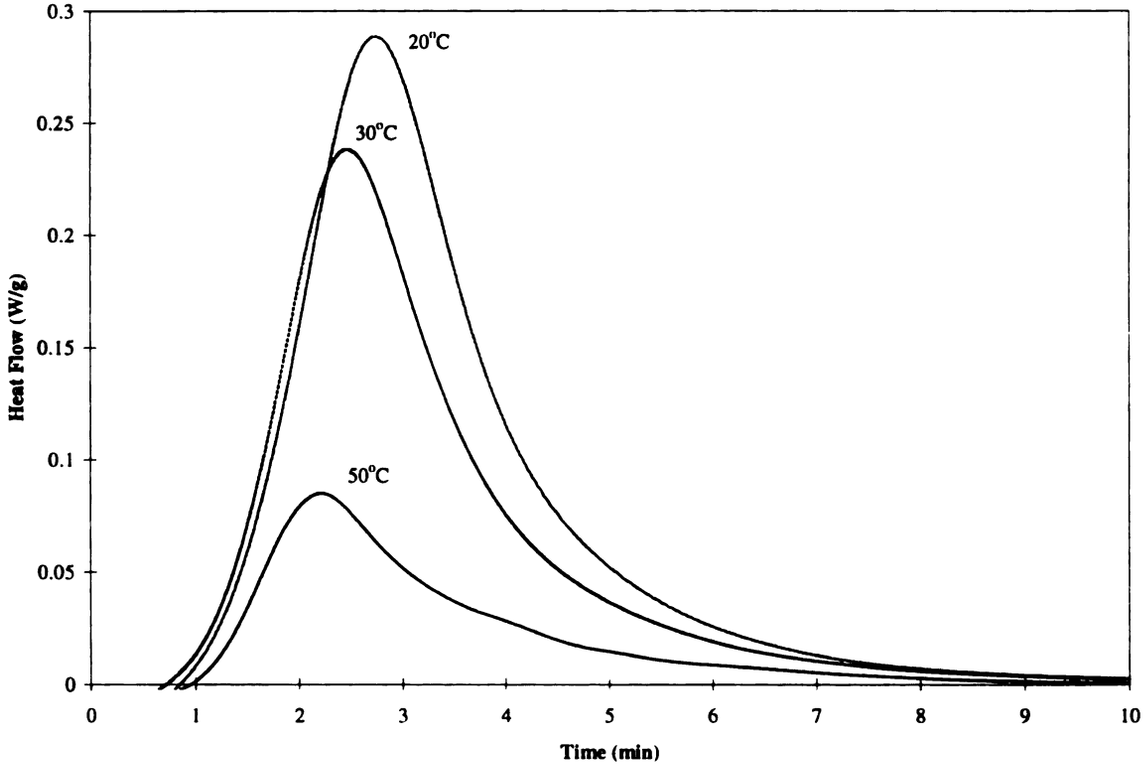

Figure 6.3. Effect of system temperature on the reaction rate profile for samples cured using 0.1 wt% Irgacure 651 to photoinitiate the polymerization.

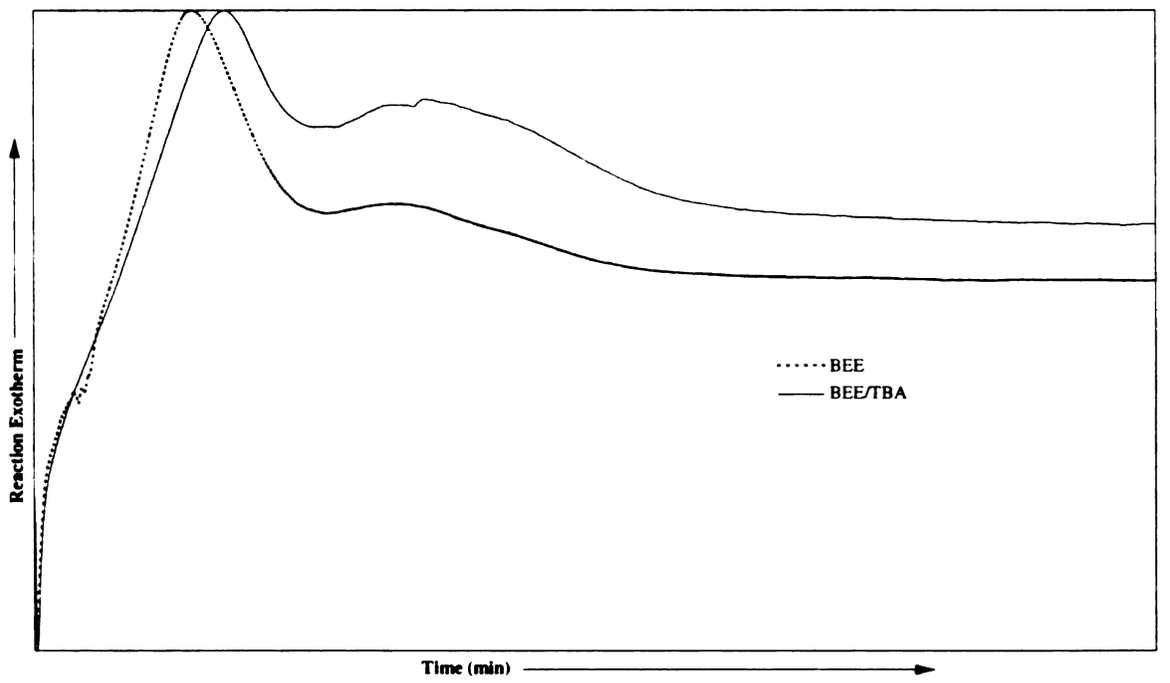

Figure 6.4. Effect of initiator formulation on the reaction rate profile for photocured (2 mm thick) vinyl ester polymers.

6.5. References

1. T. Doornkamp, Y.Y. Tan, *Polym. Comm.*, **31**, 362 (1990).

2. J.G. Kloosterboer, G.F.C.M. Litjen, *Polymer*, **28**, 1149 (1987),

3. J.G. Kloosterboer, "Network formation by chain crosslinking photopolymerizations and its application in electronics," *Adv. Polym. Sci.*, **84**, 1 (1988).

4. K.S. Anseth, C.M. Wang, C.N. Bowman, "Kinetic evidence of reaction diffusion during the polymerization of multi(meth)acrylate monomers," *Macromolecules*, **27**, 650 (1994).

5. K.S. Anseth, C.M. Wang, C.N. Bowman, "Reaction behavior and kinetic constants for photopolymerizations of multi(meth)acrylate monomers," *Polymer*, **35**, 3243 (1994).

6. R. Mallavia, F. Amat-Guerri, A. Fimia, R. Sastre, "Synthesis and evaluation as a visible-light polymerization photoinitiator of a new eosin ester with an *O*-benzoyl-α-oxooxime group," *Macromolecules*, **27**, 2643 (1994).

7. C. Decker, K.J. Moussa, "Real-time monitoring at ultrafast curing by UV-radiation and laser beams," *Coatings Tech.*, **62**, 55 (1990).

8. E.A. Grulke, *Polymer Process Engineering*, Prentice Hall, Englewood Cliffs, NJ, 1994.

9. H.E. Pebly, "Glossary of Terms," in *Composites*, **Vol. 1**, ASM International, Metals Park, OH, 3 (1987).

10. A.B. Scranton, et. al. Macromolecules paper on using dsc to characterize the polymerization rates of exothermic systems.

11. R.E. Sanders, S. Taha, "Bonding cure considerations," in *Composites*, **Vol. 1**, ASM International, Metals Park, OH, 702 (1987).

12. J.L. Courter, "Thermal Analysis," in *Composites*, **Vol. 1**, ASM International, Metals Park, OH, 779 (1987).

13. G. Odian, *Principles of Polymerization*, 3rd edition, Wiley & Sons, New York, NY, 1992.

14. E. Bortel, A. Kochanowski, W. Rys, E. Witek, "Polymerization initiated by the system triethanolamine/hydrogen sulfite with and without the cooperation of hydrogen peroxide. 1. Polymerization of acrylamide," *J.M.S. - Pure Appl. Chem.*, **A32**, 1197 (1995).

15. G. Seretoudi, I. Sideridou, "Benzil/n,n-dimethylaminoethyl methacrylate system as photoinitiator for methyl methacrylate polymerization," *J.M.S. - Pure Appl. Chem.*, **A32**, 1183 (1995).

CHAPTER 7.

THERMAL AND MECHANICAL CHARACTERIZATION OF POLYMER SYSTEMS

7.1. Introduction

In the broadest sense, any structure having a combination of two or more distinct materials where there exists a distinguishable interface between the materials can be defined as a composite.[1] However, in general terms, composites are thought of as materials having a reinforcing phase and a binder phase. In these terms, composites are distinguished by, and used for, their structural properties. Moreover, there are a number of applications where the working environment subjects the composite to thermal stresses. Thus it is important to expose the polymeric composites to a variety of thermal stresses in order to determine its thermal stability. In fact, most composites are used based on their structural properties. It was therefore important that both the mechanical properties and thermal stability of the polymeric composites developed in this research be characterized to determine their potential for industrial applications.

The phrase "mechanical properties" is a catchall term that is used to lump many different properties into one broad definition. For example, polymeric properties such as solvent, chemical and electrical resistance may be grouped with tensile properties including modulus, strength and elasticity into the definition of "mechanical properties".[2] However, there are more specific definitions of mechanical properties such as the one

offered by Pebly,[3] where mechanical properties refer to "compressive and tensile strengths, and modulus, that are associated with elastic and inelastic reaction when force is applied..." that can result in confusion when it is unclear what someone is referring to when they use the phrase "mechanical properties". To avoid any confusion, the definition offered by Pebly will be used to describe the phrase "mechanical properties" in this contribution.

A number of techniques are available which use well-developed, standard testing methods for characterizing the mechanical properties of polymers and composites. In addition, there exist a tremendous array of thermal analysis techniques such as thermogravimetric (TGA), thermomechanical (TMA) and dynamic mechanical (DMA) analysis which are commonly used to identify the thermal properties of composites. Through a combination of these techniques, one is able to obtain a detailed thermal and mechanical "history" for polymers and composites that includes the glass transition temperature, thermal stability, flexural strength and modulus, loss modulus, and thermal expansion coefficient of polymers and composites. In this research, the properties which were of most interest included the flexural strength and modulus, the thermal stability, and the dimension change. The techniques used most frequently in this research included TGA, TMA, and flexural testing because the properties of immediate interest included thermal stability, dimension change as a function of temperature, and flexural strength and modulus.

Thermogravimetric Analysis (TGA) is a useful tool for analyzing polymers and composites. In basic terms, TGA measures changes in weight as a sample is heated or cooled. When used in conjunction with mass analyzers such as gas chromatography or

mass spectrometry, TGA can be used to determine the composition of composites.[4] In this research, however, TGA was used to study the degradation kinetics for several polymer and composite systems. TGA is not ideally suited to monitoring the degradation process because it does not allow for good environmental control during the degradation process.[4] However, it can be extremely useful in determining the onset temperature for degradation, T_o, and regions where the composite is thermally stable. Finally, TGA results can be applied to specific systems to determine their long-term stability in various thermal environments under several atmospheric (oxygen, nitrogen, etc.) conditions.

Thermomechanical analysis (TMA) measures dimensional changes in a polymer as a function of temperature. Specifically, it measures minute changes in polymer length or thickness as the sample is heated at a constant rate.[5] TMA is an excellent method for measuring α, the coefficient of thermal expansion, which is critical to minimizing or eliminating stresses between fiber-matrix interfaces depending on the composite design. For example, the value of α is a significant factor when designing graphite composites.[6] TMA does not require large sample sizes, typically on the order of 0.0625 in^2, and it can also be used to measure the glass transition temperature, T_g. Unfortunately, it is often difficult to measure T_g using TMA because it is corresponds to the point where α changes. This change can be extremely minor depending on the sample, therefore it may go undetected using TMA.

Flexural modulus can be defined as the resistance to deformation while flexural strength can be defined as the amount of stress required to break a sample. Flexural modulus and strength values have units of force per area and are typically reported in units of gigapascals and megapascals, respectively. To measure the flexural modulus, a

stress is applied to a polymer of known dimension and the elongation resulting from the applied stress is measured, often as a percent elongation. To determine the flexural strength, increasing stress loads are applied to the sample at a constant rate until the sample breaks. The point at which the sample breaks is often described as the "ultimate elongation".[2] The elasticity of a given sample can also be determined using flexural testing by measuring the amount of reversible elongation.[2,3]

There are a number of methods which can be used to obtain values for the flexural modulus and flexural strength, however the most widely accepted technique for flexural testing is established by the American Society for Testing and Materials (ASTM) and is called ASTM D790.[7] The ASTM method is inexpensive, easy-to-use, and generally provides good quality-control from one sample to the next.[8,9] Unfortunately, flexural strength is not an intrinsic property, therefore careful attention has to be paid to the method of preparation in order to ensure that one does not generate slight deviations from sample to sample that result in slight variations in the flexural strength values.[8]

The focus of the remainder of this chapter is to present the results of material characterizations for polymers formed by the photoinitiation strategies (SEG and dual-cure) which have been described throughout this contribution and to discuss the impact of these results on present and future research in the area of photopolymerizations of thick polymers and composites.

7.2. Experimental

The resins used in this study were vinyl ester Derakane resins 411C50, 441 and 470 provided by Dow Chemical Company (Midland, MI). Numerous types of glass reinforcements were used in this research including powdered (E) glass fiber, 5 mm long chopped fibers, Vetrotex Certainteed (Uniflow U750, Vetrotex) fiber roving and woven glass mat. Initiators which were evaluated include benzoin ethyl ether (BEE), benzoin methyl ether (BME), benzoyl peroxide (BP), (Aldrich Chem. Co.) and α,α-dimethoxy-α-phenylaceto-phenone (sold by Ciba-Geigy under the trade name Irgacure 651). All materials were used without further purification. To prepare a photopolymerizable mixture, a predetermined amount (~0.2 wt%) of the initiator was dissolved in the resin at room temperature by stirring on a magnetic plate. These mixtures were remarkably stable in the absence of initiating light (even at elevated temperatures ~60°C). Prior to use, the reactive resins were stored in the dark at room temperature.

The primary light source used in this study was a 1000 watt Hg(Xe) arc lamp (model 6293) from Oriel Corporation, (Stratford, CT) equipped with a water filter to eliminate infrared light from the incident beam thereby reducing thermal effects. Additional experiments were performed using a 100 watt Black-Ray® long wave ultraviolet lamp (model B100AP), produced by UVP (San Gabriel, CA) and a 200 watt Hg(Xe) arc lamp (model 6291) from Oriel Corporation. Light intensities were measured using a UVP Blak-Ray ultraviolet meter (model J225), and the intensities were varied both by using the condenser lens on the lamp and by changing the distance between the sample and the light source.

Samples of the reactive formulation were polymerized in both rectangular and cylindrical geometries. These reactions were carried out in silicone molds with light projected down onto the sample, in cylindrical glass molds irradiated either axially or radially, and in rectangular acrylic (poly(methyl methacrylate)) molds irradiated either axially or radially. Composite materials were prepared by two methods. In the first method, the fiber reinforcement was placed in the mold and the mold was subsequently filled with the resin-initiator mixture. The filled mold was then placed under UV light for measured periods of time. In the second method, the powdered glass fiber reinforcement was mixed with the formulated resin to form a slurry with a desired fiber loading. This slurry was poured into the mold and irradiated with UV light for a predetermined period of time.

Flexural properties of various polymeric and composite specimens were measured using a United STM-20 instrument according to the ASTM D 790 method. All mechanical properties were measured by the three point flexural strength test, using 50.8 mm (2 inch) long samples with a length to thickness ratio of ~ 16. A 454 kg (1000 pound) load cell was used with a downdrive rate of 0.0212 mm/sec (0.05 in min^{-1}). The flexural modulus was calculated for these samples at elongations between 0.0013% to 0.0064% of a meter. The STM-20 measures the load, P, and the elongation, δ, and using these values the flexural modulus, E, can be calculated. Equation 7.1 relates the load to elongation for cylindrical rods of radius r and length L.

$$P = \left(\frac{12 \pi r^4 E}{L^3} \right) \delta \qquad (7.1)$$

The flexural modulus can then be calculated by computing the slope of the linear region of P vs. δ, then using equation 7.2.

$$E = (\text{slope})\left(\frac{L^3}{12\,\pi\, r^4}\right) \tag{7.2}$$

A similar equation was used for rectangular samples (Equation 7.3) where b is the width, h is the thickness, and L is the length of the rectangle.

$$P = \left(\frac{4\,bh^3E}{L^3}\right)\delta \tag{7.3}$$

E can be calculated for rectangular samples using Equation 7.4.

$$E = (\text{slope})\left(\frac{L^3}{4bh^3}\right) \tag{7.4}$$

Average values of measurements from at least four different samples were used for each specimen, with the error bars shown in corresponding figures representing absolute high and low values.

Thermomechanical (TMA) and thermogravimetric (TGA) analysis experiments were performed using analyzers produced by TA Instruments. TGA samples (~ 20 mg per sample) were placed in aluminum pans and analyzed in both nitrogen and air atmospheres. TMA samples were cylindrical in geometry with a length of 12 mm and a radius of ~2.7 mm. Samples that were subjected to post-cure conditions have been noted, otherwise samples were tested after irradiation.

7.3. Results and Discussion

7.3.1. Flexural Testing

In order to determine the effects of various processing parameters on the mechanical properties of the polymers and composites produced by photopolymerization, a series of experiments were conducted in which operational parameters such as initiator concentration, cure time and initiating light intensity were varied for each initiating (SEG and dual-cure) strategy. The initial flexural testing experiments were performed in order to determine if photocured samples were capable of producing polymers whose flexural properties were comparable to polymers cured using traditional (i.e. thermal) curing methods. The results of these experiments showed that values for flexural modulus of UV cured vinyl ester resins (cured for 300 seconds at an incident intensity of ~1.5 $\mu W/cm^2$) were indeed comparable to the properties of specimens cured thermally (at 363 K) for 24 hours, and were on the same order of magnitude as values reported in the literature for vinyl ester polymers.[10] For example, unfilled 411c-50 samples which were UV cured had a flexural modulus of 3.10-3.17 GPa, while thermally cured 411c-50 samples counterparts had a flexural modulus of 2.96-3.10 GPa and literature values for vinyl ester polymers were reported as 3.90 GPa.[10] These unfilled systems showed elastic behavior, as evidenced by a linear load-displacement curve, and did not fracture at the maximum displacement of 0.0013 m (0.05 inches).

The photoinitiator concentration has an effect on the modulus of the polymers formed by photopolymerization. In a sequence of experiments the initiator concentration was varied from 0.1 to 4 wt%, in neat resin. These unfilled samples were exposed to UV

light (with radial initiation of 8 mm diameter samples with a light intensity of 4.4 $\mu w/cm^2$) for a period of 240 seconds. Samples containing 2 and 4 wt% of initiator did not completely polymerize in this time frame. The flexural modulus of the remaining samples (0.1 to 1 wt% initiator) were measured and were shown previously in Chapter 4 (*Figure 4.7*). *Figure 4.7* shows that the maximum flexural modulus is achieved between 0.15-0.25 wt% of initiator. As the concentration of initiator is increased beyond this point, there is a dramatic reduction in the penetration of initiating light and decreasing percentages of the sample cure until eventually only a thin film is cured at the surface of the sample (an effect observed when the concentration of initiator in the sample reached 2 wt%). It should be noted that the optimal initiator formulation shown in *Figure 4.,7* is for the SEG strategy since the dual-cure system does not rely as heavily on efficient penetration of light as this system.

This result led to a series of experiments where the amount of time allowed for cure was varied. It was believed that, at a given intensity, the sample would cure completely if enough time was allowed for the intensity gradient to eliminate completely or be reduced significantly. If this were the case, this effect should manifest itself in the form of increased flexural modulus values. The relative importance of cure time was investigated for both SEG and dual-cure systems and proved to be somewhat dependent on the method of initiation. For these measurements the 470-45 was used with very finely- chopped (powdered) e-glass fibers. These studies were conducted on samples which were 8 mm (1/4 inch) thick, at a light intensity of 4.4 $\mu W/cm^2$. A slurry consisting of the desired fiber loading, resin, and initiator (~ 0.2 wt% BEE) was poured into a cylindrical glass mold coated with a release agent (silicone spray). The samples, which

were 8 mm (1/4 inch) thick, were exposed to the initiating light at an intensity of 4.4 $\mu W/cm^2$. The light was incident to the radial direction, and had to pass through a maximum distance of 8 mm. After exposure to the light for a predetermined period of time the mold was removed from the light and allowed to cool to room temperature. The sample was then removed from the mold and its flexural properties were tested.

The results of these studies are shown in *Figure 7.1*. This figure shows the effects of cure time on the flexural modulus of glass-filled and unfilled vinyl ester composites/polymeric materials. The results indicate that after 420 seconds (7 minutes) of cure there is no further increase in the modulus of the material. It may also be noted that there is a slight decrease in flexural modulus at higher exposure times, although this decrease falls close to the limits of experimental error. It is believed, however, that this phenomena may be due to degradation of the polymer by UV light. As expected, increasing the amount of fiber increases the flexural modulus of the samples. It can be seen that the flexural modulus increases by a factor of 3 at 50 wt% fiber loading when compared to the unfilled sample.

Figure 7.2 shows the effect of cure time on the flexural modulus of composites formed by the hybrid photo/thermal initiating mechanism. It may be observed from this figure that the plateau in flexural modulus is reached significantly sooner with the dual-cure mechanism, even at relatively high fiber loadings. This is attributable to the completeness and uniformity of cure provided by the thermal reaction. In essence, *Figure 7.2* shows that samples cured completely in less than two minutes using the dual-cure strategy.

The relative importance of the incident light intensity is highly dependent on the method of initiation. For example, when a polymer is cured using the dual-cure strategy, the intensity of the initiating source is a minor consideration. However, when the self-eliminating gradient (SEG) strategy is used to polymerize the composite, the mechanical properties become highly dependent on the incident intensity (recall *Figure 4.11*). The effects of initiating light intensity and cure time on the flexural modulus of samples initiated via the SEG strategy are shown in *Figure 7.3*. In these experiments samples containing 470-45, 0.08 wt% BEE, 0.08 wt% BME and 25 wt% powdered e-glass fibers were polymerized under UV light at various light intensities, for different periods of time. Each sample was 8 mm in diameter, and the initiating light intensity was varied between 2.2, 3.3 and 5.5 mw/cm^2. As previously observed, increasing the time of cure increased the mechanical strength of the composite. It was also observed that increasing the intensity of the initiating light resulted in an increased flexural modulus of the final composite, and also reduced the cure time. This suggests that higher light intensities allow the samples to cure more completely in shorter periods of time, resulting in a higher flexural modulus. Indirectly, this experiment also shows that, while they are effective initiators for thick photopolymerization, benzoin ethers do not produce a *completely* self-eliminating gradient. *Figure 7.3* supports this contention because, in theory, the flexural modulus values at each light intensity should approach an asymptotic limit given enough time to cure. However, this does not occur, therefore it is likely that low intensity light sources will be less efficient than moderate or high intensity light sources at curing thick samples.

One final set of experiments were conducted to determine the effect of cure time on flexural strength. The results of this experiment are presented in *Figure 7.4*. The samples in this figure were cured using 0.2 wt% BEE as the photoinitiator with finely chopped e-glass fibers employed as the reinforcing material at a loading of 50 wt%. The fibers were similar in texture to baby powder and they provided an extremely low aspect ratio. Therefore, they were not expected to provide a large amount of stiffening. Instead they were selected for this set of experiments because they were the most challenging system available because their presence in the reactive resin maximized the light scattering and presented the highest number of resin/fiber interfaces. The result of this formulation is a system that is perhaps the most difficult photopolymerize. To emphasize this, one need only compare the neat and fiber-filled polymers after each had been photocured. While the unfilled polymers were clear with a light yellow color, the composites obtained using the powdered fibers were gray, opaque, and produced almost a marble-like finish once they had been completely cured. *Figure 7.4* showed that the samples had reached a maximum value of ~ 0.1 GPa after being exposed to incident light of ~ 1.5 $\mu W/cm^2$ for a total of 5 minutes. The plateau achieved for samples cured for five minutes or longer indicated that the samples had cured completely after five minutes.

7.3.2. Thermal Analysis

Thermogravimetric analysis of the vinyl ester samples showed that there was virtually no degradation at 573 K. *Figure 7.5* shows TGA curves for each of the vinyl ester resins used in this research. Each of the samples in *Figure 7.5* was cured for eight minutes at a light intensity of 3.13 $\mu W/cm^2$ using a 0.1/0.1 BEE wt%/BP wt% initiator formulation.

As this figure shows, the lowest viscosity resin begins to degrade first (470-45, around 378°C) followed by the medium viscosity resin, 411c-50 (384°C) and finally 441-400, the most viscous resin (~ 390°C). The results of this experiment support the contention that these polymers are suitable for use temperatures < 275°C.

The final set of experiments performed on the cured composites were designed to characterize the thermal expansion coefficient, α, and the glass transition temperature, T_g, for neat polymers and composites. The effects of initiator formulation and cure time on are shown in *Table 7.1* for 470-45 and 441-400 vinyl ester resins.

Table 7.1. Thermal expansion coefficient as a function of initiator formulation and cure time for vinyl ester polymers.

Resin	Initiator Formulation	Cure Time (min)	α (mm/m°C)
470-45	BEE	3.5	23.52
470-45	BEE	8	23.06
470-45	BEE/BP	3.5	23.46
470-45	BEE/BP	8	21.82
441-400	BEE	3.5	34.23
441-400	BEE	8	26.12
441-400	BEE/BP	3.5	30.44
441-400	BEE/BP	8	26.43

The results in *Table 7.1* show that as the cure time was increased for each sample, the thermal expansion coefficient decreased for each sample regardless of initiator

formulation or resin type. This is likely a result of enhanced cure as the amount time allowed for cure was increased. Further scrutiny of *Table 7.1* shows that, for the most part, the thermal expansion coefficient was slightly smaller for samples cured using the dual-cure method. Again this would seem to suggest that the dual-cure method cured samples more completely than the SEG strategy. A final observation of this table shows that α was ~ 37% larger for the highly viscous (441-400) resin than the low viscosity resin (470-45) when the sample was cured for 3.5 minutes, however it was only 17% larger when the samples were cured for a total of 8 minutes. This seems to suggest that the effect of viscosity can significantly affect the kinetics of the reaction.

The effect of fiber loading on α was also studied in addition to cure time, initiator formulation, and resin type. *Figure 7.6* compares α values for neat polymers and composites having a 50 wt% fiber loading of powdered e-glass fibers. As expected, α values decreased for each viscosity resin as fibers were added to the polymer.

For the most part, both DSC and TMA proved to be somewhat ineffective at determining the glass transition temperature for the polymers investigated in this research. Due to the highly crosslinked structure of the polymers formed in these reactions, any evidence of a T_g would be subtle. With this in mind, TMA did show T_g values between 120-150°C for vinyl ester samples. *Figure 7.7* shows TMA curves for two vinyl ester polymers photocured for 3.5 minutes at a light intensity of 3.13 $\mu W/cm^2$. T_g is determined as the point where the slope of the specific volume curve changes. *Figure 7.7* This occurs at ~ 125°C for 441-400 and 145°C for 470-45. The higher T_g value for the low viscosity resin may in part be due to a higher degree of cure (and an increased high

degree of crosslinking). In general, T_g values determined via TMA experiments were in the 120-150°C range for each of the Derakane resins investigated in this research.

7.4. Research Conclusions/Chapter Summary

The results presented in this chapter show that the materials produced by SEG and dual-cure strategies exhibit mechanical properties comparable to composites cured using traditional (i.e. thermal) methods. The effects of basic operational variables such as cure time, light intensity, photoinitiator concentration, fiber loading and temperature on the performance of the composites have been established. Additional experiments have shown that increasing the fiber loading of the samples reduces both the rate of reaction and the temperature rise in the sample. Increasing the initiating light intensity not only enhanced the reaction rate but also increased the flexural modulus of the final composite. These studies demonstrate the tremendous potential of photopolymerizations for the affordable manufacture of composite materials, and show that with careful attention to detail, photopolymerizations can be used to rapidly produce products with outstanding mechanical properties.

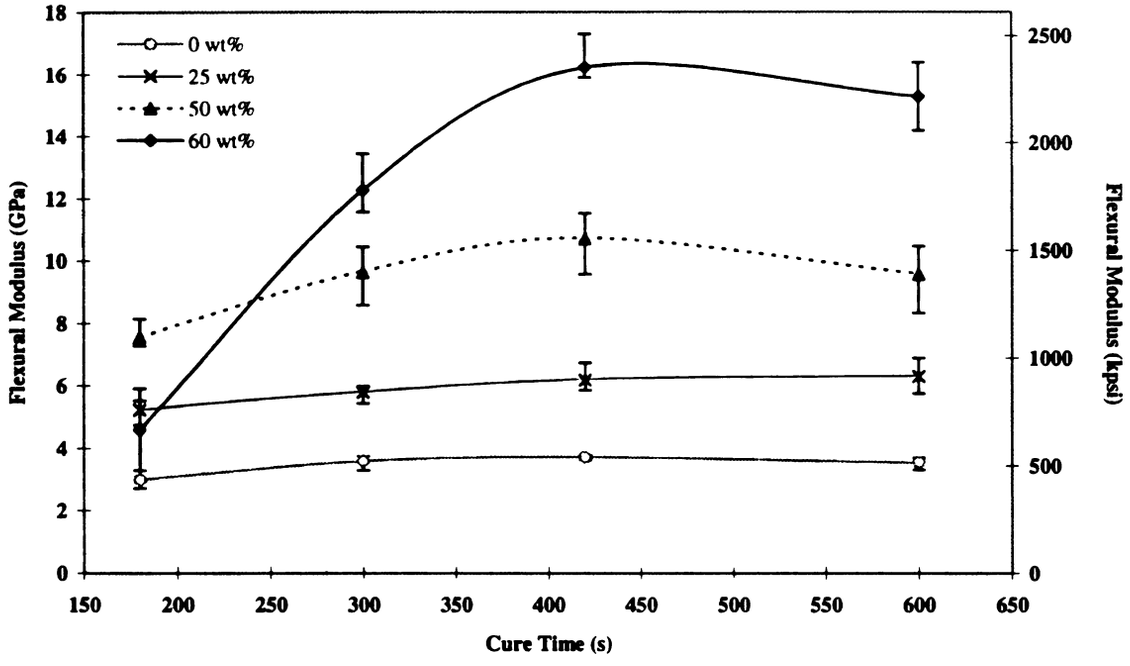

Figure 7.1. The effect of irradiation time and degree of fiber loading on the flexural modulus of vinyl ester polymers cured using the SEG strategy.

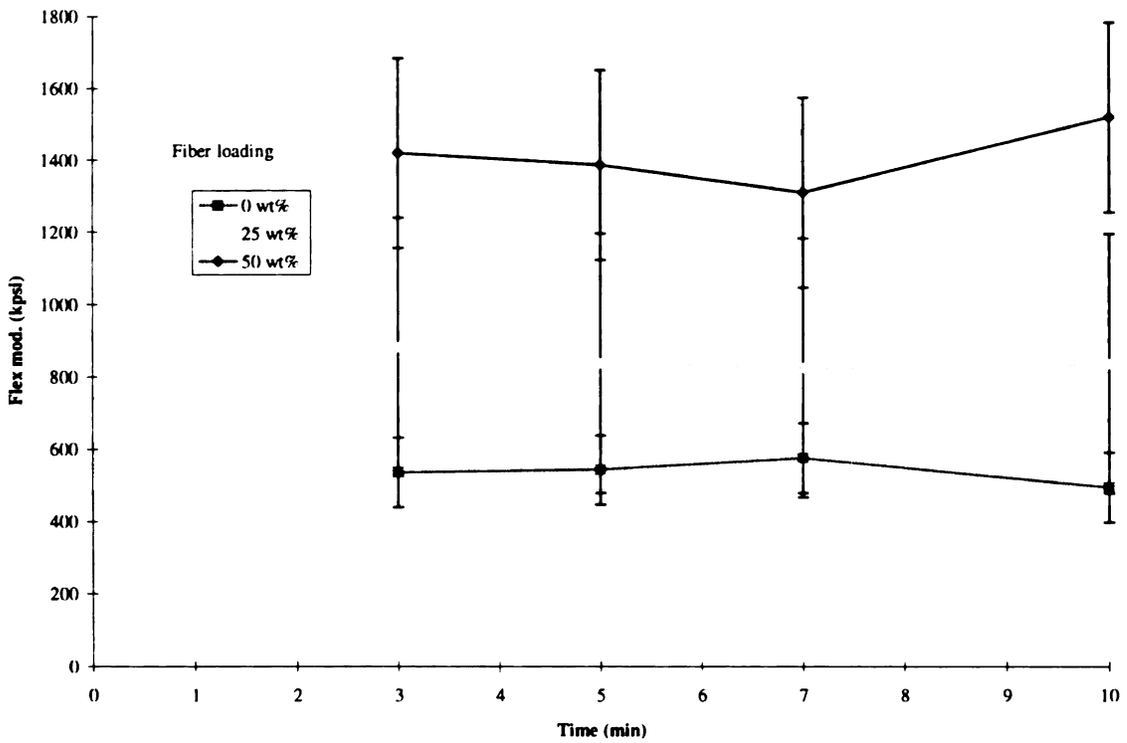

Figure 7.2. The effect of irradiation time and degree of fiber loading on the flexural modulus of vinyl ester polymers cured using the dual-cure method.

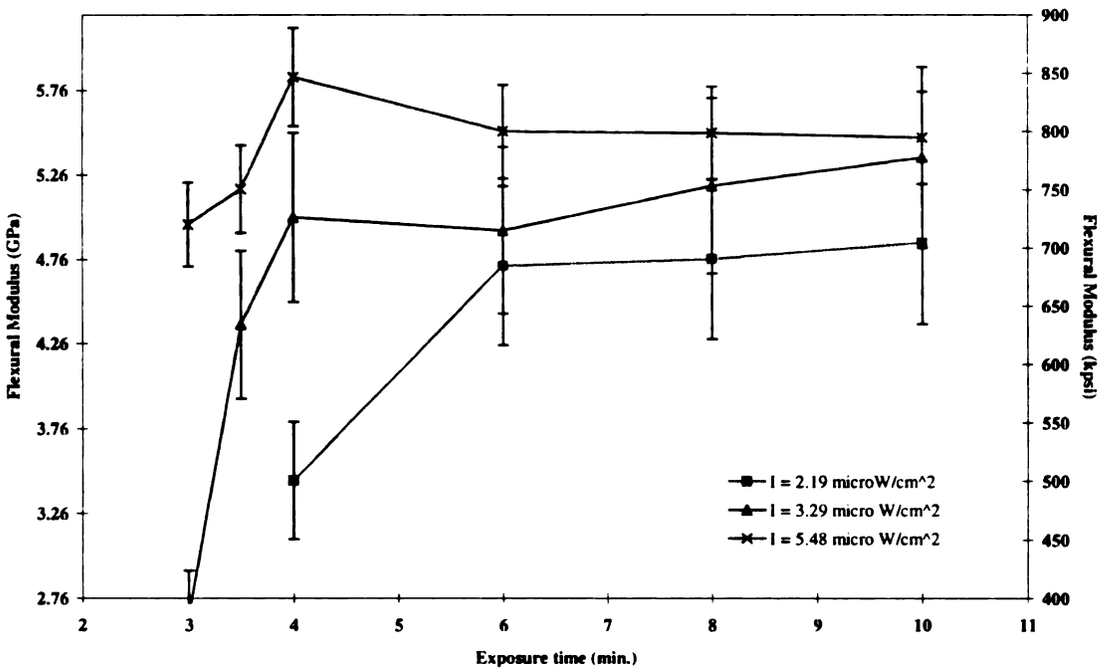

Figure 7.3. The effects of light intensity and cure time on the flexural modulus of composites with a 25 wt.% fiber loading.

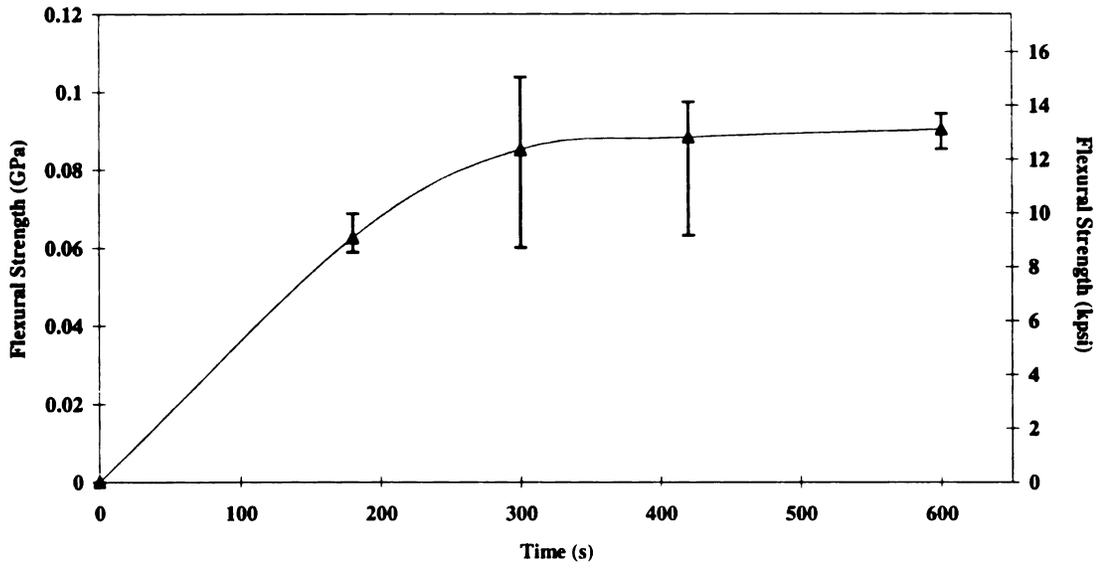

Figure 7.4. The effect of cure time on the flexural strength of vinyl ester composites with a 50 wt% chopped e-glass fiber loading.

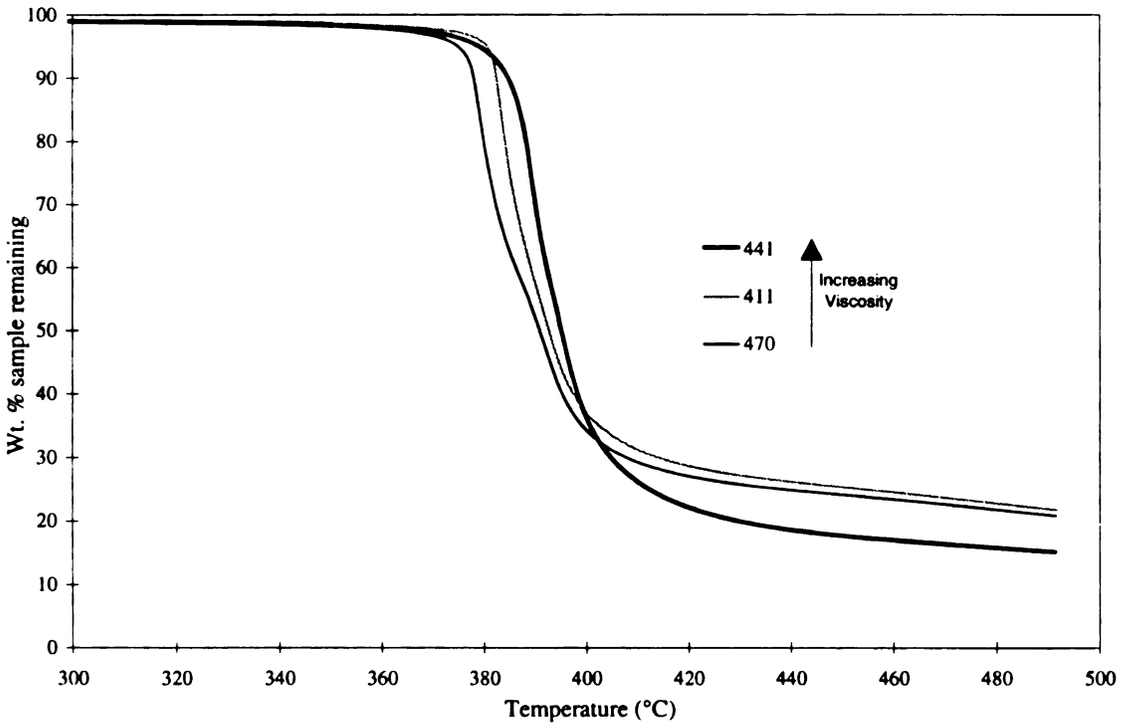

Figure 7.5. TGA profiles for vinyl ester resins as a function of temperature.

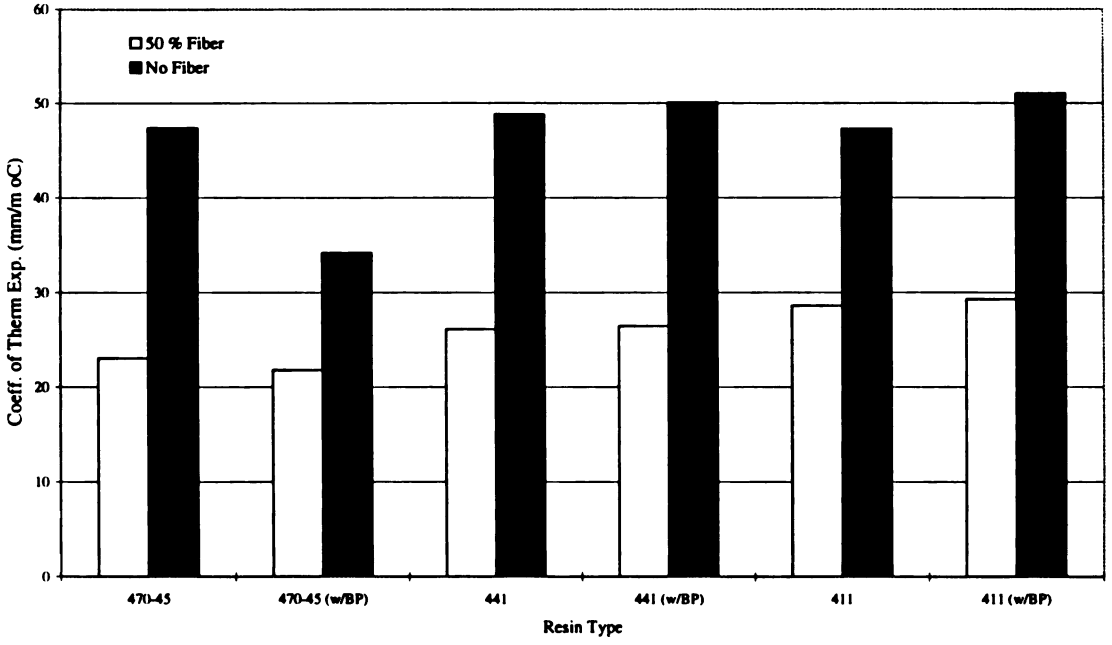

Figure 7.6. Effect of fibers on the thermal expansion coefficient of vinyl ester polymers.

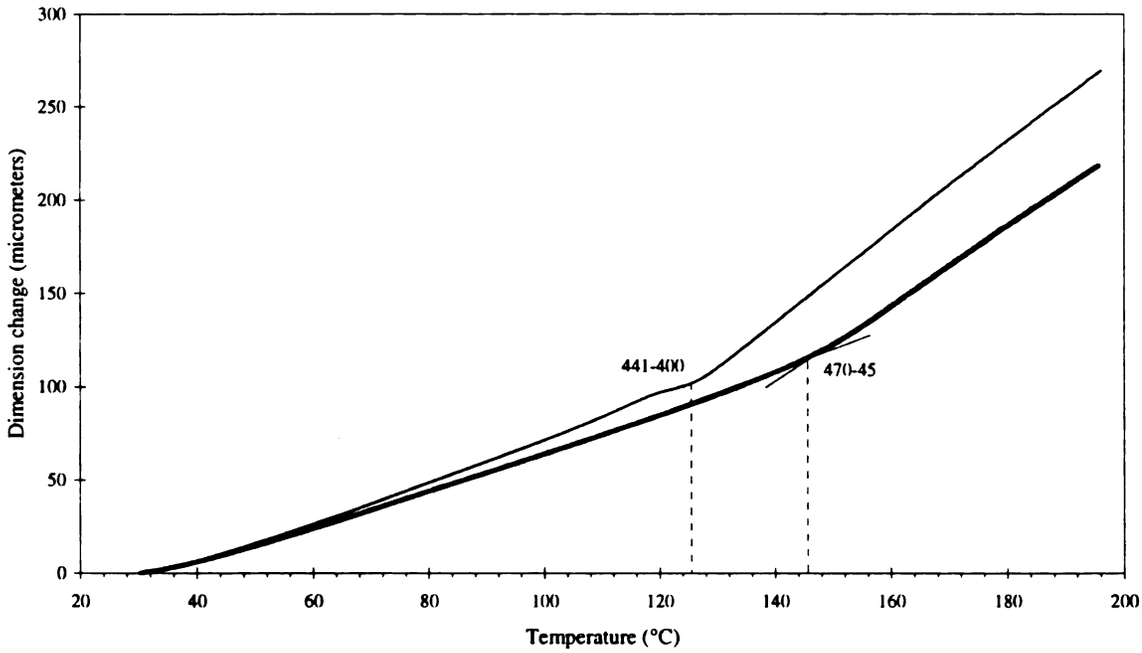

Figure 7.7. Determination of the glass transition from TMA profiles for vinyl ester polymers.

7.5. References

1. T.J. Reinhart, L.L. Clements, "Introduction to composites," in *Composites*, **Vol. 1**, ASM International, Metals Park, OH, 27 (1987).

2. G. Odian, *Principles of Polymerization*, 3rd edition, Wiley & Sons, New York, NY, 1992.

3. H.E.Pebly, "Glossary of terms," in *Composites*, **Vol. 1**, ASM International, Metals Park, OH, 3 (1987).

4. E.A. Grulke, *Polymer Process Engineering*, Prentice Hall, Englewood Cliffs, NJ, 1994.

5. J.L. Courter, "Thermal analysis," in *Composites*, **Vol. 1**, ASM International, Metals Park, OH, 779 (1987).

6. R.H. Stone, "Dissimilar material selection," in *Composites*, **Vol. 1**, ASM International, Metals Park, OH, 716 (1987).

7. "Standard test methods for flexural properties of unreinforced and reinforced plastics and electrical insulating materials," **D 790**, American Society for Testing and Materials.

8. N.R. Adsit, "Mechanical properties and environmental exposure tests," ," in *Composites*, **Vol. 1**, ASM International, Metals Park, OH, 295 (1987).

9. R.B. Pipes, R.A. Blake, "Test methods," in *Composites Design Encyclopedia*, **Vol. 6**, University of Delaware, 68 (1983).

10. C.D. Dudgeon, "Polyester resins," in *Composites*, **Vol. 1**, ASM International, Metals Park, OH, 90 (1987).

CHAPTER 8.

INVESTIGATION OF ADDITIONAL POLYMER SYSTEMS

This chapter summarizes work performed at the initial stages of this research in the area of polymer networks. Specifically, this work focuses on ladder polymers and interpenetrating polymer networks (IPNs). This work served as the groundwork for the more detailed research on photopolymerizations by providing valuable experience in the areas of radical and cationic chain polymerizations. In addition, a number of experiments used in the development of novel photopolymerization strategies were first tested on these polymer networks. Finally, the inclusion of thermal initiators in the dual-cure system evolved in part from the working knowledge that had been established during this introductory research.

This chapter will be divided into two main sections, one detailing research performed on ladder polymers and one describing a potential method for producing interpenetrating polymer networks. The majority of pre-photopolymerization research was on ladder systems, thus the focus of experimental work in this chapter will be on these types of polymeric structures.

8.1. Ladder Polymers

Ladder polymers, or fused-ring chain polymers, have received attention for their ability to achieve both superior resistance to molecular weight losses *and* high thermal

stability. This class of polymers is so named because its chemical structure physically resembles a ladder. Ladder polymers occur when several bifunctional monomers or aromatic rings are linked together to form an uncrosslinked polymer. These polymers exhibit strong resistance to decreases in molecular weight and superior thermal resistance due to the fact that for chain scission to occur there must be at least two cleavages within the same ring structure. This is a statistically unlikely condition unless massive oxidation occurs.[1] Their unique structure allows ladder polymers to approach the maximum serviceability temperature limits of organic polymers, widely reported to be in the 250-300°C range,[2,3] while their superior properties make them industrially useful for aeronautical applications, as fiber materials, and as composite parts.[1,2] Additionally, the excellent thermal resistance of ladder polymers makes them ideal for high-temperature applications such as aerospace charring ablators.[4]

Ladder polymers are unique in the sense that every polymer contains bifunctional monomers where both functionalities have been polymerized to form two distinct polymeric backbones. The degree of polymerization for each functionality within each individual ladder polymer determines whether or not the ladder structure is perfect or imperfect. Structures having no cleavages in either backbone may be described as perfect ladder polymers while a single cleavage in either polymer backbone results in an imperfect ladder polymer. The production of imperfect ladder polymers is not a desired reaction since they fail to enhance either the thermal or the mechanical properties when compared with their linear chain analogs.[5]

Early attempts to produce ladder structures centered on sequentially polymerizing bifunctional molecules. However, this technology has seen only limited success because

there does not appear to be a reaction that is capable of completely "closing up" each individual ring without some degree of cleavage or crosslinking once one of the functionalities have been reacted to produce a linear polymer with dangling chain ends. As a result of this, the majority of ladders formed are imperfect with little or no enhancement in mechanical or thermal properties while the perfect ladders typically have very low molecular weights. For these and other reasons, ladder polymers synthesis has focused primarily on two polymerization methods.

The first method used to form ladders involves a Diels-Alder reaction. In this reaction, each "rung" of the ladder is a single monomer unit, and the sides of the ladder are formed when that monomer undergoes 1,3-dipolar addition with a second monomer, thereby forming a ring where *both* sides of the monomer react at the same time. A strength of the Diels-Alder reaction is the fact that either both of the functional groups react or neither of the functional groups react, therefore no incomplete or imperfect rings may be formed.[6] However, a drawback of the Diels-Alder mechanism is rearrangement into more thermodynamically stable, non-ladder structures due to a lack of stability in the newly formed bonds.[2] An additional problem with the Diels-Alder method is that it typically forms low molecular-weight polymers with little or no enhancement in properties that are directly related to molecular weight. These problems limit the potential of this mechanism as an alternative for polymerizing ladder structures.

The second method used most often to produce ladders involves step copolymerization of two aromatic molecules such as imides, benzimidazoles or quinazolones.[7-10] The resulting polymers still fail to produce perfect ladder structures in most instances when formed using this method. For example, Ghafoor and Still[10] have

synthesized polymers from polyquinazolones and other aromatic molecules which were then cyclized to form only partial ladder structures. The problem with these structures is that only a single cleavage is required to cause significant decreases in the molecular weight. An additional problem with this mechanism is the cyclization step. Cycylization may not always occur, thereby creating an imperfect ladder structure because of the single linkages in the polymer.

8.1.1. Novel Ladder Synthesis Method

Scientists have been studying ladder polymers for a number of years with limited success in an attempt to develop a process which is capable of producing perfect ladder structures repeatedly. While some methods can guarantee that both functionalities of a given monomer will react in the proper manner (i.e. they will not cyclize), these same methods can not guarantee that the reaction will occur to a high degree of conversion. As a result, low-molecular weight polymers are formed which exhibit only slight increases in thermal and mechanical properties due to their (relatively) light weight. Although perfect ladder polymers exhibit excellent thermal and mechanical properties, they have not been used extensively in industrial applications because of the numerous difficulties inherent in their formation.

The initial thrust of this research effort was to produce ladder polymers from the monomer glycidyl methacrylate (GMA), also named 2,3-epoxypropyl methacrylate. The structure of a GMA monomer is shown in Figure 8-1. GMA is a bifunctional monomer (it contains an acrylate linkage and an epoxy functionality) that can be polymerized via a number of chain polymerization reactions. This monomer was thought to be ideal for

ladder polymer systems because its functionalities are mutually exclusive, meaning active cations will not initiate a propagation reaction in acrylate monomers while free-radicals are likewise unable to react with epoxides. The novelty of this research was underscored by the fact that it combined two chain polymerization mechanisms while insuring that there would be no crosslinking or reaction between systems whether the systems were reacted simultaneously or sequentially. This approach differed dramatically from research on network systems which had been investigated previously. In fact, the majority of networked polymer systems that require each system to be distinct from the other involve a combination of step and chain polymerizations to maintain the homogeneity of the polymers within the network.

Poly(glycidyl methacrylate) (PGMA) may form a number of ladder-like structures ranging from perfect, two-dimensional ladders to three-dimensional "ladders" to imperfect ladders. An additional structure which may be formed is a "crosslinked" polymeric ladder. This type of network is not actually a crosslinked polymer, instead it links poly(epoxy) homopolymers with poly(methacrylate) homopolymers via the "crosslinking agent" glycidyl methacrylate. Its unique structure allows GMA to polymerize via two distinct methods, therefore simultaneous polymerization of GMA may result in a number of homopolymer chains which are linked together through the backbone of the monomer. Some potential, ladder-like structures of PGMA are shown in Figure 8-2.

8.2. Ladder Polymer Research Experiments

A large majority of this research involved attaining a better understanding of the kinetics involved in these reactions. Specifically, a large amount of time was devoted to optimizing an experimental setup such that experimental conditions such as temperature, pressure, and method of initiation were repeatable. Although pressure changes during these reactions were generally not significant due to small-scale reactions and typically unsealed vessels, the temperature of the reaction was prone to large fluctuations depending on a number variables. Thus the temperature was monitored over the course of reaction in order to determine optimal conditions for these particular simultaneous reactions.

Determining the optimal reaction temperature, T_{op}, for these reactions involved multiple experiments and calculations. The first step involved in this process was to determine if the kinetics of the radical and cationic reactions were similar under usable conditions (i.e. suitable initiating temperatures). Once a theoretical T_{op} was calculated, thermal profiles for each reaction were obtained to determine an experimental T_{op}. In addition, the thermal profiles for each reaction were studied thoroughly to determine if they could provide any evidence of simultaneous reactions.

8.2.1. Theoretical prediction of T_{op}

In order for the simultaneous mechanism to be successful, the reactions must behave similarly, that is they must polymerize over similar time scales under identical conditions. *In situ* temperature-monitoring of these reactions was important because it provided

qualitative information on the time requirements for each reaction both individually and simultaneously. To determine if the epoxide functionality and the acrylate functionality could be polymerized in similar times, two theoretical curves were calculated. To get an approximation of this temperature, theoretical studies were conducted to predict polymerization rates for the cationic and radical reactions as a function of temperature. A general method for predicting the polymerization rate for radical reactions is shown in Equations 8.1-5. An extensive derivation of Equations 8.1-5 is readily available in a number of sources including Odian, therefore only the resulting equations are shown here.[3]

$$Ri = 2fk_d[I] \tag{8.1}$$

$$R_p = k_p[M](fk_d[I]/k_t)^{1/2} \tag{8.2}$$

$$\ln R_p = \ln\{k_p(k_d/k_t)^{1/2}\} + \ln\{[M](f[I])^{1/2}\} \tag{8.3}$$

$$\ln k_p(k_d/k_t)^{1/2} = \ln A - E_R/RT \tag{8.4}$$

$$\ln R_p = \ln\{ A_p(A_d/A_t)^{1/2}\} + \ln\{[M](f[I])^{1/2}\} - E_R/RT \tag{8.5}$$

A similar expression for the theoretical determination of R_p versus temperature for cationic mechanisms can be derived in a manner similar to that performed in Equations 8.3-5. The resulting equation shows the dependence of cationic reactions on temperature

$$\ln R_p = \ln(Kk_ik_p/k_t) + \ln\{[I][ZY][M]^2\} \tag{8.6}$$

where K, k_i, k_p, and k_t are all temperature-dependent. Determining the effects of temperature on these quantities is more difficult than for radical reactions, and existing data is much more limited. However, there are a few sources that list k values at various temperatures, including Odian[3] and Subira.[11,12] These values are not extremely accurate, however, therefore there are potentially large errors in these calculations.

After deriving the rate expressions for both mechanisms, experimental values were reported in order to predict an optimal theoretical temperature. The values used to make this determination were extremely liberal in their application, however it must be emphasized that these temperatures were only used in order to make a ballpark estimation for T_{op}. With this in mind, the values shown below in Table 8.1 were substituted into Equation 8.5 to predict Rp as a function of temperature. Table 8.1 shows literature values for methyl methacrylate (the comparable structure to the radical functionality of GMA) as a function of temperature.

Table 8.1. Constant values for theoretical calculation of R_p[3,13].

$A_p \times 10^{-7}$	$A_d \times 10^{-14}$	$A_t \times 10^{-9}$	[M] (mol/L)	[I] (mol/L)	f	E_R (KJ/mol)
0.087[a]	7.38[a,b]	0.11[a]	7.04	0.006	0.8[c]	82.15

[a]has units of liters/mol-sec.
[b]calculated using reported k values at 60°C.[3]
[c]typical values for *f* range from 0.3 - 0.8.

Predicting the propagation rate of the epoxide functionality provided an even less reliable approximation for R_p versus temperature. Literature has reported that E_p typically ranges from 20-80 KJ/mol and may vary greatly according to specific reaction conditions.[14] Increases in temperature generally lead to increases in the rate of polymerization. These facts were used in conjunction with typical ranges for some of the reaction variables in Equation 8.6 to *estimate* an equation relating R_p with temperature. The point resulting from the intersection of the lines produced from Equations 8.5 and 8.6 was determined to be T_{op}. This point ranged from approximately 25°C to 140°C when varying the limits of cationic reaction variables, therefore median values for each cationic

reaction variable were used, resulting in a predicted optimal temperature of 82°C. This intersection point is shown in Figure 8.3.

8.2.2. Thermal profiles

Polymerization of either functionality of glycidyl methacrylate results in a highly exothermic reaction which gives off tremendous amounts of heat over very short periods of time. The large amounts of heat liberated during reaction would be a source of concern in any industrial application employing simultaneous reactions, hence it is important to characterize the thermal profiles of these reactions. Although both the cationic and radical reactions of glycidyl methacrylate are highly exothermic, they are not identical. Therefore, one can gain insight into the actual kinetics of each reaction by monitoring the temperature of the system throughout the polymerization. Moreover, thermal profiles might lead to conclusive evidence of simultaneous reaction if any had occurred. A computerized thermocouple system, developed by Omega Thermal Systems, was used to monitor the temperature of these reactions *in situ*.

The thermal profiles obtained from the computerized thermocouple provided valuable insight into the kinetics of both reactions. A number of variables proved to be important when observing the thermal history of the reaction, thus these variables required substantial examination to determine their effects on the rate of polymerization and the amount of time required for reaction. Some of the variables we studied included initiation temperature, sample size, and initiator concentration. These variables were studied in order to determine their effects on the reaction kinetics of both (radical and cationic) polymerization methods.

The effect of the initiator concentration on the reaction rates is shown in Figure 8.4, where the epoxide functionality of GMA samples was polymerized using three different concentrations of $FeCl_3$. This figure shows dramatically decreasing reaction times as the amount of initiator increases. Intuitively this makes since a higher initiator concentration means more active species present. Unfortunately, the concentration can only be raised so high because higher concentrations will result in the formation of oligomers or lower molecular-weight polymers, thereby diminishing the physical properties which are directly proportional to molecular weight. Experimental determination of the limits for the concentration of radical and cationic initiators were inhibited by the fact that simultaneously polymerized samples were insoluble in all solvents tested including alcohols, methylene chloride, and various acids. However, many researchers including Dusek *et al.*[15] have used radical initiator concentrations around 0.1 wt%, with similar concentrations being used for cationic initiation by Lewis acids. This led to the decision to use both radical and cationic initiator concentrations of approximately 0.1 wt% for simultaneous polymerizations.

A final set of experiments were conducted using the thermocouple to determine if it could be used to detect simultaneous polymerization to a noticeable degree. In order to do this, three samples were made up from bulk solutions of 99.8 wt% GMA and 0.2 wt% AIBN and 99.8 wt% GMA and 0.2 wt% $FeCl_3$. The three samples were a bulk radical solution (AIBN as the initiator), a bulk cationic solution ($FeCl_3$), and a simultaneous solution (both). The simultaneous solution was prepared by mixing equal parts of the radical and cationic solutions, thereby diluting each initiator concentration by 50 wt% while maintaining the monomer concentration. The initiator concentration in the bulk

samples were diluted down to 0.1 wt% by adding GMA to the samples to insure that they would be consistent with the simultaneous solution. These samples were then polymerized at 76.9°C in a water bath. Figure 8.5 shows the accelerated polymerization in the simultaneous sample relative to the radical and cationic samples. The simultaneous polymer reaches its maximum temperature in roughly half the time of either the cationic or radical polymers. This may occur because the reaction is non-isothermal, hence as reaction occurs the system gets hotter, resulting in an increased production of radicals and cations capable of initiating polymerization.

8.2.3. Computer Modeling

Computer modeling, or molecular modeling as it is sometimes called, can provide a vast amount of useful information. Using the technology now available, researchers are able to study many different aspects of polymers on a microscopic level that were once impossible to simulate. For example, programs exist today which are capable of predicting various physical properties, structures, surface composition, and volume of polymers in solution. These examples are only a small percentage of what can be predicted by various software packages, however they represent the broad area of polymer technology which can now be studied electronically. Moreover, computer modeling can be extremely useful when trying to determine likely structural conformations of new polymers or when attempting to create a polymer having specific properties. These experiments were carried out using Polygraf™, molecular simulation software for the design, simulation, and analysis of polymeric materials, on a Silicon Graphics Supercomputer (IRIS 4D/220GTX).

Polymeric structures based on GMA were created using POLYGRAF™; and the total energies of each structure were determined. Each structure was formed from the same monomer and its energy was computed in order to make qualitative comparisons. A POLYGRAF™ energy minimization package was used to transform each structure from its original conformation to its most probable conformation (i.e. conformation having the lowest total energy).

To ensure that the structures were in their "best" conformation, each structure was first subjected to an energy minimization process. Next, the structure was perturbed from its minimum energy for an average of five picoseconds and minimized again to determine if it had reached a local or global minimum energy. This was repeated *n* times until the *n*th energy was approximately equal to the *(n-1)*th energy, meaning that the structure had reached its global minimum. This value is reported as the total energy of that particular structure. This process was repeated for each of the structures listed in Table 8.2.

Table 8.2. Total energy for various compounds as predicted by computer modeling.

Structure	Total Energy (kcal/mol)
Glycidyl methacrylate monomer	129.878
Radical homopolymer	1450.818
Cationic homopolymer	193.326
Perfect ladder polymer	2539.952
Imperfect ladder polymer	2408.233
3 strand ladder with epoxy backbone	2894.584
3 strand ladder with acrylate backbone	1538.396

The energy contributions of bonds, angles, van der Waals forces, and hydrogen bonds[16] are totaled to obtain the energy values listed in Table 8-2. The energy values produced during these simulations are the sum of the kinetic and potential energies for each structure. To produce each structure, ten glycidyl methacrylate repeat units were manipulated in order to produce energy values that could be quantitatively compared to other polymeric structures (with the exception of the energy associated with the single monomeric unit) to determine which structure is more likely to exist in nature. Structures having lower energy values would more likely be formed in polymerization reactions. For example, it is more likely that an imperfect ladder will be produced from glycidyl methacrylate than a perfect ladder, because the imperfect ladder requires approximately 100 less kilocalories per mole than the perfect ladder structure. It is important to realize that the energies listed in Table 8.2 are not related to the amount of energy required to

polymerize a functionality, rather they are the amount of energy associated with a particular structure under standard conditions (25°C, 1atm).

8.2.4. Conclusions of Ladder Polymer Research

The molecular modeling experiments led to the conclusion that it would be highly unlikely that a high molecular weight perfect ladder would form in a simultaneous radical and cationic chain polymerization scheme. In addition, it is very difficult to "match" the kinetics of two distinct reactions such that the rate of polymerization for each is identical under identical conditions. Since the conditions of a simultaneous polymerization involving two different reaction mechanisms are by definition identical, thus there exists an extremely complicated logistical problem which must be solved in order for a perfect ladder structure to be formed. These problems and others made it clear that the formation of perfect ladder polymers in a simultaneous, one-step polymerization of two distinct functionalities would meet with extremely limited success, at best.

8.3. Interpenetrating Polymer Networks

Interpenetrating polymer networks (IPNs) consist of at least two physically intertwined polymer networks which are inseparable. IPNs have attracted attention as a special type of polymer blend for crosslinked polymer systems which allows the synergistic combination of two polymers, thereby creating a network with properties superior to those of each individual constituent polymer.[17] In addition, IPNs may show higher resistance to deformation as measured by initial stress divided by elongation.[18] An

example of this increased resistance is a rubbery polymer/glassy polymer IPN, which exhibits both increased strength and impact resistance when compared with the strength and impact resistance of its single chain analogs.[19]

IPNs are particularly attractive to research scientists because their properties can be tailored to specific applications by proper construction of the network. An additional advantage of IPNs is the fact that they combine properties of existing polymer systems to form one polymeric network whose properties are superior to any and all individual polymers in the network. Hence new polymer technology is not required in the development and production of IPNs. These advantages plus the fact that IPNs can be produced with inexpensive components (polymers) make them potentially suitable for a number of industrial applications. Despite these obvious advantages as well as other benefits of IPNs, they have not yet been used in many industrial applications due to process limitations. For example, many of the previously reported methods involve the use of large amounts of solvent and require significant time for swelling.

A goal of this research was to to circumvent many of the problems associated with the formation of IPNs by reacting two distinct, crosslinkable monomer systems simultaneously to form an IPN. To test this strategy, the possibility of initiating one monomer via a radical chain reaction while at the same time polymerizing the second monomer via cationic chain reactions was investigated. Successful development of such a process would yield at least two major advantages: it would drastically reduce time requirements for both reactions to reach equilibrium; and the process would be environmentally benign because it is solvent-free.

While such a process would have obvious advantages over current IPN processing methods, there are a number of disadvantages which drastically reduce the rewards associated with developing such a process. A significant disadvantage of this method is the fact that it greatly limits the number of IPNs which can be produced. There will be at least two different active species present in measurable amounts due to the fact that there are two reactions occurring simultaneously. This limits the availability of useful monomers right from the start because no monomer may be initiated by more than one active species during the course of the reaction or the structure most likely to form will be a single copolymer as opposed to an IPN. For example, polystyrene/polyacrylate IPNs would not be possible because an active radical could propagate through either the acrylate or the styrene, thus resulting in a polystyrene/polyacrylate copolymer instead of an IPN. The initial hurdle in selecting a system is determining if the selected monomers will undergo the same type of chain polymerization. Table 8.3 (adapted from Odian[3]) shows various monomers which will undergo radical or cationic polymerization exclusively. In order for our process to be amenable to a specific system, the monomers must come from separate columns (of Table 8.3). This table is by no means comprehensive, however it affords one the opportunity to determine if their system is fundamentally capable of producing an IPN based upon this technology. Furthermore, selecting monomers from each column of Table 8.3 does not guarantee a successful IPN since there are other compatibility questions such as miscibility and reaction kinetics which were not contemplated during the course of this research.

Table 8.3. Type of chain polymerization undergone by various unsaturated monomers.

Type of Initiation	
Radical	*Cationic*
ethylene	α-olefins
halogenated olefins	1,1-dialkyl olefins
vinyl esters	vinyl ethers
acrylates	aldehydes, ketones
acrylonitriles	epoxides
acrylamides	

8.3.1. Classes of IPNs

Three methods are currently used to synthesize IPN's. The first method (A) is a multiple-step process in which one network is formed, then swollen by the second monomer, which is then polymerized and crosslinked *in situ*. The second method (B) is also a multiple-step process in which both monomers are mixed initially and the IPN is formed by sequentially polymerizing and crosslinking the monomers in the system. The final method (C) involves mixing all network ingredients at once, followed by polymerization and crosslinking of both networks in a truly simultaneous, one-step process in which one monomer typically undergoes chain polymerization while the other undergoes a step polymerization.[20] Method C is best-suited for industrial applications because it does not involve swelling of polymer networks, dramatically reducing the overall cure time of the IPN. Despite the improved processability in the simultaneous

method, solvent capable of producing unwanted side reactions is still required, which can result in complications in the formation of one or both polymer networks. Moreover, the amount of solvent evaporated during reaction can be excessive and may be damaging to the environment.

The classification of IPNs is generally based on the method used to form the IPN. Polymer networks produced by method A or method B are classified as sequential IPNs while method C produces simultaneous IPNs which are more commonly known as SINS. Both sequential and simultaneous IPNS may be further divided into subclasses based on the number of crosslinked homopolymers within the network. The most significant class of interpenetrating polymer networks in terms of industrial potential are the *simultaneous IPNs*, commonly referred to as SINs. SINs display the highest industrial potential for many reasons ranging from their facile synthetic process to significant time and energy reductions. Interpenetrating polymer networks synthesized simultaneously are less time-intensive in both the preparation of the monomeric solutions as well as in the production of the SINs; hence parts produced using this method are more amenable to large-scale processing methods such as resin transfer molding (RTM) and reaction injection molding (RIM). Despite their promise, SINs are the least researched and therefore most poorly characterized class of interpenetrating polymer networks.

SINs are formed when all components of the final network, including monomers, initiators and crosslinking agents, are mixed together either in bulk or in a solvent to form a reactive formulation. This formulation is then exposed to a set of experimental conditions such that two distinct polymerization mechanisms are able to proceed at approximately equal reaction rates. Nearly all SINs involve one monomer system

proceeding via chain polymerization while a second monomer undergoes step polymerization. These polymerizations occur in a manner such that each reaction will progress towards completion without interference from the other. Monomers that "overlap" (i.e. polymerization will occur via either reaction mechanism) will be ineffective because they will likely yield one large, crosslinked polymer instead of two intertwined, crosslinked homopolymers. Therefore the selection of restrictive reaction schemes is vital to the formation of SINs. The choice of monomeric and/or oligomeric precursors as well as the rates at which these components polymerize are also crucial to the success of the network. For example, the rate of polymerization for each component of the system must be equal or nearly equal to the rate of polymerization of other components in the network or a SIN will not form.

Interpenetrating polymer networks synthesized from (at least) two monomers, each polymerizing and crosslinking in the presence of the other, involve extremely complex reaction kinetics. The crosslinking reaction for each component is complicated by the added reaction that exists when a second monomer is synthesized and polymerized *at the same time*. Researchers have tried to largely circumvent this problem by using low molecular-weight polymers which may still be solubilized instead of monomers, and crosslinking these homopolymers to form SINs.[21-23] In addition, IPNs may be sensitive to environmental changes, both before and during polymerization.[24]

Composition, like temperature and pressure, has a large affect on the morphology and physical properties of IPNs. For example, Frisch et al.[25] stated that an elastomeric/glass IPN would be a reinforced rubber if the elastomeric phase dominated, while an IPN having the same components present in different composition would yield

an impact resistant plastic if the glass phase dominated. The ability to design the IPN so that the properties can be controlled by the composition of the IPN is considered by Frisch[25] to be one of the biggest advantages of IPNs.

8.3.2. IPN Experiments

IPN research in this laboratory centered on epoxy/acrylate polymer networks. The original model system selected for this study was propylene oxide / methyl methacrylate. These monomers were chosen because they were the single-chain analogs of glycidyl methacrylate, a monomer whose kinetics for both the radical and cationic reactions were characterized in the ladder research. This model system proved to be shortsighted from the beginning because the monomers were incompatible in a number of areas ranging from the boiling point of each monomer to the density difference. Initial experiments attempting to polymerize 50/50 mixtures at 65°C belied some of the fundamental problems of this system. The results of these initial experiments showed that roughly 40% of the solution had been converted to a solid after 20 minutes, an extremely low yield when compared with ladder experiments. After attempting to polymerize propylene oxide individually, the problem became clear almost immediately.

A reactive formulation consisting of 98.9 wt% propylene oxide, 1.0 wt% (triethylene glycol) divinyl ether, and 0.1wt% $FeCl_3$ was mixed and stored in a refrigerator. A 3g sample was placed in a plastic vial, capped, and placed securely in a water bath maintained at 65°C. The sample was removed from the water bath after 20 minutes, only to find that nearly all of the solution had vaporized. This process was repeated seven times with improvements made each time to seal the vial and prevent the

vial from vaporizing. In each case, there was less than 2% of the monomer remaining at the conclusion of the experiment.

8.3.3. Discussion/Conclusions of IPN Research

The experiments with the propylene oxide/methyl methacrylate system led to the immediate conclusion that production of an IPN based on a thermally-initated simultaneous radical/cationic chain polymerization would be extremely difficult due to a number of considerations including monomer compatibility, competing reactions, and lack of (thermal) control over the reaction. In fact, the lack of control led to the initial investigations using photoinitiators to polymerize the individual networks.

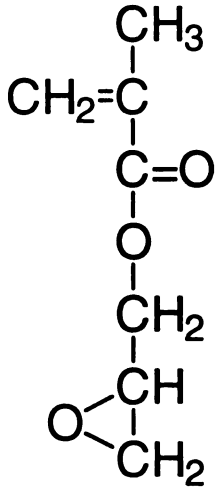

Figure 8.1. Chemical structure of glycidyl methacrylate.

PERFECT 2-DIMENSIONAL LADDER

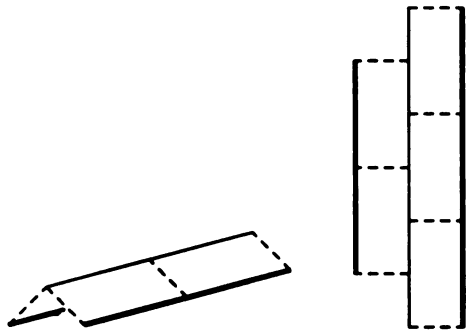

3-DIMENSIONAL "LADDER"

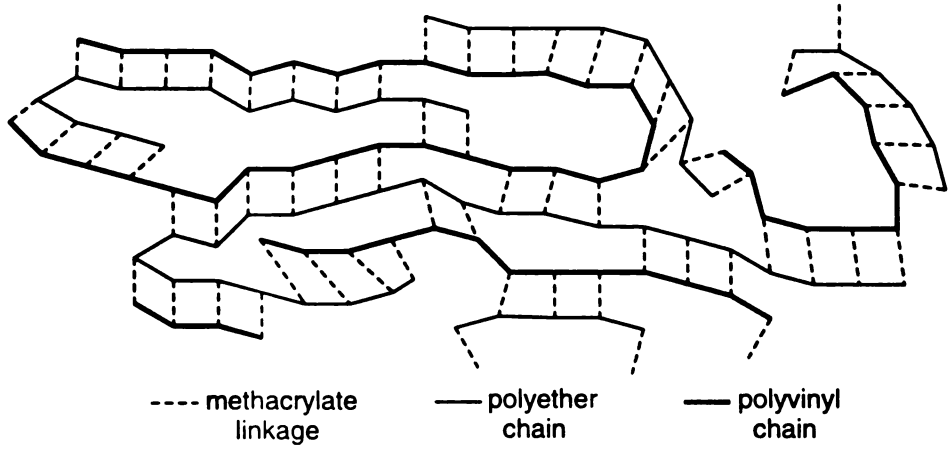

"CROSSLINKED" LADDER

Figure 8.2. Potential structures of poly(glycidyl methacrylate).

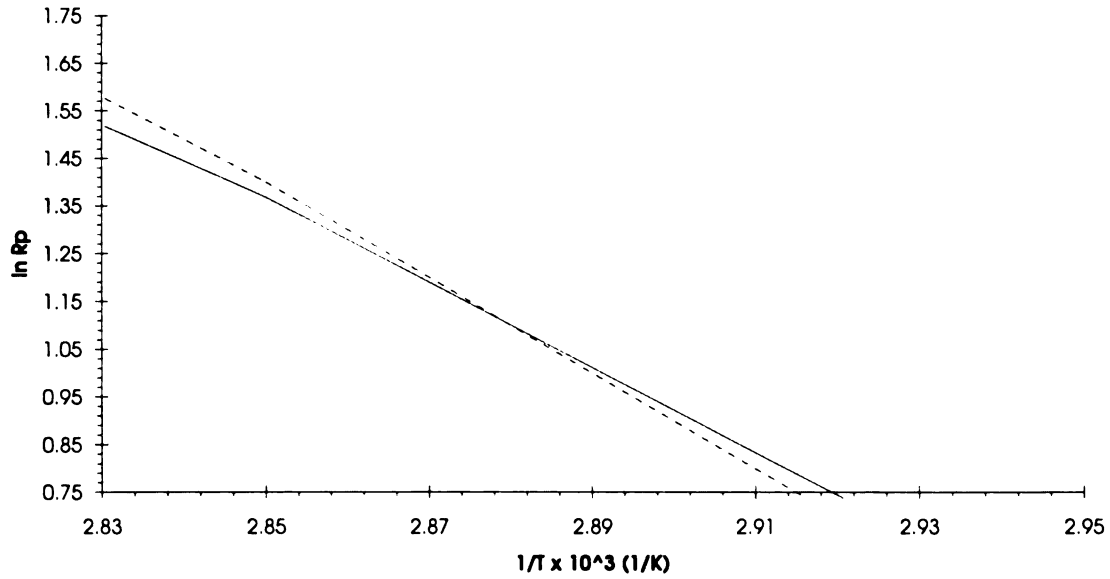

Figure 8.3. Predicted propagation rates of MMA (—) and propylene oxide (- -) as a function of temperature.

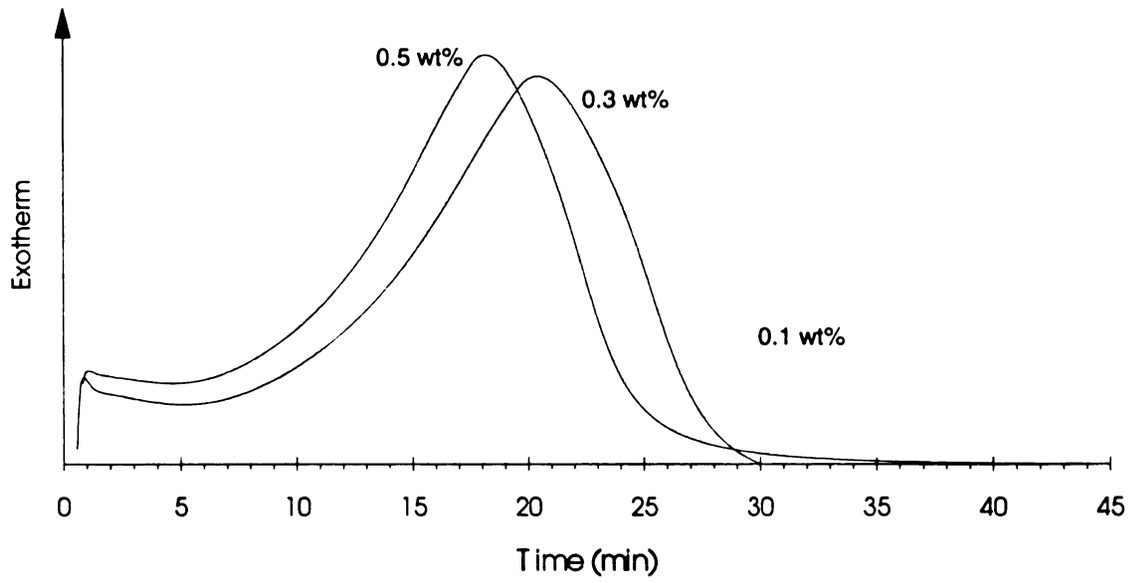

Figure 8.4. R_p versus initiator intensity for GMA polymerized cationically at 73°C.

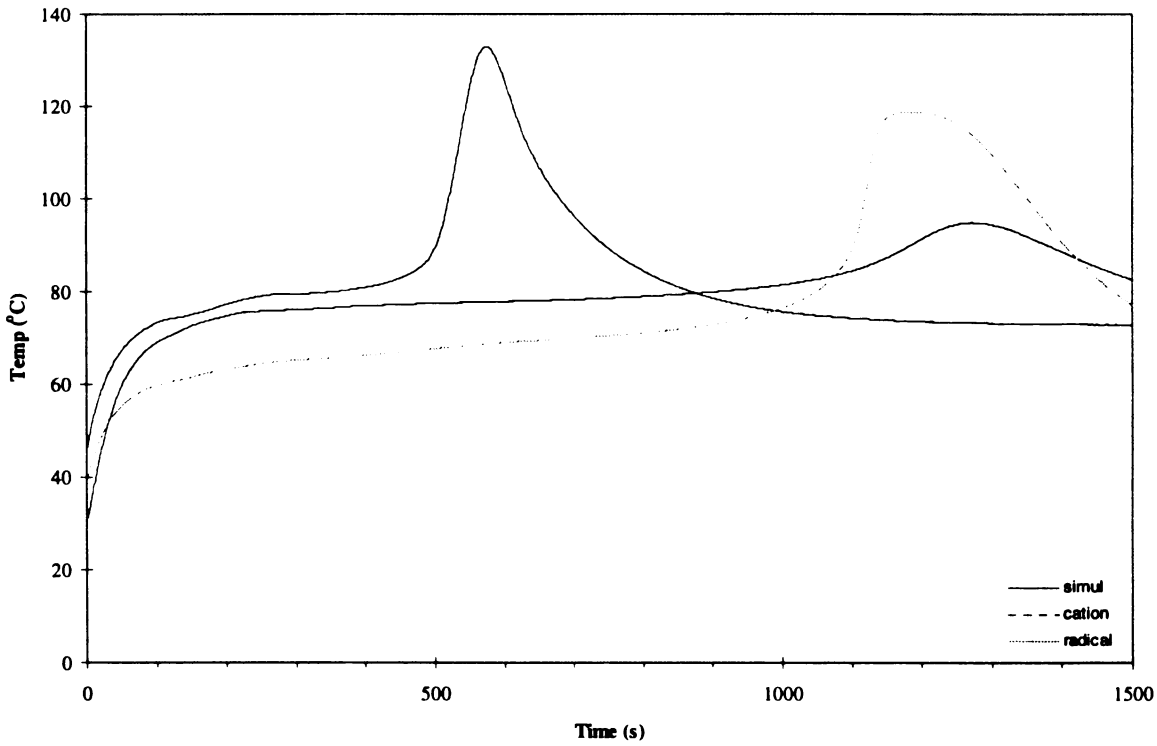

Figure 8.5. Thermal profiles of glycidyl methacrylate polymerized radically, cationically, and simultaneously.

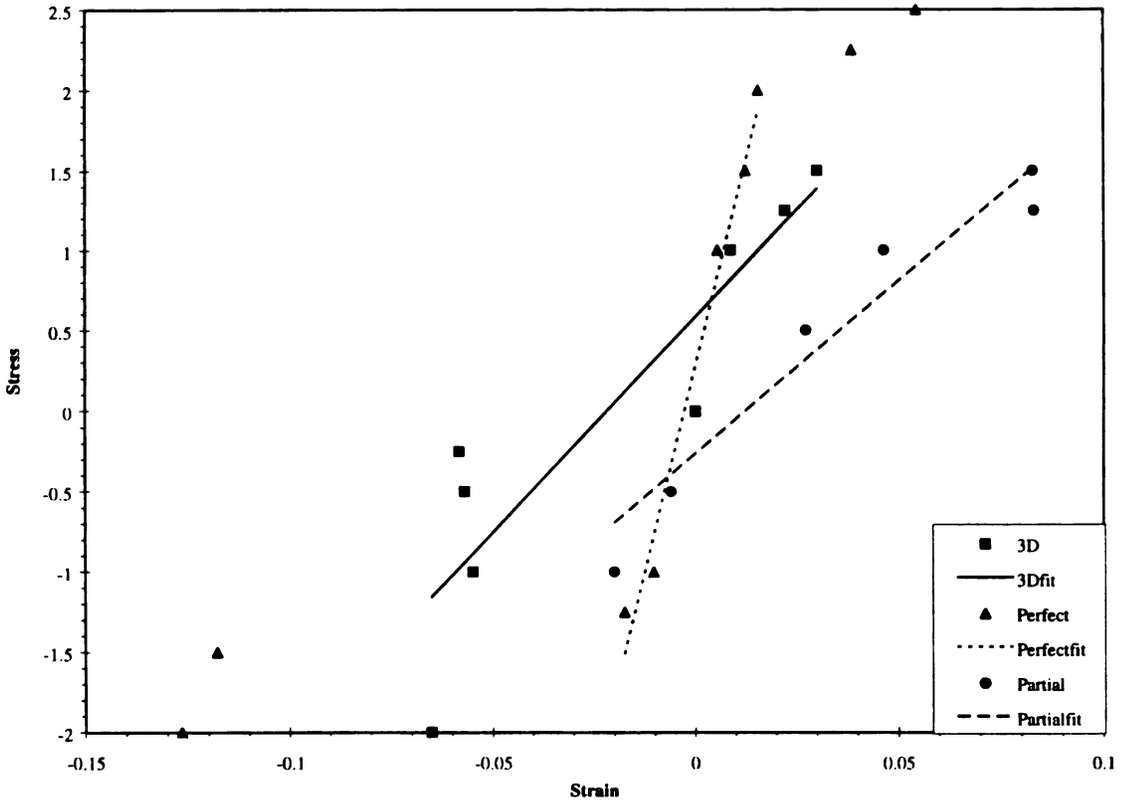

Figure 8.6. Simulated stress/strain curves for poly(glycidyl methacrylate) ladder structures.

8.4. References

1. M.S.M. Alger, in "Specialty Polymers," R.W. Dyson, Ed., Chapman and Hall, New York, 64 (1987).

2. W.J. Bailey, *Polym. Mat. Sci. Eng.*, **60**, 400 (1989).

3. G. Odian, "Principles of Polymerization," 3rd Ed., Wiley-Interscience, New York, 149 (1991).

4. J.I. Jones, *Rep. Prog. Appl. Chem.*, **27**, 544 (1968).

5. M.M. Tessler, *J. Polym. Sci., Part A*, **1**, 2521 (1966).

6. J. McMurray, "Organic Chemistry," Brooks/Cole Publishing, Monterey, California, 423 (1984).

7. W.R. Dunnavant, *J. Polym. Sci., Part B*, **6**, 49 (1968).

8. B.H. Lee, C.S. Marvel, *J. Polym. Sci., Polym. Chem.*, **21**, 83 (1983).

9. S.A. Jenekhe, *Macromolecules*, **24(1)**, 1 (1991).

10. A. Ghafoor and R.H. Still, *J. Appl. Polym. Sci.*, **21**, 2905 (1977).

11. F. Subira, G. Sauvet, J.P. Vairon, and P. Sigwalt, J. Polym. Sci. Symp., **56**, 221 (1976).

12. F. Subira, J.P. Vairon, and P. Sigwalt, Macromolecules, **21**, 2339 (1988).

13. J. Brandup and E.H. Immergut, Eds. (with W. McDowell) in "Polymer Handbook", Wiley-Interscience, New York, II-316 (1989).

14. J.C.W. Chien, Y.-G. Cheun, C.P. Lillya, *Macromolecules*, **21**, 870 (1988).

15. K. Dusek and J. Spevacek, *J. Polym. Sci., Polym. Phys.*, **18**, 2027 (1980).

16. POLYGRAF Reference Manual, v3.1, Molecular Simulations, Waltham, MA, 5-15 (1992).

17. D.R. Paul, J.W. Barlow and H. Keskkula , in "Encyclopedia of Polymer Science and Engineering," **12**, H.F. Mark, N.M. Bikales, C.G. Overberger and G. , Eds., Wiley-Interscience, New York, 399 (1988).

18. R. Pernice, K.C. Frisch and R. Navare, in "Polymer Alloys III," **20**, D. Klempner and K.C. Frisch, Eds., Plenum Press, New York, 219 (1983).

19. A. Morin, H. Djomo and G.C. Meyer, *Polym. Eng. Sci.*,**23(7)**, 394 (1983).

20. H. Djomo, A. Morin, M. Damyanidu, G. Meyer, *Polymer*, **24**, 65 (1983).

21. D.J. Hourston and M.G. Huson, *J. Appl. Polym. Sci.*, **46**, 973 (1992).

22. M.S. Lin and K.T. Jeng, *J. Polym. Sci., Polym. Chem.*, **30**, 1941 (1992).

23. M.S. Lin and R.J. Chang, *J. Appl. Polym. Sci.*, **46**, 815 (1992).

24. D.J. Hourston and M.G. Huson, *J. Appl. Polym. Sci.*, **45**, 1753 (1992).

25. H.L. Frisch, K.C. Frisch and D. Klempner, in "Chemistry and Properties of Crosslinked Polymers," S.S. Labana, Ed., Academic Press, New York, 205 (1977).

CHAPTER 9.

RESEARCH SUMMARY AND RECOMMENDATIONS FOR FUTURE WORK

Through fundamental "proof-of-concept" and characterization studies, this research effort has demonstrated the tremendous potential of photopolymerization processes for the production of composites and thick polymers. The initiation strategies developed in this research can in fact be used to produce thick polymers and composites. As described in the preceding chapters, it is clear that the advantages afforded by photopolymerizations can be extremely advantageous in the production of thick and fiber-filled polymer composites. A general summary of this research effort as well as recommendations for the continuation of research in this area are presented in the remainder of this chapter.

9.1. Research Summary

Two novel strategies for the production of thick polymers and composites based on photoinitiation methods have been developed in this research effort. The first strategy employs careful selection of initiators, resins and system "extras" including photosensitizers, accelerators, dyes and pigments to establish a system where the transverse light intensity gradient that exists in thick samples is initially modest. This

strategy relies on efficient penetration of light into the bulk of the sample as the reactive formulation polymerizes. The second strategy capitalizes on the fact that these reactions are highly exothermic to use a hybrid photo/thermal initiation mechanism. In this method, ultraviolet light excites a photoinitiator, causing it to undergo some type of decomposition reaction resulting in the generation of active sites. These active sites initiate polymerization in the sample while simultaneously elevating the temperature of the system. This causes a second, thermal initiator to undergo some type of decomposition reaction which results in the generation of additional active sites throughout the bulk of the sample, thereby enhancing the reaction.

A reactive formulation consisting of a radical photoinitiator (benzoin ethyl ether), a vinyl ester resin, and occasionally a thermal initiator (benzoyl peroxide) was employed to demonstrate the initiation strategies developed in this research. A number of resin and initiators were investigated in addition to the materials used in the representative system. A summary of investigated materials is shown in Table 9.1. A series of fundamental investigations were conducted in order to establish the validity of these initiation strategies and to establish their potential as new methods for producing composites and thick polymers. Fundamental "proof-of-concept" studies that were completed to validate the concepts of "self-eliminating gradients" and hybrid "photo/ thermal" initiation methods consisted of a number of important system variables including:

- optimization of initiator concentration and overall initiator formulation including concentration of photoinitiator, thermal initiator and photosensitizer;
- optimization of operating window including careful selection of initiator formulation, incident light intensity and wavelength range;

- investigating the effects of fiber type, treatment, and loading on the cure time and mechanical properties of resultant composites;
- mechanical and thermal characterization of the resulting composite parts.

Combined, these studies present a picture that clearly shows the domain of photopolymerization applications can be expanded to include thick polymers and composites using either the concept of self-eliminating light intensity gradients or the notion of a hybrid photo/thermal initiation scheme. Widely accepted photoinitiator classes which have proven to be successful catalysts for either strategy developed in this research include benzoin ethers and the so called "Irgacure" initiators produced by Ciba Geigy. These initiators can be used to cure important classes of monomers and resins such as vinyl esters, acrylates and methacrylates. Additional experiments have demonstrated the ability to decouple mold filling and reaction, resulting in the rapid production of thick and fiber-filled polymer composites which exhibit good mechanical properties.

In conclusion, these initial studies have confirmed the potential of these novel processing schemes for the production of photocurable composites. This research represents a significant breakthrough in UV technology. It has used novel strategies based on photoinitiation processes to cure products that are considerably thicker than what was once thought possible. However, before employing either of the strategies outlined in this research commercially, considerable work must be put in to optimize the composite products and to develop applications.

Table 9.1. Resins, photo and thermal initiators studied in the development of the initiation strategies.

Monomers/Resins	Photoinitiators	Thermal Initiators
Derakane	Benzoin ethers	Benzoyl Peroxide
470-45	Benzophenone	2,2'-azobisobutyronitrile
411c-50	Benzoin Methyl Ether	Wako V-70
441-400	Benzoin Ethyl Ether	Wako VA-044
511	Camphorquinone/TBA	
8084	Irgacure 639	
Methyl Methacrylate	Irgacure 651	
Glycidyl Methacrylate	Eosin B	

9.2. Recommendations for Future Work

Although photopolymerizations offer several advantages when compared with traditional thermal polymerizations, their use in the production of thick and fiber-filled composite parts has been limited due to problems associated with poor mechanical properties arising from non-uniform and incomplete cure. In order to fully exploit the findings of this research, it is recommended that this research branch off in three directions: further development of the radical system; research into cationic systems; and investigations and development of industrial applications.

9.2.1. Development of Radical Systems

A general objective of this research has been to validate the concept of using photopolymerizations to produce thick polymers and composites. As a result of this, only minor attention has been paid to characterizing the kinetics of these systems. While effects of system variables have been qualitatively analyzed and radical propagation and termination constants are well-established for vinyl ester resins, it would still be beneficial to quantify the overall kinetics of these reactions.

Although the mechanical properties of these systems have been characterized, they were optimized for an extremely limited number of glass-fiber reinforcement materials which were chosen to provide the most optically challenging systems possible instead of providing the best mechanical properties. It is therefore worthwhile to investigate available reinforcement materials in order to optimize the composites to achieve the highest performance levels possible (although the level of performance is dictated somewhat by the particular application). While it is highly unlikely that they would be well-suited for SEG strategy due to the opaque nature of the composite, carbon fibers should be investigated in addition to the aforementioned glass fiber systems as reinforcement materials for composites cured using the dual-cure strategy. Initial polymerizations involving relatively modest degrees of carbon fiber loading (~ 25 wt% or less) have met with some success. However, by no means can any conclusion be drawn as to their ability or inability to be used as reinforcing materials for the photocurable composites.

Characterization of the chemical resistance for the vinyl ester polymers and composites has recently been initiated and should be continued. Preliminary results from

swelling studies indicate that most of the Derakane polymers are stable in a number of chemical environments ranging from water to methanol to 10 % solutions of sodium hydroxide and hydrochloric acid. Still, these experiments have been initiated very recently and are highly limited in scope.

The final area of research which merits attention for the Derakane vinyl ester resins is to determine how different variables such as initiator concentration and formulation, incident intensity, resin type and fiber type and degree of loading affect the extent of cure for these polymers and composites. Techniques for determining the extent of cure have been discussed in this contribution and could be performed to better characterize the effects of operational variables on the ultimate properties of resultant polymers and composites. Infrared (IR) spectroscopy is an additional technique that can be used to quantitatively characterize the extent of cure for polymeric systems. IR experiments performed in this research proved to be inconclusive, however there are a number of peaks in the IR spectrum such as the vinyl bond and the ether linkage which can be monitored to quantitatively determine the extent of cure.

9.2.2. Fundamental Research into Cationic Systems

Preliminary studies have indicated that the cationic initiation systems may be successfully used to cure thick polymers and composites, however further development and characterization is necessary. Development of a strategy based on photoinitiation of cationically polymerizable systems would allow one to cure important classes of commercially available resins such as epoxies. This research may serve as a guide for the future efforts in cationic systems. Specific efforts in this area should focus on

establishing the following operating conditions for a representative epoxy system: development of usable photoinitiator systems including photoinitiator, photosensitizer and thermal initiator; optimizing the *monomer/resin formulation* for desirable viscosity, curing rate and temperature control; and characterizing the effects of cure time, incident intensity and wavelength range on the reaction kinetics. In addition, photoinitiator formulations based on diaryliodonium salt/anthracene systems have been investigated and it has been established in this research that these systems exhibit the self-eliminating characteristic even more dramatically than the radical systems employed in this research (see *Chapter 4 - Developing the Polymerization Strategies: Fundamental Experiments*).

These fundamental studies will provide an understanding of the relationships among reaction variables, thereby allowing efficient process development. Because general strategies have been developed which can serve as guidelines for this research and potential initiator formulations have already been established, research efforts should focus primarily on developing suitable epoxy systems and not on investigating new initiator formulations (although investigations of new initiators should not be completely overlooked).

9.2.3. Investigation and Development of Potential Applications

It is strongly recommended that research in pursuit of applications based on this technology be performed in tandem with industrial contacts. The input of industrial collaborators in terms of both financial and technological support is invaluable and offers insight into many of the problems which one might face when trying to take a product from the prototype stage to production. With these comments in mind, a number of

potential applications which merit further attention have been investigated in the course of this research.

Potting Compounds. Prototype samples for photocurable potting compounds have already been developed and tested at three industrial sites. Based upon the industrial feedback, adjustments in the formulation should be made to make the compounds industrially feasible for specific applications. An objective of research in this area should be to develop several formulations which can be used to meet a variety of industrial needs depending on the particular application. For example, highly adhesive formulations may be desired for repair applications while some applications such as systems where two or more structures are bonded temporarily may require formulations which exhibit fair or even poor adhesion.

Photocurable prepregs. This application exploits the rapid response and high degree of control provided by photoinitiation to partially polymerize a resin-impregnated fiber mat to a precise, predetermined degree of cure. In this partially polymerized, intermediate state, the resin is cured to an extent that it will not flow, but the prepreg will be pliable (i.e. tacky but shapeable) and can be worked with and formed into the desired shape before photocuring to form to a rigid composite. Since light rather than heat provides the initiating energy, these prepregs will have the unique characteristics of superior working times in the absence of UV light, but short cure times upon illumination at room temperature.

This novel design of these photocurable prepregs is based upon fundamental aspects of the photoinitiation and free radical termination processes. Due to the underlying photochemistry, the production of active centers occurs rapidly, consuming a

portion of the photoinitiator upon illumination by the appropriate wavelength of light. When the prepreg is removed from the light, the active center concentration decreases rapidly due to radical termination reactions and will decay to zero in a few seconds, allowing the part to cure to an intermediate state that is both predictable and reproducible. The degree of intermediate conversion is readily manipulated by changing the illumination time, hence the system can be tailored to achieve an intermediate prepreg with the desired characteristics. The final photocure (after forming) utilizes the unconsumed portion of photoinitiator to rapidly form a stiff, fiber-reinforced composite. If necessary, this cure could readily be achieved using a second photoinitiator and a different wavelength of light than the initial partial cure.

Perforated, Composite, Acoustic Panel Face Sheets. Although the photocurable prepregs may find many applications, they are ideally suited for the production of perforated composite acoustic panel face-sheets for the aerospace industry. Perforated, cylindrical composite structures are used to surround jet engines to provide acoustic dampening. These acoustic panel face-sheets are difficult to manufacture due to the curvature of the structure and the ordered pattern of perforations. Since these radial perforations must extend through the thickness of the part, it is impossible to remove these structures from a cylindrical mold containing pins to produce the perforations. Due to this problem, current methods of production are tedious and inefficient. A photopolymerizable prepreg offers an efficient and elegant method to produce such structures. For this application, the resin-impregnated fiber mat may be partially polymerized in a flat mold equipped with ordered pins to produce the perforations. The semi-cured prepreg can be easily removed since the mold is flat. The perforated prepreg

will then be shaped around a cylinder to impart the proper curvature, and the cure will be completed. The perforations will remain intact, therefore no pins are required in the cylindrical geometry and the finished part is easily removed.